Simulation of Emerging Smaller-Scale Tri-Generation Systems

by

FRANCESCO CICCIARELLA
Laurea Triennale, Politecnico di Torino, Turin, Italy, 2013

THESIS

Submitted in partial fulfillment of the requirements
for the degree of Master of Science in Mechanical Engineering
in the Graduate College of the
University of Illinois at Chicago, 2015

Chicago, Illinois

Defense Committee:

William Ryan, Chair and Advisor
Michael Scott
Marco Carlo Masoero, Politecnico di Torino

The impossible could not have happened,

therefore the impossible must be possible in spite of appearances.

Agatha Christie, Murder on the Orient Express.

ACKNOWLEDGMENTS

First and foremost, I wish to thank both my advisors.

Prof. William A. Ryan for his precious guidance throughout this work and for the constant enthusiasm with which faces his work.

Prof. Marco C. Masoero for being my reference during these years and for his complete willingness to help, something that every professor should demonstrate.

Furthermore, I am particularly grateful to the person who has shared with me this experience day by day. Thanks to Cesare for teaching me how time does not count for feeling real friends. Thanks to another Cesare, whose endless patience in listening my stream of consciousness has provided me the necessary clarity to face my challenges.

Thanks to Giuseppe, Marco, and Michel for always reminding me my achievements rather than my failures and for giving me the silent awareness of the existence of a place called home.

I thank from the deep of my heart my whole family, for standing by my side in every important moment of my life. Whatever I do, whatever I chose, they will always be happy if I am too. This is love.

FC

TABLE OF CONTENTS

TABLE OF CONTENTS (Continued)

LIST OF TABLES

LIST OF FIGURES

LIST OF FIGURES (Continued)

FIGURE **PAGE**

LIST OF FIGURES (Continued)

FIGURE **PAGE**

LIST OF FIGURES (Continued)

FIGURE **PAGE**

LIST OF ABBREVIATIONS

CCGT	Combined Cycle Gas Turbine
CHP	Combined Heat and Power generation
CI	Critical Infrastructure
COP	Coefficient Of Performance
CWT	Chilled Water Temperature
DOE	Department Of Energy
GHG	Green House Gases
HRSG	Heat Recovery Steam Generator
HVAC	Heating, Ventilation and Air Conditioning
IEA	International Energy Agency
IGCC	Integrated Gasification Combined Cycle
MOB	Medical Office Building
NPV	Net Positive Value
O&M	Operations and Maintenance
PLR	Partial Load Ratio
PNNL	Pacific Northwest National Laboratory

LIST OF ABBREVIATIONS (Continued)

PRSEC	Percentage Reduction in Source Energy Consumption
SCR	Selective Catalytic Reduction
USD	United States Dollars
VAV	Variable Air Volume
WHP	Waste Heat to Power
WRH	Wasted Recoverable Heat

SUMMARY

Support for renewable energy and for actions aiming at increasing energy efficiency represents a fundamental objective for both governments and private investors. Depletion of energy resources and global pollution effects, produced by the exploitation of non-renewable energy sources, represent major concerns for the social and environmental sustainability of energy production in the immediate future. This concern is compounded by steady increase of the global energy consumption, despite of the limited availability of non-renewable fuel resources. As the energy demand and the pollution concerns continue to grow, the research on energy efficiency and the need to design new environmental friendly power generation is becoming more crucial than ever.

This study is aimed to analyze the energy needs of a health care facility in order to define a strategy to improve the efficiency of the energy supply. Using eQuest® software, the facility is simulated and electricity and natural gas consumption is evaluated assuming the direct purchase of both from external grids.

The analysis continues by adding cogeneration. To adequately simulate the behavior of this kind of plant, a detailed study of gas turbines has been carried out to produce an up-to-date model of this component. Different layouts, including different sizes of gas turbines, are simulated in order to identify the best plant layout.

The next step of this study focuses on trigeneration. Once again, preliminary task was to develop a detailed study of its components. In this phase, the object of analysis is the absorption chiller. Using eQuest® the cogeneration layout of the facility is further improved through the installation of the absorption chiller, to exploit the thermal energy content of the gas turbine exhaust gas during the cooling season. Several simulations have been performed to define the layout of the plant that ensures the best performance.

The simulation results allow two kinds of analysis; first, an economic analysis for defining the most profitable layout and second an analysis on source energy consumption to determine the layout providing the best exploitation of resources.

CHAPTER 1

THE HEALTH CARE FACILITY

This study deals with satisfying the energy needs of a health care facility in an innovative way. Solutions like cogeneration or trigeneration have more chances to be realized in a profitable way in hospitals, because of the frequent, large, and simultaneous need for electricity, heat and cold [1]. These facilities are characterized by prolonged operation, 24 hours a day and 7 days a week, and predictable significantly high energy demand. This is the main reason the energy consumption od hospitals is on average 2.5 times larger than an average commercial building. This results in shorter investment payback time, with respect to other facilities, due to an almost constant energy usage [2].

Moreover, hospitals require the continuity of electric supply and the reliability in case of grid outage or hazardous weather conditions. Indeed, hospitals are regarded as critical infrastructures (CI). The CI are those networks, assets and facilities which, if it did not properly operate it would have a dramatic negative impact on the national security, economic or public health safety [16]. These requirements drive the choice of designers and managers toward the introduction of this kind of innovative solutions. The importance of on-site electricity generation as a safety alternative to the supply by external grid has been highlighted in recent years in the US. The combined heat and power (CHP) production systems are more independent from the external grid than conventional systems, which may suffer from disruptions or instabilities during severe weather conditions or technical accidents. For instance, in 2012 during the super storm Sandy, energy disruption led the Long Island South Oak Hospital Campus to operate its CHP system for more than two weeks, supplying the necessary electric and thermal power to the facility. The installation of a cogeneration or trigeneration system prevented the occurrence of the tragic scenario represented by the absence of electricity in a hospital.

Beyond reliability, economical savings also constitute an interesting motivation which increase the interest in cogeneration in hospitals. The economic advantages produced by cogeneration also bring interest for small facilities. In the past they were not interested in on-site energy production because of the relatively small size of their power demand. Changes in the market have been produced thanks to the smaller sizes of the equipment developed by manufacturers. Thanks to the efforts in research, cogeneration and trigeneration has become interesting applications for smaller facilities.

1.1 Current Status in the US

The existing CHP installations in US hospitals are 212 facilities, with an overall installed capacity of 756.6 [MW]. Looking at the overall market of energy usage, health care facilities account for more than the 9% of the energy use in commercial buildings in US and the 8% of the greenhouse gas emissions in the country. The current shares of installed power are shown in figure 1, there they are classified on the basis of the adopted prime mover. The installed sizes in this market typically range from 100 [kW] to 6 [MW] and the most common prime movers installed are reciprocating engines, followed by gas turbines [3]. Looking at further possibilities to expand this market, the potential generating capacity in US is about 6,411 [MW] and 10,6% of CHP market penetration resides in hospitals. Table I and figure 2 show the

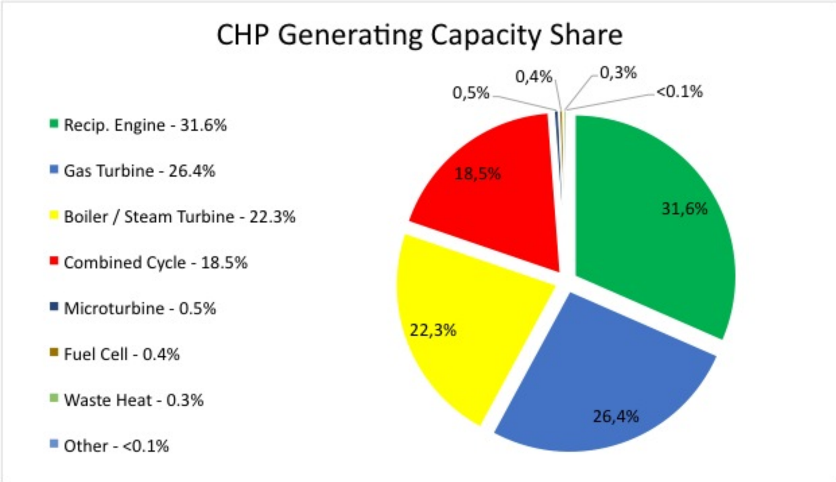

Figure 1: Shares of installed capacity for health care facilities by prime mover.

existing installations by region and provide information about the average installed sizes. In Table I is shown as a capacity of 104.4 [MW] is installed in the Midwest area, which is a result comparable to the other regions of US. Therefore the Chicago area, which is the area chosen as reference for weather condition and utilities rates estimation, has one of the highest technical potential, in particular concerning the installation of systems with a size ranging between 1 and 5 [MW] [4].

Key information have also been collected to obtain a background in this field and to analyze the possible effects on the economic balance of the facilities and to the environment. In US the health care organizations spend more than 6.5 billion dollars every year in order to manage their facilities and to better meet patients' needs. An European study focuses the attention on the possible effects on the economic balance of an hospital due to the installation of a

TABLE I: EXISTING INSTALLED CHP CAPACITY IN THE US.

Region	Sites	Capacity [MW]	Ave. Size [MW]
Mid-Atlantic	23	113.1	4.9
Midwest	36	104.4	2.9
Northeast	77	244.9	3.2
Northwest	0	0	0
Pacific	54	173.3	3.2
Southeast	13	46.9	3.6
Southwest	9	74	8.2
Total	212	756.6	3.6

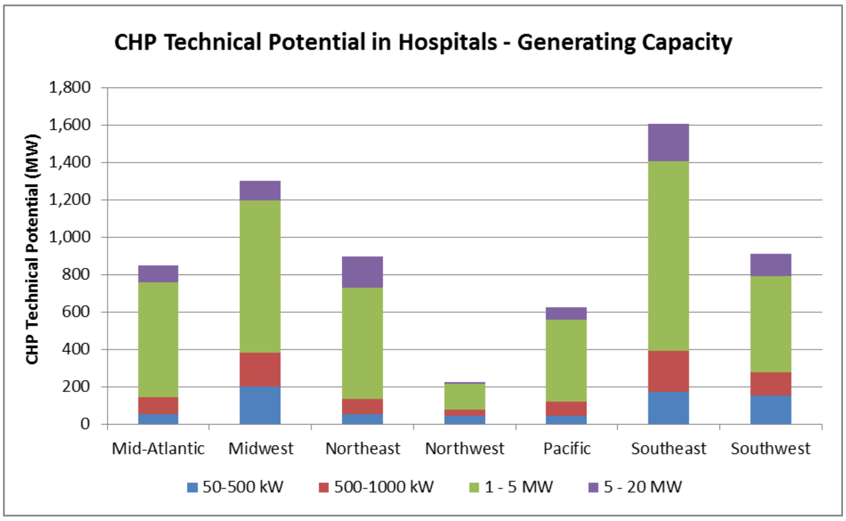

Figure 2: Technical potential in hospitals divided by generating capacity.

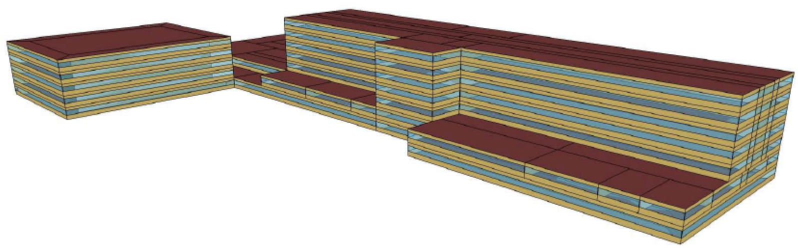

Figure 3: 3D rendering of the prototype hospital.

cogeneration system [5]. The study provides an estimation of the economic savings based on the number of patients which the hospital can accommodate. The costs reduction of energy supply is estimated to be between the 30% and 40%. For an European hospital, the absolute value of the savings is around 200,000 euro (220,000 2015 USD) for hospitals which have a capacity of 300 patients and up to 400,000 euro (440,000 2015 USD) for bigger hospitals which have around 500 patients.

1.2 The Hospital Prototype

In order to analyze the market sector of health care facilities, the study is conducted through the simulation of a single facility, which represents the average US hospital. A 3D render of the analyzed building is shown in figure 3. The model prototype for the hospital is the result of the implementation on eQuest® of the design addressed by the National Renewable Energy Laboratory (NREL). [7] [8]. The model implemented on eQuest® has been validated in previous works [4] and it has been further improved through the fix of some irregularities found through the analysis of the output records, in this study.

The guidelines for the definition of the prototype hospital are the result of US Department of Energy (DOE) support to the development of commercial building energy codes and standards. The Commercial Buildings Group at NREL developed the model of the hospital and its technical support document under the direction of the U.S. Department of Energy Building Technologies Program. The study was ment to document the analysis performed and the resulting design guidance that will enable to achieve energy savings of 50% over ASHRAE Standard 90.1-2004. This report also documents in detail the modeling methods used to demonstrate that the design recommendations meet or exceed the 50% energy savings goal. The NREL's codes are available on its website because of the will to promote the transparency of the NREL's actions in its support, and to promote the circulation and validation of its work through the public review and application of the developed products.

ASHRAE Standard 90.1 (Energy Standard for Buildings Except Low-Rise Residential Buildings) is a US standard providing the minimum accepted requirements for the design of energy efficient buildings. The analyzed building categories cover a wide range of buildings typologies although there are some exemption; as example the low-rise residential buildings are not taken into account by the standard. The first release of the ASHRAE Standard 90 was in 1975. Through the years many upgrades and review have been released and the ASHRAE is always spending effort to further improve the standard itself. Some of the noteworthy editions were released in 1999, when the standard on continuous maintenance was included. Since that moment, additional upgrades have been done in 2004, 2007, 2010, and 2013. The need for upgrades is the reflection on legislation of the changes produced by newer and more efficient technologies development.

The NREL contributes to DOE's support to ANSI/ASHRAE/IES Standard 90.1 through the application and the development of models of prototype buildings, which can approximately cover, according to NREL analysts estimation, the 80% of the commercial and residential building in the US. These prototype buildings are obtained by the analysis of reference building models produced by the DOE. According to the updates of ANSI/ASHRAE/IES Standard 90.1, NREL implement the revisions to the prototype building models. The prototype models include 16 commercial building types in 17 climate locations (across all of the eight US climate zones). The current combination results in an overall set of 1,088 building models developed through the years and available in the latest release of the documentation (EnergyPlus™ Version 8.0). Among all of the analyzed buildings also an health care facility has been studied.

Starting from the ASHRAE Standard 90.1 and NREL data, the implementation of the prototype hospital on eQuest® has been possible [7] [8]. From now on, the model prototype will be referred as *base model*, to distinguish it from other possible layout, e.g., the trigeneration or the cogeneration layout. These information can be summarized and classified according the following categories:

- building internal layout description;
- building shell description;
- internal loads;
- occupation and equipment schedules;

- lighting schedules;
- Heating, Ventilating and Air Conditioning information;
- Service Water Heating;

The model prototype has a total surface of 527,000 [ft^2] (49,000 [m^2]). This surface is divided in two main buildings: the hospital (427,000 [ft^2] divided into seven stories) and the medical office building (MOB) (100,000 [ft^2] divided into five stories). The maps of each floor are reported in appendix as developed in the previous works [4]. No fixed prescription were available on the fenestration surface, so the assumption of a 40% fraction of fenestration to gross wall area had been adopted. Concerning the structure of the building itself, the prototype accounts for a steel frame construction and an arrangement of the roof with insulation above deck.

Base model heating, ventilation, and air conditioning equipment consists of central air handling units, chillers, boilers, chilled and hot water air handling unit coils and terminal units with hot water reheat coils [7]. This information are strictly true for the base model only; the upgrade of the plant configuration through the realization of a cogeneration plant will bring to the installation of a heat recovery for the hot water production. Moreover, the further upgrade of the plant configuration through the realization of a trigeneration plant will also include the installation of an absorption chiller. Some of the presented features are summarized in Table II.

1.3 Model Improvement

The improvements made in this study to the *base model* are aimed to fix some errors produced by the direct implementation of the *base model* specifications on eQuest®. Analyzing

TABLE II: PROTOTYPE HOSPITAL LAYOUT MAIN INFORMATION.

Parameter	**Value**	
Total Floor Area	527,000 [ft^2]	48,960 [m^2]
Hospital floor area	427,000 [ft^2]	39,670 [m^2]
MOB floor area	100,000 [ft^2]	9,290 [m^2]
Floor-to-floor height	10 [ft]	3.05 [m]
Number of floors (Hospital)	7	
Number of floors (MOB)	5	

the detailed report produced by eQuest®, some issues rose by the analysis of the data provided by the thermostats of each space in the facility. For a considerable number of hours per year, some spaces of the facility resulted to be at a temperature lower than the design one. These issues are the result of the conflicts rising from the interaction of the thermal load with some default parameters in the eQuest® heating, ventilation and air conditioning (HVAC) properties.

The first modification produced consists in the adoption of a pre-heat coil in each of the variable air volume (VAV) HVAC systems, which are not provided in the default set up of the software. These components have to be manually introduced in the layout of the system. This choice ensure the proper operation of the system especially during winter months, when external air is introduced in the system at a temperature lower than the freezing point of water. This condition could cause damages to the cold deck coils because of the freezing of the water

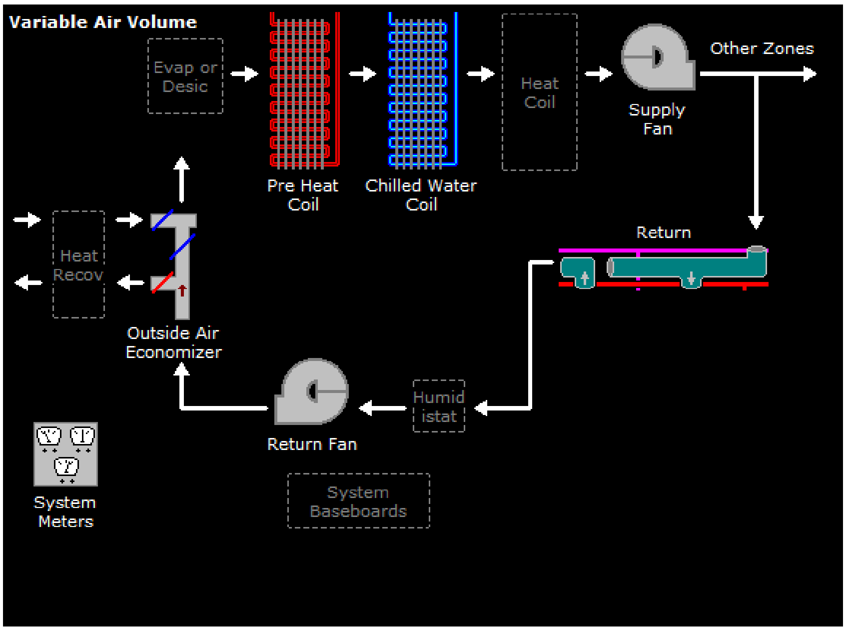

Figure 4: Layout of the VAV HVAC system - it does not include reheat coils.

contained inside it. In figure 4 the adopted layout for the HVAC system is shown through a screenshot of the eQuest® piece of software. The picture does not include the presence of the terminal units for hot water reheat.

An additional modification adopted for all the VAV systems in the facility deals with the coils technical specifications. The software's properties called *Reheat Delta T*, which represents the maximum increase in temperature for supply air passing through the reheat coils, has been increased from 30[F] to 50[F] [9]. These modifications ensure the possibility to satisfy the requirement about the inlet temperature of the supply air.

Unfortunately, additional simulations have shown how these changes are not sufficient to allow all of spaces to reach the design temperature, although fix the previously mentioned problems about the thermal needs for some of them. To better understand where those spaces are located inside the facility a schematic representation of the facility subdivision is reported in figure 5. A *space* represents one or more rooms characterized by the same desired thermal conditions and managed by the same VAV system; subdividing the facility in several spaces is necessary for the proper operation of the software [9]. The number of spaces is a function of the complexity of the thermal control strategy of the building itself. Because of this constrain the building has been divided according the following list of 9 different spaces:

- MOB - Medical office building, five stories building;
- PT - Patient Tower, five stories (from third to seventh floor);
- BLD3 - Building 3, two stories;
- BLD4 - Building 4, two stories;
- BLD5 - Building 5, one story;
- BLD6 - Building 6, two stories;
- BLD7 - Building 7, three stories;
- BLD8 - Building 8, one story;
- BLD9 - Building 9, two stories (located below the PT);

The further changes produced in this work to the *base model* are adopted for the spaces listed in Table III, which are those affected by the lack in heating power and causing the impossibility to reach the design temperature. The objective of the improvement is connected with the sizing ratio. The sizing ratio is a key parameter in eQuest®, it represents a multiplier of the program-calculated values of air flow rate and coil size. This key word is used to deliberately oversize or undersize the equipment in the system [9]. This value has been changed for all the listed spaces from the default value of 1 to the value of 1.15. Resulting in an oversizing of the 15% of the system. The final simulations performed show how the combined effects of the increase in the reheat temperature supported by the oversizing of some of the coils of the VAV systems can fix the errors in the previously developed model, ensuring the meeting of the design condition in all the spaces and thus the proper simulation of the thermal needs of the facility.

The modeling and analysis described in this section are used to develop the *base model* building. It provides a reference point for evaluating the energy needs of the facility and to evaluate the effectiveness of the energy efficiency improvements produced by the installation of cogeneration and trigeneration systems.

1.4 Energy Demand Profiles

The energy demand profiles of the prototype hospital have been determined through the simulation of its behavior on eQuest®. The energy demand profiles refer to the hourly heat demand and the hourly electricity demand profiles. Studying and collecting detailed information about the energy demand of the facility is the first step of any work meant to intervene in changing the layout of the energy supply. Post processing of the hourly results was done to obtain a chart where the value of the electric demand (expressed in [MW]) is reported for the 8760 hours of the year. This graph is shown in figure 6.

TABLE III: ZONES OF UNMATCHED TEMPERATURE.

Building	**Zone**	**Building**	**Zone**
PT	South Perim Zn (G.S1)	MOB	South Perim Zn (G.S1)
PT	East Perim Zn (G.E2)	MOB	East Perim Zn (G.E2)
PT	South Perim Zn (G.S3)	MOB	West Perim Zn (G.W4)
PT	East Perim Zn (G.E4)	MOB	South Perim Zn (M.S6)
PT	North Perim Zn (G.N5)	MOB	East Perim Zn (M.E7)
PT	North Perim Zn (G.N7)	MOB	North Perim Zn (M.N8)
PT	South Perim Zn (G.S9)	MOB	West Perim Zn (M.W9)
PT	South Perim Zn (M.S12)	MOB	South Perim Zn (T.S11)
PT	East Perim Zn (M.E13)	MOB	East Perim Zn (T.E12)
PT	South Perim Zn (M.S14)	MOB	North Perim Zn (T.N13)
PT	East Perim Zn (M.E15)	MOB	West Perim Zn (T.W14)
PT	North Perim Zn (M.N16)	MOB	Core Zn (T.C15)
PT	North Perim Zn (M.N17)	BLD4	South Perim Zn (G.S1)
PT	North Perim Zn (M.N18)	BLD4	East Perim Zn (G.E2)
PT	South Perim Zn (M.S20)	BLD4	West Perim Zn (G.W)
PT	South Perim Zn (T.S23)	BLD4	South Perim Zn (T.S6)
PT	East Perim Zn (T.E24)	BLD4	East Perim Zn (T.E7)
PT	South Perim Zn (T.S25)	BLD4	West Perim Zn (T.W9)
PT	East Perim Zn (T.E26)	BLD6	NE Perim Zn (G.NE1)
PT	North Perim Zn (T.N27)	BLD7	NNE Perim Zn (G.NNE2)
PT	North Perim Zn (T.N28)	BLD9	South Perim Zn (G.S1)
PT	North Perim Zn (T.N29)	BLD9	East Perim Zn (G.E4)
PT	West Perim Zn (T.W30)	BLD9	North Perim Zn (G.N5)
PT	South Perim Zn (T.S31)	BLD9	South Perim Zn (T.S12))
PT	West Perim Zn (T.W32)	BLD9	North Perim Zn (T.N16)
PT	Core Zn (T.C33)		

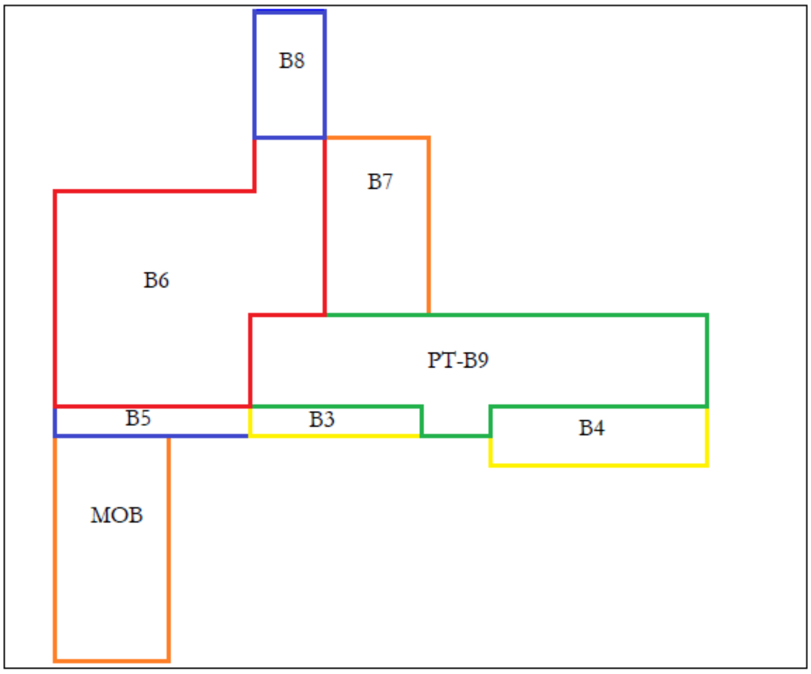

Figure 5: Scheme of the spaces inside the facility.

The same approach has been applied for the analysis of the thermal demand. The analysis of the thermal demand has been approached analyzing the fuel consumption (figure 8) of the facility, rather then just the values of thermal needs. The thermal needs are those necessary for producing hot water both for the heating system and the domestic water system. connected to the hot water demand (figure 7). The fuel demand takes into account not only the thermal demand due to domestic hot water and hot water for space heatings purposes, but also the amount of fuel required by other equipment inside the facility, such as the kitchen or the laundry. Moreover, analyzing the fuel demand rather than the heat demand, the analysis also

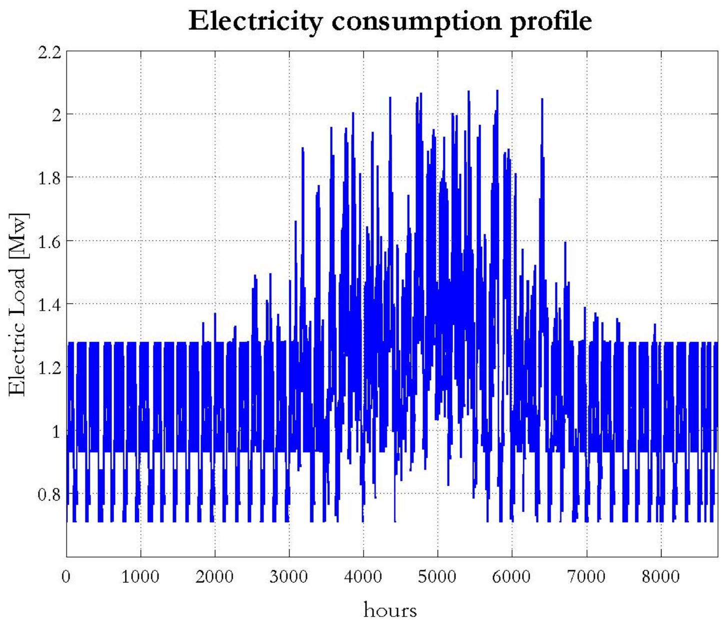

Figure 6: Electric demand profile throughout the year.

take into account the efficiency of the conversion system (e.g., the efficiency of the boilers). In this way it is provided a more general description of the needs of the facility. The entirety of this approach lies in the fact that the heat demand (excluding the fuel needs by kitchen and laundry) is a constant value, which is not affected by how the heat is produced. On the other hand, the fuel demand is strictly connected not only to the heat demand, but also to the efficiency of the employed equipments. Comparing the fuel demand profiles of different solution, provides information on how the primary source consumption is affected by switching from a technical solution to another one.

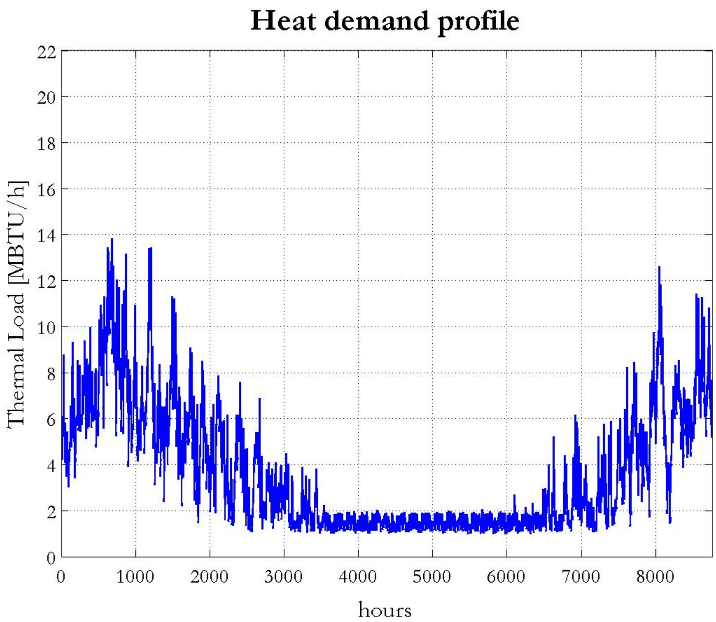

Figure 7: Heat demand profile throughout the year.

Analyzing figure 6 the main feature, other than the daily fluctuation of the electric load due to the recurring occupation of the structure and the recurring usage of electric equipment, is the increase in the electric needs during summer. The steep raise in the electric demand is connected to the cooling demand by the HVAC system. In the *base model* this demand is satisfied using electric industrial chillers to produce chilled water and feeding the cold coils of the system.

The fuel demand profile depicted in figure 7 shows the same cycling behavior of the electric demand profile; the reasons of this behavior are basically the same of the previous case. An opposed behavior of the average value of the fuel demand is highlighted by the comparison

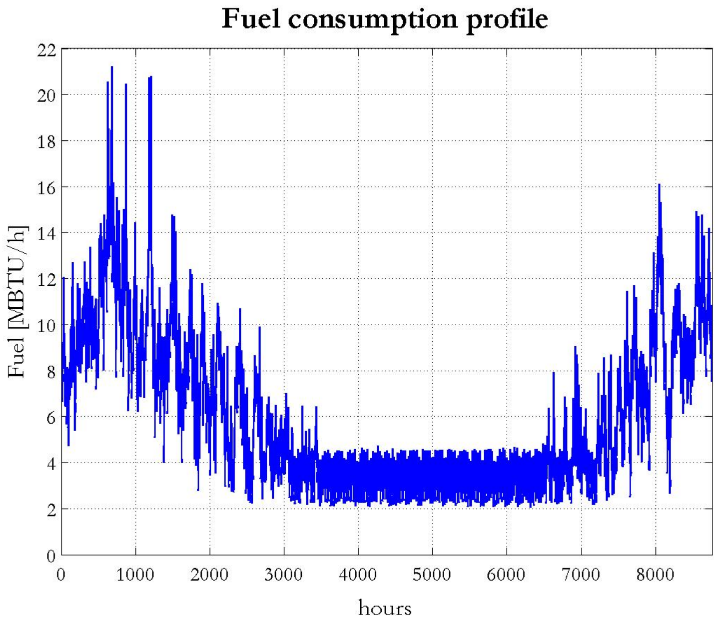

Figure 8: Fuel demand profile throughout the year.

with the electric demand. While the electric demand reaches the highest value of the year in summer months, the fuel demand reaches its maximum during winter. Obviously this is connected to the thermal request of the heating system which works at full load only during winter months. On the other hand during summer months the heat request, and thus the fuel request, is substantially reduced being due just to the domestic hot water demand, to the heat request by the re heat coils of the HVAC system and to the kitchen's demand. During this period the fuel request is sufficiently steady (neglecting the daily fluctuations).

The presented graphs provide a detailed representation of the load throughout the year, however they are not the best way to present the information needed to analyze the energy

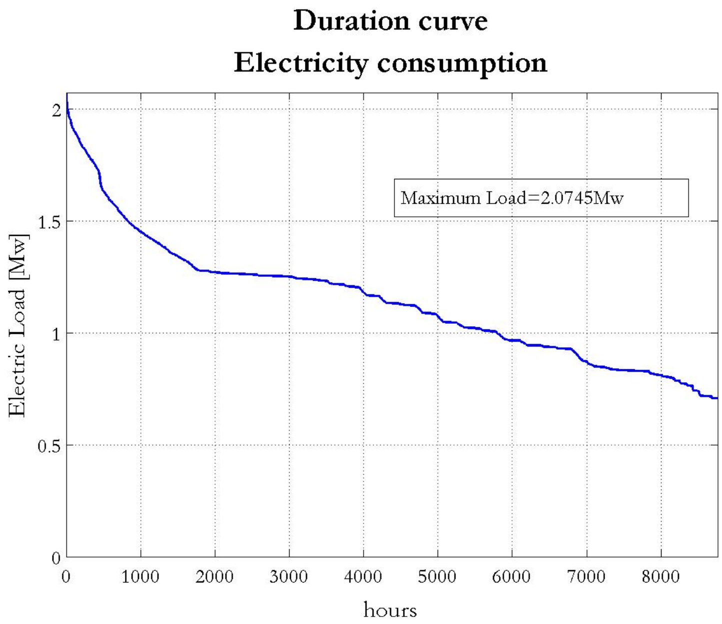

Figure 9: Electric duration curve.

demand and to size the equipments of the cogeneration or trigeneration system. For this purpose, duration curves can better provide important information about the analyzed facility. A load duration curve illustrates the time duration of the magnitudes of a load. On the y-axis the magnitude of the load is reported. On the x-axis the number of hours for which that load persist is reported. Using this approach, the duration curve is always a decreasing curve, used to represent the maximum number of hours in which a load equal or higher than the analyzed one occurs. Duration curves refer to a specific period of time, thus it is possible to find graphs on a daily base or, for example, on an annual base. The results obtained for the analyzed health care facility are shown in figure 9 and figure 10.

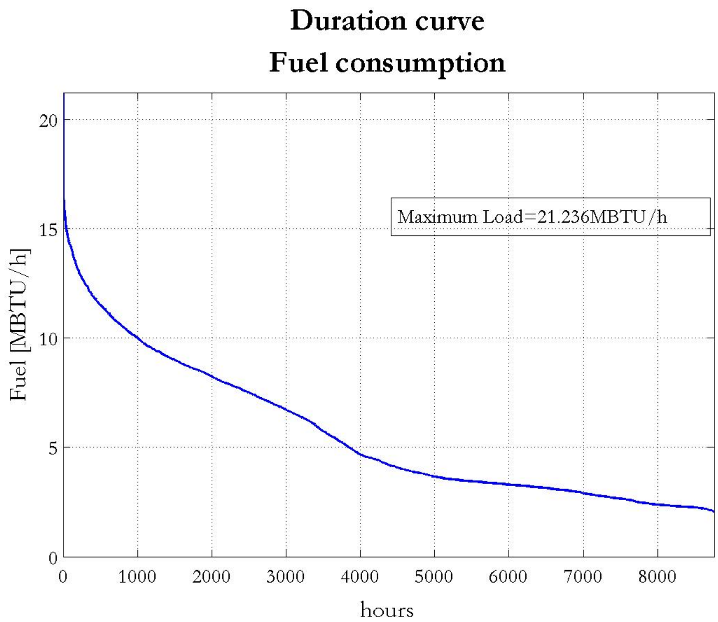

Figure 10: Fuel duration curve.

Looking at the electric duration curve it is possible to estimate the number of hours at which a prime mover will work at full load if installed in the facility. Looking at the chosen size of the prime mover, it is possible to determine the full load hours for that equipment by reading the intersection of the curve with that value. Because of the decreasing shape of the curve, rising up the size of the proposed prime mover, a reduction of the full load hours occur, increasing the number of hours at which the equipment works in partial load condition (or partial load ratio, PLR). In the opposite way, reducing the size of the installed equipment, it is possible to size a component working at full load and in steady state condition for a number of hour larger than the previous case.

CHAPTER 2

GAS TURBINE

2.1 General Introduction

The birth of this technology hails from the beginning of the twentieth century: however, gas turbines began to be employed for electricity generation purposes at the end of 1930s. The successful results achieved in power generation field have brought this technology in the last twenty years to become a popular choice for new plant installations in the US. Nowadays, gas turbines are fabricated in sizes ranging from 500 [kW] to more than 300 [MW]. The future of this technology is moving toward the realization of smaller sizes, down to 25 [kW]; these emerging sizes are regarded as micro turbines [10].

Gas turbines represent a common solution in power-only generation or a key element of more sophisticated layouts. As an example, a layout including a heat recovery system, which allows the combined heat and power (CHP) generation. In the previous decades, this kind of equipment has been extensively used by energy producers to satisfy the power demand peaks. More recently, the evolution of power generation industry and the developments of technology, caused the launch of gas turbines in the electricity production for base-load electrical power. Nowadays combined cycle gas turbines (CCGT) play an important role in satisfying the electric base-load of the country. At the same time, single gas turbines (without cogeneration) are frequently used to satisfy peak-loads. Recent data prove that gas turbines represent the 32%, 315 [GW], of the overall power plant capacity in the US. Moreover gas turbines represent 62%, 51.5 [GW], of the overall operating CHP capacity. Among the previously mentioned CHP capacity, large CCGT constitute the 80% of the total. Thanks to efficiencies higher than those of other technologies, large CCGT plants maximize the power production delivered to the electrical grid. From the 80s onward, the efficiency and reliability of such equipment (ranging in sizes from 1 up to 50 [MW]) have reached high enough standards to let small gas turbines become an attractive opportunity for industrial and small users, usually for CHP applications [10].

One of the key factors, which has increased gas turbine popularity across the market, especially for CHP purposes, is connected to the relatively high quality of the exhausts produced by this prime mover. The quality of exhaust gas is connected to the temperature at which they are produced and to the amount of corrosive and heavy substances within it.

A gas turbine, and in general any kind of prime mover, can be installed into different frameworks. The prime mover is regarded to be in simple cycle operation if the only output is the produced electricity. Another possible layout is the combined heat and power (CHP) configuration. This definition is used when the thermal energy content of gas exhaust is directly used in another application. For instance, a prime mover producing electricity and simultaneously employing the exhaust gas in a direct heating process (or producing steam / hot water in a device such as a HRSG) is defined as an example of CHP application. On the other hand, if the plant employs the exhaust gas to feed a HRSG producing steam, which is in a later stage used to feed a steam turbine, the system is considered to be a combined cycle unit. In this case, there is no direct thermal use of the recovered heat and the system is no longer considered to be CHP. This different application is regarded as a waste heat to power (WHP) system.

Nowadays in the market gas turbines are considered to be among the cleanest (non-renewable) ways of producing electricity, with reduced emissions of oxides of nitrogen (NO_X). This important result is obtained through the operation of catalytic exhaust cleanup processes and also through the installation of lean premixed combustors (usually referred to as dry low-NO_X combustors). Furthermore because of the quite high efficiency achieved and the common usage of clean fuels, e.g., natural gas, which is one of the cleanest fuels available for industrial energy production, gas turbines produce less carbon dioxide (CO_2) than any other fossil technology available on the market (the comparison is based on a fixed amount of produced energy adopted as yardstick).

Huge differences in the performances of the gas turbines are found according to the main purpose of the equipment itself. Emergency power units usually show lower efficiency but also reduced investment cost than other turbines intended as prime movers, with high annual capacity factors, which reveal larger efficiency values and investment costs.

The number of working hours per year of gas turbines represents a strong point for this technology; manufacturers data proved that gas turbines can be reliable power generators. Typical value of time between subsequent maintenance operations ranges between 25,000 and 50,000 hours. This feature represents a key factor in the choice of an equipment meant to satisfy a base-load, thus an equipment meant to work without interruption for most of the year. The importance of continuous operation, and thus the reliability of the prime mover, is highlighted when the electric load is a facility whose operation interruption could be fatal.

The on-site power generation, which represents just one of the several fields of application for this technology, is the main topic of this analysis. On-site power generation is the situation that occurs when the equipment works to provide energy to a single specific load, without any connection to the external electric grid for the distribution of the produced electricity. In this field, the choice of a gas turbine usually aims to realize a CHP system; this target is pursued by recovering the energy in the turbine exhaust gas through a heat exchanger and delivering it directly to the final user. Examples of CHP installations include: chemical products production plant, paper production factory, food processing industry, and all those big public buildings where the electric and thermal demand are strictly connected, such as university campuses and hospitals. An example of CHP application is a university campus where a 5 [MW] gas turbine is installed. From its exhaust gas, it is possible to recover enough heat to produce around 8 [MW] of hot water. The hot water is then pumped into the hot water loop. This loop can feed the domestic hot water needs or the space heating system during the heating season or also provide the thermal power needed to run an absorption chillers, which is adopted to satisfy chilled water needs during summer season(trigeneration application) [10].

2.2 Performance Analysis

The reference thermodynamic cycle for a gas turbine is the Joule-Brayton cycle. The Joule-Brayton cycle is actually performed using a compressor, a combustion chamber, and an expansion turbine. The expansion turbine as seen in figure 11 is divided into two elements. The first one is the gas producer, here the mechanical power output drives the compressor. The second one is the power turbine, whose power production drives the electric generator.

The compressor works by increasing the external air pressure to the feeding pressure of the combustion chamber. The external air temperature is then raised up by the combustion process occurring in the combustion chamber. The last step occurs in the expansion turbine, where the expansion work of the exhaust gases is transformed into shaft work. The produced shaft work is necessary to move the electric generator and to drive the compressor at the same time.

Today, several variations of the Joule-Brayton cycle exist, each aiming to efficiency improvement. For example, the fuel consumption can be reduced and the efficiency can be improved by preheating the outlet air form the compressor using recovered heat from the expansion turbine exhaust gas; this process is carried out by using a regenerative heat exchanger. Another strategy to increase the efficiency of the gas turbine is achieved by reducing the work required by the compressor. The amount of work required by a compressor is directly proportional to the density of the air at the compressor inlet. This amount of work can be reduced, and thus the net power of the gas turbine can be increased, by using intercooling strategies in a multistage compressor or pre-cooling the inlet gas.

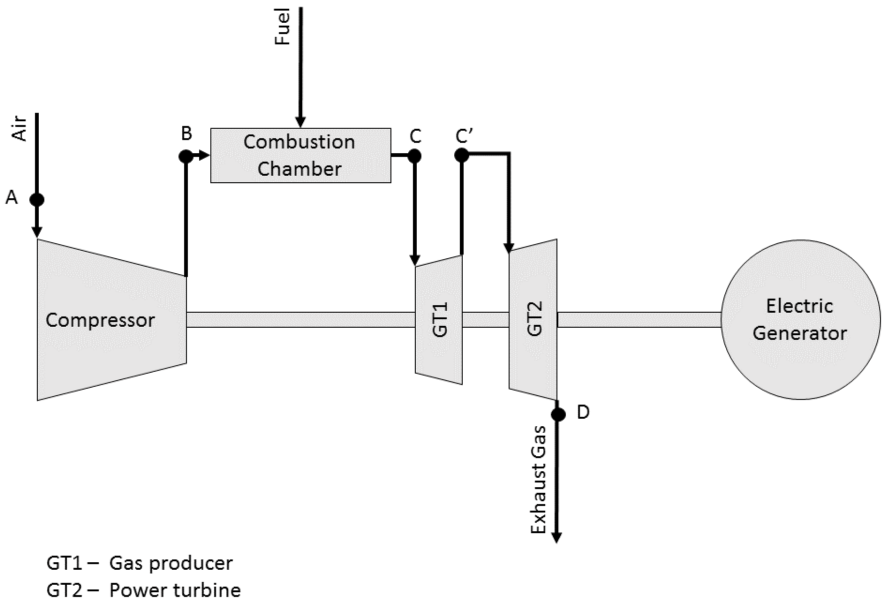

Figure 11: Gas turbine scheme.

Analyzing the ideal thermodynamic cycle shown in figure 12, the calculated efficiency of the thermodynamic cycle is expressed using Equation 2.1

$$\eta = 1 - \frac{T_D}{T_C} = 1 - \frac{1}{\rho^{\frac{\gamma-1}{\gamma}}} \tag{2.1}$$

- η Overall efficiency of the equipment;
- T_D Outlet temperature of the exhaust from the power producer section of the gas turbine;
- T_C Inlet temperature of the exhaust in the gas generator section of the gas turbine;
- ρ Pressure ratio of the turbine $\rho = \dfrac{p_C}{p_D}$;

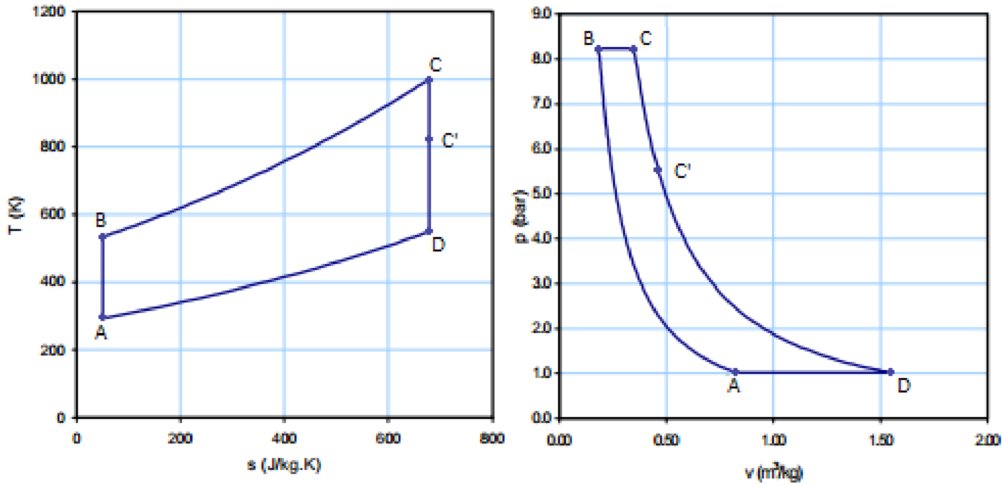

Figure 12: Joule-Brayton thermodynamic cycle.

- γ Air specific heat ratio.

Looking at Equation 2.1, a direct dependence between efficiency and the increase of the temperature T_C is shown. T_C represents the absolute temperature of the exhaust gas at the inlet of the gas producer section of the gas turbine. Consequently, it is obvious that one of the main challenges in increasing the performance of these devices have been connected to the need of operating the turbine at the highest practical temperature. The main constraints are connected to the performance of the blade materials, which have to be adequate to tolerate the high temperatures. Increasing both the gas temperature at the gas producer inlet and the pressure ratio of the equipment, it is possible to improve the efficiency. Thus, the trend adopted by manufacturers in enhancing performance has been in the direction of increasing both temperatures and pressures.

Another important information can be obtained analyzing Equation 2.1. Gas turbines off-design operation, and thus power output management, is obtained by reducing the amount of fuel burnt in the combustion chamber. This management strategy has a direct consequence on the inlet temperature of gases in the expansion turbine and thus on the values of efficiency achievable during partial load operation. This information will represent an important factor choosing the turbine size during the design phase of the energy production plant. Oversizing the gas turbine will produce undesired economic effects if this choice implies the need to run the equipment at partial load for a considerable number of hours per year.

2.3 Partial Load Performance

Gas turbines are usually designed to allow the user to control the output power. This goal is obtained by changing the amount of fuel burnt in the combustion chamber of the gas turbine (heat provided in the process from point B to point C in figure 12). Reducing the fuel consumption causes a reduction of the temperature of the inlet gas in the expansion turbine. The amount of work produced by the expansion section of the gas turbine is directly proportional to the inlet temperature of the gas in the component (T_C). Under the simplifying assumption of an ideal machinery, the expression of the output power produced by the gas turbine is presented in Equation 2.2 (the adopted notation refers to figure 12):

$$P = (G_a + G_f) \cdot l_t - G_a \cdot l_c = \tag{2.2}$$

$$P = (G_a + G_f) \cdot c_p \cdot (T_C - T_D) - G_a \cdot c_p \cdot (T_B - T_A) = \tag{2.3}$$

$$= (G_a + G_f) \cdot c_p \cdot T_C \cdot \left(1 - \frac{T_D}{T_C}\right) - G_a \cdot c_p \cdot T_A \cdot \left(\frac{T_B}{T_A} - 1\right) = \tag{2.4}$$

$$= (G_a + G_f) \cdot c_p \cdot T_C \cdot \left(1 - \left(\frac{p_C}{p_D}\right)^{\frac{1-\gamma}{\gamma}}\right) - G_a \cdot c_p \cdot T_A \cdot \left(\left(\frac{p_B}{p_A}\right)^{\frac{\gamma-1}{\gamma}} - 1\right) = \tag{2.5}$$

$$= (G_a + G_f) \cdot c_p \cdot T_C \cdot \left(1 - (\beta_t)^{\frac{1-\gamma}{\gamma}}\right) - G_a \cdot c_p \cdot T_A \cdot \left((\beta_c)^{\frac{\gamma-1}{\gamma}} - 1\right) = \tag{2.6}$$

$$= (G_a \cdot c_p) \cdot \left(\left(\frac{1+\alpha}{\alpha}\right) T_C \cdot \left(1 - (\beta_t)^{\frac{1-\gamma}{\gamma}}\right) - T_A \cdot \left((\beta_c)^{\frac{\gamma-1}{\gamma}} - 1\right)\right) = \tag{2.7}$$

- P Power output from the gas turbine;
- l_t Work produced by the gas turbine;
- l_c Work required by the compressor;
- G_a Air mass flow rate;
- G_f Fuel mass flow rate;
- c_p Constant pressure specific heat;
- β_t Pressure ratio of the turbine $\beta_t = \frac{p_C}{p_D}$;
- β_c Pressure ratio of the compressor $\beta_c = \frac{p_B}{p_A}$;
- γ Air specific heat ratio;
- α Air to fuel ratio $\alpha = \frac{G_a}{G_f}$;

Unfortunately, the change in the inlet temperature of the exhaust gas in the expansion turbine has also the undesired consequence to reduce the efficiency of the whole equipment.

Moreover, in order to take into account also environmental issues, the amount of pollutants emitted by the gas turbine is generally increased at part load conditions. The effect is stronger when the partial load ratio (PLR), which is the ratio between the produced power to the design one, approaches half of the load and below.

2.4 Improved Gas Turbine Model

eQuest® requires a model to describe the behavior of the gas turbine and to properly define the power output and the fuel consumption of the equipment during its operation in the framework of the cogeneration plant. As example, among the most important required information there is the relation existing between the partial load ratio at which the gas turbine is working and the efficiency corresponding to that condition. In this analysis an improved model has been developed starting by the technical information provided by SOLAR® [11][12]. The need to produce a new model starting by the information provided by the manufacturer is due to the obsolescence of the default model provided by the eQuest®.

2.4.1 PLR Effects

The new proposed model is developed from the information about the SOLAR® turbine named Taurus 60™. This model has been choosen although the size of this turbine is of about 5 [MW], which is larger than the gas turbine's average size suitable for the health care facility. Taurus 60™ has been adopted rather than the smaller size model by SOLAR®, named Saturn 20™. The Saturn 20™ has a size of about 1 [MW], which could better meet the needs of the hospital; however, this is a really obsolete model whose performance is far from the latest model produced by the manufacturers.

In figure 13 the performance curves of the eQuest® model and of the new improved model are depicted. At full load condition the improved model approaches efficiency of around the 30% while the eQuest® model is below the 20%. Moreover, at partial load operation the eQuest® model shows a steeper reduction of performance than the improved model. The improved model has been developed starting from the techinal sheets provided by SOLAR®. Some points have been retrived from the curves in the technical sheets, after that, through an interpolation process, a new quadratic relationship was developed to replace the default one on eQuest®. The range for PLR is from 10% to 100%; the lower limit is the result of manufacturer's prescription about the minimum required power output to safely operate the equipment. The obtained expression is Equation 2.8, which replaces Equation 2.9 in eQuest®.

$$\eta_{SOLAR} = 2.61E - 3x^2 + 0.464x + 8.52 \tag{2.8}$$

$$\eta_{eQuest} = 2.98E - 4x^2 + 7.56E - 2x + 8.42 \tag{2.9}$$

2.4.2 External Temperature Effects

To better describe the behavior of the gas turbine, the eQuest® software requires also a model describing the relation occurring between the external air temperature and the performance of the equipment. The external conditions, both in terms of pressure and temperature, associated to the operation of a gas turbine have a strong influence on the produced power and also on the overall efficiency. Because of the fixed installation of the equipment this study

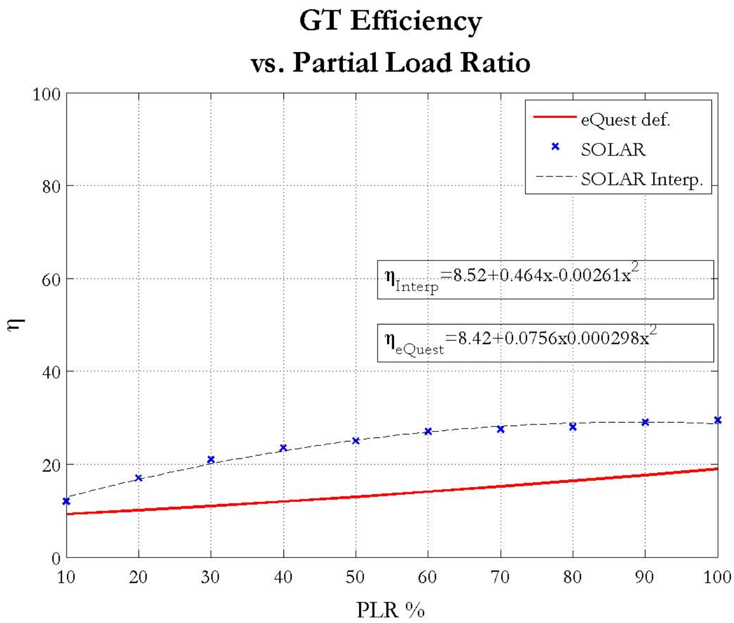

Figure 13: GT performance curve for eQuest® model and improved model.

does not deal with the effect of atmospheric pressure on performance. When an increase in the inlet air temperature occurs, both the produced power and the efficiency of the equipment are negatively affected. The causes of this reduced performance are linked with two main factors. The first factor is the reduction of the gas mass flow rate through the equipment (this occurs because the density of air decrease when its temperature increases). The second underlying factor for the efficiency drop is the increase of work per air mass unit required by the compressor. For a fixed pressure ratio of the compressor, the work required is proportional to the inlet air temperature. Looking at Equation 2.7, it is possible to understand how increasing T_A, the net power output (P) decreases.

These effects have led through the years to the need to establish fixed and widely accepted reference conditions to evaluate gas turbine performances. The reference condition fixed by the International Organization for Standards (ISO) consists of an outdoor pressure equal to the pressure at the sea level (101.325 [Pa]) and an ambient temperature equal to 59 [F] [13]. As an example of the correlation provided by the manufacturer, when the external temperature reaches 100 [F], power output can be reduced to 90% of the power output estimated following the ISO standard. On the other hand, by reducing the inlet temperature to about 50 [F], the net power output rises up to 105% of the power output estimated following the ISO standard. The comparison between the eQuest® default model and the SOLAR® based model [11][12] has been carried out in terms of the analysis of the air temperature effect on the equipment performance. The results are shown in figure 14. The trend of the eQuest® model is steeper than the improved model, this represents a more marked sensitivity to the changes of ambient conditions. The related equations are: Equation 2.10 for the new model and Equation 2.11 for the eQuest® model.

$$\eta\%_{SOLAR} = -0.24x + 114.6 \tag{2.10}$$

$$\eta\%_{eQuest} = -0.41x + 124 \tag{2.11}$$

The obtained information about the SOLAR® turbine and the production of the new model will produce an improvement in the quality of the analysis conducted on eQuest®. The updates made to the default equipment's performance provides the basis for the realization of analysis able to accurately reproduce the case studied.

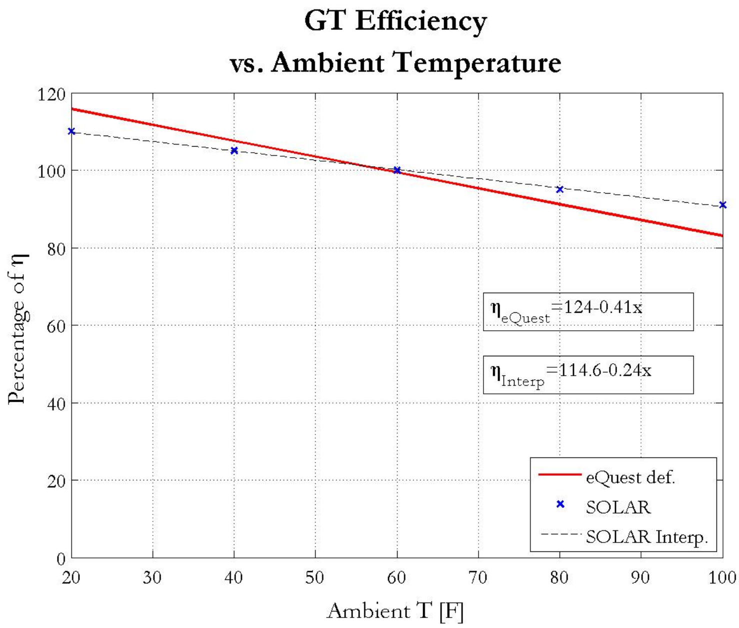

Figure 14: Effects of the external air temperature on efficiency.

2.5 Economic Information

The presented analysis focuses on the estimation of the costs for the realization of a CHP system and also attempts to estimate the costs for its safe operation. A general knowledge of the elements constituting the system is required to be able to analyze them.

A simple gas turbine system is constituted by several components. The basic elements are the gas turbine itself, the gearbox, the electric generator, the ducting, and all the other auxiliary systems such as: lubrication and cooling systems, inlet air filtration, starting system, and exhaust silencing [10]. Starting from data provided in the *ICF*'s report for several types of gas turbines, throughout some simplifying assumptions about the layout of the system, the costs for the realization of different sizes plants have been determined and summarized in Table IV. The collected data refer to five different systems of different sizes. The analyzed gas turbine are:

- SOLAR® Saturn 20™;
- SOLAR® Taurus 60™;
- SOLAR® Mars 100™;
- General Electric® LM2500™;
- General Electric® LM6000™;

TABLE IV: TURBINES TECHNICAL FEATURES.

	Saturn 20	**Taurus 60**	**Mars 100**	**LM2500**	**LM6000**
Nominal capacity [kW]	1,000	5,000	10,000	25,000	40,000
Actual capacity [kW]	1,150	5,460	10,240	23,330	46,560
Electrical Efficiency	21.3%	27.7%	28.4%	34.3%	37.0%
Total CHP Efficiency	66.3%	69.8%	68.4%	70.7%	72.1%
Power/Heat Ratio	0.47	0.66	0.71	0.94	1.06

2.5.1 Investment Costs

The economic data presented in Table V represent an approximated assessment of the real plant realization, which are strongly influenced by the installation region, market competitiveness , special requirements connected to the installation site and to emissions reduction policies.

The costs estimates refer to plant layouts providing pollutants control thanks to a selective catalytic reduction (SCR) system; moreover the costs take into account the installation of an heat recovery system, a water treatment system and basic utility interconnection (required when the utility is not an off-grid utility).

2.5.2 O & M Costs

The initial investment cost of the plant is just a part of the whole expenses connected to the operation of a gas turbine. The complete cost analysis has also to take into account the variable costs connected to the normal operation of the system and its maintenance. The fuel cost estimation is part of chapter 3. With regards to operations and maintenance (O & M), costs evaluation is based on gas turbine manufacturer estimates for service contracts, which have been collected in *ICF*'s report [10].For the sake of better clarity about costs estimates composition, it is expedient to classify the maintenance in two main categories:

- Routine inspections;
- Scheduled overhauls;

Routine maintenance operations are those performed both while the equipment is working and when a scheduled stop is required. Those belonging to the first category are: the daily data acquisition, performances measurement, fuel consumption monitoring and vibration analysis. Daily system maintenance takes into account visual inspection by the maintenance staff of filters and general site conditions.

Most of the activities connected to the stop of the equipment are instead constituted by predictive maintenance procedures. They are usually performed every 4,000 hours to guarantee

TABLE V: DETAILED GAS TURBINE PLANT COSTS IN THOUSANDS OF USD.

	Saturn 20	Taurus 60	Mars 100	LM2500+	LM6000PD
Nominal capacity [kW]	1,000	5,000	10,000	25,000	40,000
Actual capacity [kW]	1,150	5,457	10,239	23,328	46,556
Combustion turbine	1,015	2,733	6,102	12,750	23,700
Electrical	411	540	653	1,040	1,575
Fuel system	166	177	188	251	358
Water treatment system	74	180	293	370	416
Heat recovery	508	615	779	1,030	1,241
Total equipment	2,173	4,246	8,015	15,440	27,290
Construction	769	1,402	2,568	4,947	8,744
Total Process Capital	2,942	5,648	10,583	20,387	36,034
Project/Construction Management	271	402	664	1,279	2,260
Shipping	47	89	164	317	559
Development Fees	217	425	802	1,544	2,729
Project Contingency	116	177	276	532	940
Project Financing	230	431	799	1,540	2,721
Total Plant Cost	3,822	7,172	13,288	25,598	45,243
Total Plant Cost per net kW ($)	3,324	1,314	1,298	1,097	972

the proper operation of the turbine. Great attention is given to the presence of dramatic vibrations caused by excessively worn bearings and ruined blades. Moreover, the maintenance actions also include exhaust gas chemical analysis and non destructive components testing to ensure the functionality of some critical components.

Scheduled overhauls for a gas turbine are performed every 25,000 to 50,000 hours depending on the features of each installation. They usually include the complete inspection, substitution or rebuild of components. These actions are required for restoring the gas turbine performance to installation conditions. The most important actions performed during a scheduled overhaul are dimensional inspections of worn components, components upgrade following manufacturer release, testing turbine and compressor functionality, rotor disassembling, bearings, blades and clearances inspection.

All these actions have costs depending on how severe the maintenance actions are. Plant maintenance actions change substantially depending on the quality standards of the adopted programs. Another factor affecting the required actions is connected to the operating conditions. For example, operating a gas turbine for long periods over the nominal capacity will markedly increase the number of stops for maintenance. Maintenance costs are summarized in Table VI for all the analyzed sizes of gas turbine. The source of the data presented is the *ICF* report [10].

Information on proper operating conditions have to be tracked in order to keep the availability of the system as high as possible. Indeed, the proper sizing of the gas turbine with respect to the load of the facility can ensure the best operating condition for the system, avoiding

TABLE VI: COSTS SUMMARY OF MAINTENANCE ACTIONS.

	Saturn 20	**Taurus 60**	**Mars 100**	**LM2500+**	**LM6000PD**
Electric Capacity [kW]	1,000	5,000	10,000	25,000	40,000
Variable [$/kWh]	0.006	0.006	0.006	0.004	0.0035
Fixed [$/kW-yr]	40	10	7.5	6	5
Fixed [$/kWh] (8,000 hrs/yr)	0.005	0.0013	0.0009	0.0008	0.0006
Total O&M Costs [$/kWh]	0.0111	0.0074	0.007	0.0049	0.0042

undesired or too frequent maintenance actions. Numerous operational conditions have direct repercussions on the failure rate of the components constituting the gas turbine. Frequent starts and stops produce heavy damages due to thermal cycling, resulting in higher rate of mechanical failure than gas turbines working at constant load condition.

Choosing unclean fuels for feeding the combustor, especially those rich of impurities (i.e. alkali, sulfur, and ash), causes the increase of the radiative heat transfer to the combustor walls, thus overheating the combustor chamber. This phenomenon is more marked for heavy fuels than for clean gaseous fuels. The opposite situation of discontinuous operation with heavy fuels, is the constant load condition, burning fuels with a reduced content of impurities. The latter situation lets gas turbines operating for a year without need for shutdown. The availability of a gas turbines properly working (i.e. without marked and frequent power cycles) burning clean gaseous fuels, such as natural gas, is estimated to be higher than 95% [14].

This information is a crucial one. Although the hospital is connected to the electrical grid, thus shut down of the prime mover will not result in a dramatic interruption of energy resources for the facility, the availability of the gas turbine is a key factor when the opposite situation occurs. The purpose of cogeneration is not only economical savings but also ensuring a reliable source of energy. A gas turbine prime mover characterized by such high availability and reliability is undoubtedly a trusted choice.

CHAPTER 3

COGENERATION

This chapter is meant as an intermediate step in the process of analysis of the energy needs of the health care facility and of CHP to satisfy them. Before defining of the layout of a trigeneration system, a cogeneration layout is analyzed to show the fuel and economic savings of this simpler system. Cogeneration allows the simultaneous production of heat and electricity by the same source. Through the years, the positive effects of cogeneration have been extensively proven and it represents a valuable alternative to the separate production of heat and electricity. The scaling of this technology constitutes the frontier of improvements in this field. Although its efficiency and economic advantages have been proved for big facilities, new attempts are made to reduce the size of the plants, moving toward the smaller cogeneration systems is challenging.

3.1 Description of the Technology

Combined heat and power (CHP) technology comprises a group of reliable and profitable systems which play a role in the world production of heat and electricity. Thanks to the improved efficiency of the energy production and to the improved exploitation of the fuel's energy content, CHP is part of the energy efficiency policies and green house gases (GHG) emissions reductions strategies. The best results are usually obtained by the coupling with other efficient ways to use energy, such as district heating systems. Most of the studies conducted all around the world confirm the benefits produced by CHP and suggest to increase the efforts made to achieve new technology advancements in this field toward a less polluting and more efficient way to satisfy the always increasing energy demand. Some of the well known features about CHP, resulting from all of the studies conducted in this field are summarized in a study published by the International Energy Agency (IEA) in 2008 [15], are here reported:

- CHP can produce positive effects on the CO_2 emissions. The estimated reduction by 2030 is more than 10% (950 [Mt/year]) of the overall annual CO_2 emission in 2008. Thus, CHP can have a marked effect on the reduction of emissions of pollutants required to avoid future major climate changes;
- Through on-site electricity production, reduction in the needs of distribution grids improvements could be expected, followed by the reduction of the linked investments. Valuations show how an increased use of CHP could cause a reduction of power sector investments by 795 billion USD over the next 20 years (2008 data);
- If the energy savings and investment costs benefits achieved through CHP installation will be addressed to increase its electricity production, the estimated growth in CHP market can produce a reduction of the delivering costs of electricity to the final users;

The possibility to recover the thermal energy content in the exhaust gas of a prime mover represents a crucial factor to preserve the economic benefits of the examined application. Dealing with gas turbines, the great thermal energy content of its exhaust gas, which generally represents from 60 to 80% of the energy content of the burned fuel, constitutes a valuable re-

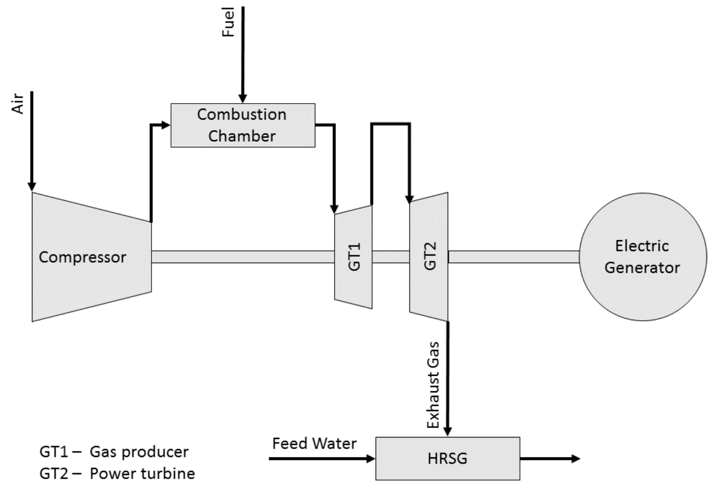

Figure 15: Layout of a cogeneration plant.

source in terms of energy savings. The most widespread way to exploit this recovered energy is the steam generation in unfired or supplementary fired HRSG. Moreover, the gas turbine exhaust gas are also commonly used as a source of direct process energy for unfired or supplementary fired process fluid heaters (hot water production), see figure 15.

For the sake of better clarity a detailed definition of all the energy fluxes across the CHP plant is required. For this purpose a scheme of the plant and of the fluxes is reported in figure 16. The fuel's energy content is partially transformed by the prime mover in mechanical energy and then in electricity through an electric generator. The unexploited energy content is lost as heat. Part of this heat represent an unrecoverable loss, in this analysis this energy flux is regarded as *Wasted Heat*. The *Wasted Heat* is contitued by all the thermal losses through the prime mover and the heat recovery system. The other amount of heat can be potentially recovered and efficiently exploited, as example the energy content of the exhaust gas of a prime mover. This heat flux is called *Recoverable Heat*.

The *Recoverable Heat* is just potentially available, the real amount of recovered energy depends on the thermodynamic constrains (e.g. the temperature of the secondary fluid in an heat exchanger) fixed by the user and from the demand profile for thermal energy. As example, if the exhaust gas temperature is 950 [F] and the user requires steam at 10.3 [bar] (the related boiling temperature is 359 [F]) the amount of recovered heat is smaller than if the user requires steam at a pressure of 4 [bar] (the related boiling temperature is 291 [F]), because of the different temperature of the exchange fluid.

Finally, if the heat is available when it is not required by the final user, it is inevitably wasted. Thus a further classification of the *Recoverable Heat* is required. The term *Wasted Recoverable Heat* (WRH) is used to refer to the amount of thermal energy in the exhaust gas that despite being available is not recovered through the heat exchanger (or through the HRSG). In other terms, the WRH represents an energy resource obtainable by the exhaust gas which is wasted because it is not used in the plant. The WRH have not to be confused with the *Wasted Heat*, which represent the amount of heat discharged into the ambient because it is not possible to recover it. Finally the *Recovered Heat* represent the amount of heat which is really used by the facility.

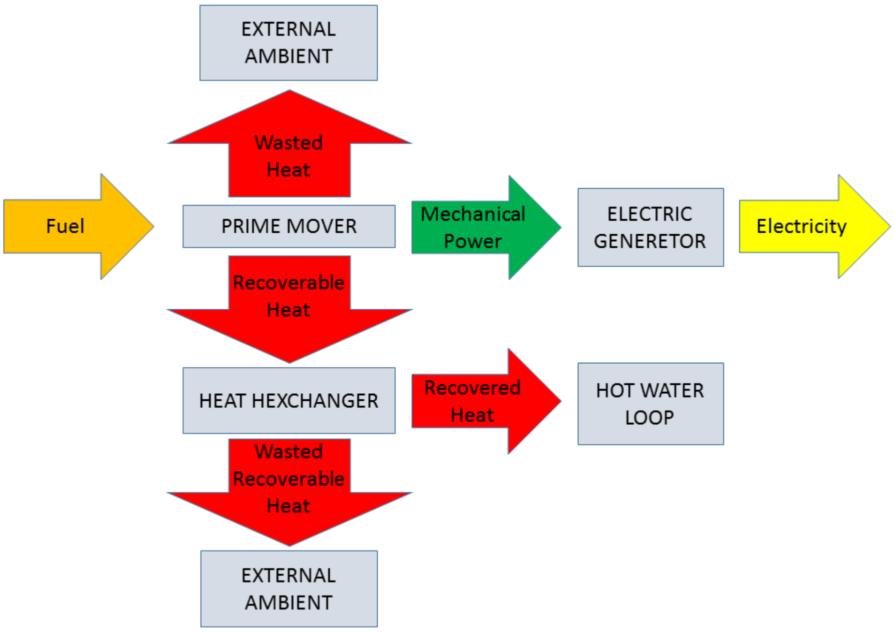

Figure 16: Main energy fluxes in a CHP system.

3.2 Management Strategies

Hospitals are characterized by a high energy demand at a constant daily rate and by a large base load through the whole year. This situation may allow a CHP plant to work with global efficiencies up to 85% for a large amount of hours per year.

In the past, these systems were generally designed to satisfy the thermal load of the facility and to use the electric output as an extra product that reduces the amount of power purchased from the external grid. In this approach the electricity does not represent the main product of the plant but rather a secondary one to increase the economical sustainability of the investment.

Through the years, the plant management strategy has changed toward operating the system in order to produce electricity in an economically convenient way. Using this different approach the electricity can be seen as the main output of the system. This increases the economic benefits in a framework characterized by growing rates of primary sources [6].

Moreover, this is the approach ensuring the best reliability of the electric supply. Emergency electric generators are not designed for continuous operation, especially because they are usually diesel fired, causing high emissions and having a limited fuel storage. On the other hand, cogeneration and trigeneration plants are designed to operate continuously and to meet either the electrical or the thermal load of the facility. Therefore they are more reliable power providers. In addition, emergency generators, which are still required in the system in case of CHP breakdown, can be designed with lower capacity than the prime mover of the CHP system itself. Using this approach the energy generators are meant to feed only the critical loads, e.g., operating rooms, and become *the backup of the backup*, making the overall system more reliable.

Focusing again on the reliability of the system, severe weather events draw the attention on power supply reliability. In this situation emergency power generators appeared to be not the best applicable solution; they may not operate as expected during outages and they may be limited by the fuel storage, e.g., diesel engines. The longer is the duration of the outages, the higher is the probability of the emergency system malfunctioning, which may have catastrophic consequences in a hospital.

Taking also into account economic considerations, emergencies electric generators are considered as dead assets for the economic balance of the hospital. This is caused by the impossibility to operate a backup system in a profitable way. Conversely, CHP plant is regarded as a dynamic asset, because it provides economic returns during the regular operation and it can provide an additional backup power during emergencies. The choice to install a CHP system allows hospitals to avoid to over-sizing emergency generators, while still having a reliable system for prolonged outages.

The hospitals' economic strategy is addressed to improve the health care services for the patients. Therefore, energy management is often a minor priority and the most common applied energy savings strategies have $1-2$ years payback period for the investments [5]. However, it is possible to create a parallel source of earnings for the facility if a longer payback period and also a larger investment cost is accepted. At the same time, it is possible to reduce the influence of the energy price variations on the hospital's budget.

3.3 Case Study

Several simulations of the hospital in cogeneration mode have been performed to collect a wide range of data on the possible sizing option of a CHP system. The output of the simulation in terms of data about the electricity and fuel consumption have been used as a starting point to perform an economic analysis and choose the best layout of the plant. The proposed layout consist of a gas turbine, whose exhaust feeds an heat exchanger to produce hot water to satisfy the thermal request of the hot water loop of the hospital.

The simplifying assumption of just hot water use has been adopted, rather than the double request of both steam and hot water. This assumption does not effect the estimation about the absolute value of the energy demand but considerably simplifies the realization of the simulation on eQuest®.

When the recovered heat is not enough to satisfy the heat request of the facility, a conventional boiler is operated being connected to the same water loop. The needs of domestic water are satisfied using the same heat recovered by the gas turbine, being the domestic hot water load assigned to the main hot water loop in the software. This approach does not represent the real plant layout, where domestic hot water and hot water for heating are addressed to different loops. However, it is the only approach allowing the simultaneous exploitation of the recovered heat to satisfy both energy demands. Although this choice has been implemented, eQuest® requires the existence of a domestic hot water loop and of its boiler to perform the simulation. Thus a domestic hot water loop has been created, although the adopted size of its boiler has been set to zero.

Finally, the cooling needs of the hospital are satisfied through electric chillers, which satisfy the cold demand of the cold water loop. The scheme of the analyzed layout is reported in figure 17 as it is shown on eQuest®; the picture does not provide information about the installed prime mover.

Several sizes of gas turbines have been analyzed, from 600 [kW] up to 1300 [kW]. Comparing the sizes of the equipment with the duration curve of the hospital it is possible to estimate how many hours per year the gas turbine will work at full load. The result are shown in figure 18

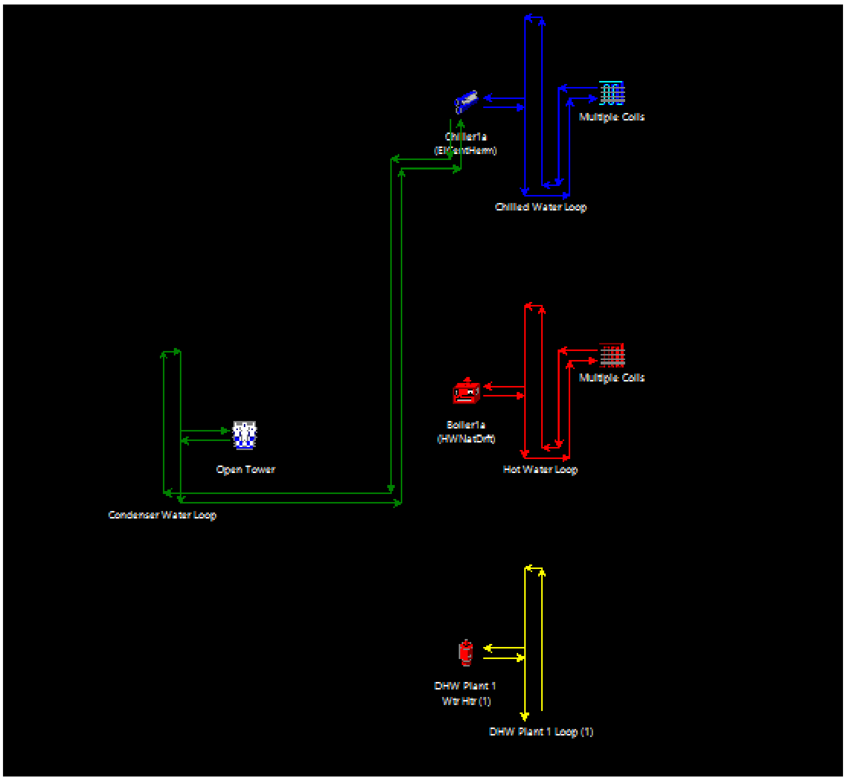

Figure 17: Layout of the cogeneration plant - prime mover is not depicted in eQuest® scheme.

by a visual comparison on the duration curve for electricity demand of the health care facility. Moreover the exact numbers of full load working hours are calculated and summarized in Table VII.

TABLE VII: FULL LOAD HOURS FOR SEVERAL GAS TURBINE SIZES.

Size [kW]	**600**	**700**	**800**	**900**	**1000**	**1100**	**1200**	**1300**
Full Load Hours [h]	8,760	8,760	8,172	6,880	5,798	4,771	3,950	1,699

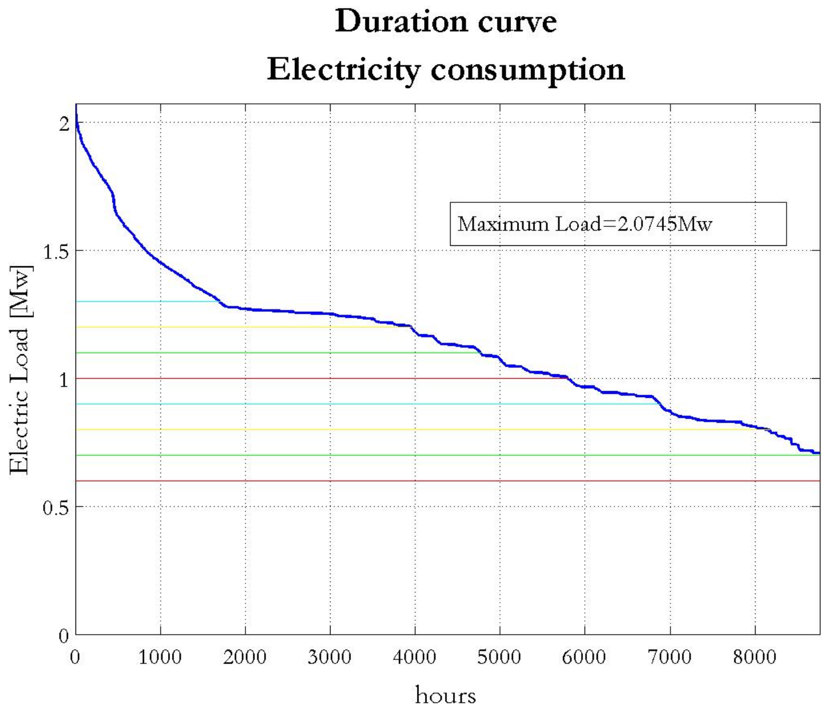

Figure 18: Electric duration curve if the hospital load and gas turbines proposed sizes comparison.

3.3.1 Electric Analysis

The number of hours at which an equipment works at full load is an important parameter to define if a system is well designed. Working at partial load for long periods all along the year is an undesired result, especially for equipment like gas turbines, which offer modest performance in off design condition and suffer early wear in this situation. Thus, partial load operation is an undesired operating condition because in turn it represents a non-profitable condition. In our case, prolonged partial load operation occurs for gas turbine larger than 1100 [kW]. Although extensive simulations and data collection have been performed for all the proposed sizes, here only some of the most significant graphs and results are reported to be discussed. The complete information and results are reported in the appendix.

The first important effect produced by the installation of the gas turbine is the change on the profile of the electricity demand. From now on, unless otherwise stated, referring to the *electric demand profile* it is meant the amount of electricity purchased by the external grid, which is evaluated as the difference between the facility need and the produced electricity by the gas turbine. Because of the on-site production of electricity, a pronounced reduction of the electric demand is noticeable. Obviously the reduction is proportional to the size of the installed gas turbine; the bigger is the size of the prime mover the larger is the amount of electricity produced thanks to the possibility to better cover the peaks of the hospital's electric demand.

The result of the simulation are reported in figure 19,figure 20, and figure 21. In the graphs, the blue line represent the electric demand of the facility and the red dashed line represents the electricity produced by the gas turbine. Hour by hour the difference in the y-coordinate values between the two plotted curves represent the power purchased by the external grid. The trend is extremely clear, increasing the installed capacity a reduction of the amount of power requested by the external grid occurs.

Looking figure 19,figure 20, and figure 21 the other important information provided is how the smaller equipment works at full load, in steady state conditions, for the whole year, while the 1300 [kW] gas turbine operating condition fluctuates during the same period, resulting in a equipment not fully exploited and working at low values of PLR for extended periods.

However, small fluctuations in the power production profile also occur during summer season in the 600 [kW] gas turbine. They represent the effects of the external temperature on the gas turbine electricity production. As explained in chapter 2, the proposed model for simulating the gas turbine behavior takes into account the effect of external temperature on the equipment's performance (High temperature occurring in summer cause a reduction of the efficiency and power output). These effects occur also in the other cases studied, however their effect are not as evident because of the simultaneous fluctuation of the operating condition of the gas turbine.

The previously mentioned results in terms of reduction of the electric demand are shown in figure 22, figure 23, and figure 24 where a comparison between the duration curve of the *base model* of the hospital (hospital without cogeneration plant) and the cogeneration layout is presented for the sizes of 700, 1000 and 1300 [kW]. The graph also shown the peak value of the electric demand in both the configurations for each presented case. In the 700 [kW] layout the facility uses the external grid supply for all the year, although the required electrical power is around the 50% of the *base model* demand. The peak value is reduced from 2.07 [MW] to 1.43

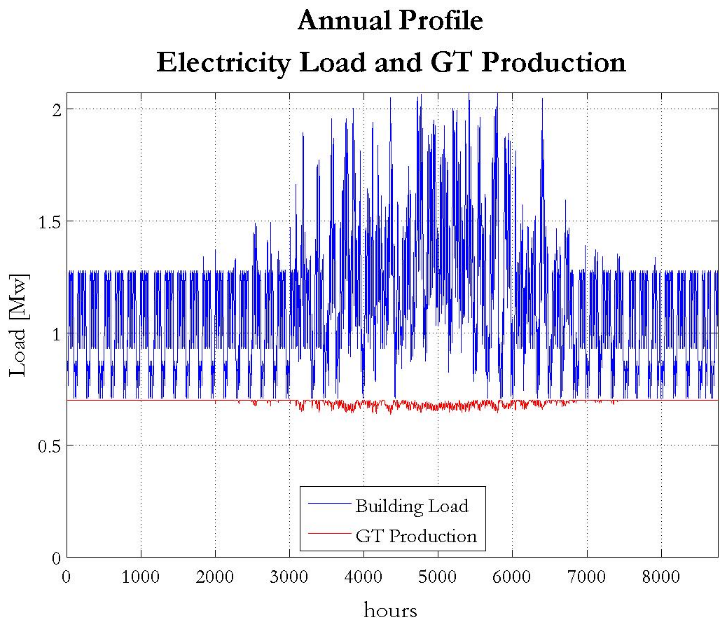

Figure 19: Hourly profile of the electricity production - GT 700 [kW].

[MW]. The situation is considerably different for the 1300 [kW] layout. In this case the health care facility is electrically independent from the external grid for up to 7,000 hours per year, while the power demand is reduced to 40% of the original demand. The peak value is reduced from 2.07 [MW] to 0.88 [MW].

The size of the gas turbine, produce a noticeable effect, on the overall amount of purchased electricity. The amount of electricity bought by the facility, month by month, is the result of the difference between the electric needs of the facility and the on-site production. In figure 25, figure 26, and figure 27 the electricity production and the monthly electricity needs for three different sizes of gas turbines: 700, 1000 and 1300 [kW]. Graphs about the electricity production

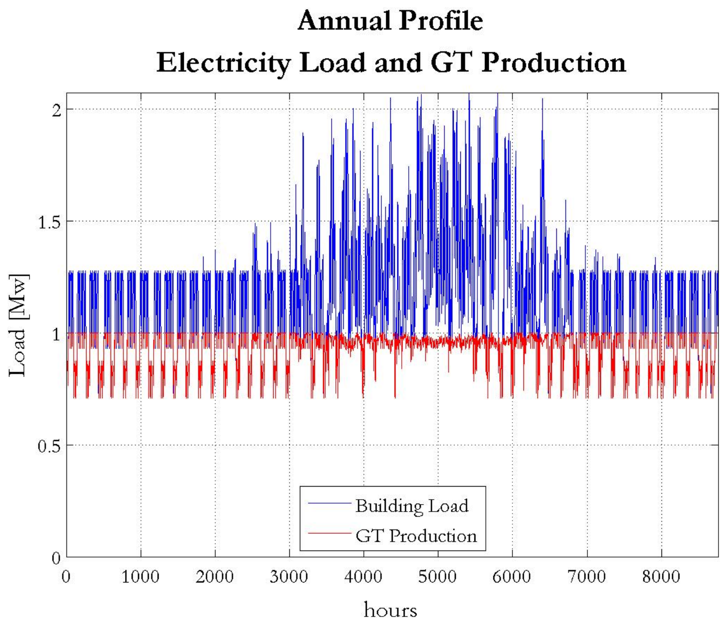

Figure 20: Hourly profile of the electricity production - GT 1000 [kW].

for all the analyzed sizes are reported in appendix. Although graphs are reported, the results about electricity production throughout the year are reported in Table VIII for all the gas turbine sizes analyzed.

Analyzing the data it is possible to see how rising up the size of the equipment, the overall production approaches the value of 10,015.20 [MWh], which represents the overall amount of electricity needed by the hospital in one year. The complete satisfaction of the electrical needs of the facility is not generally the purpose of a cogeneration plant. Indeed, the 1300 [kW] gas turbine layout results in a device working for the most of the year at very low efficiency because of the reduced working load with respect to the design one (low value of PLR). This

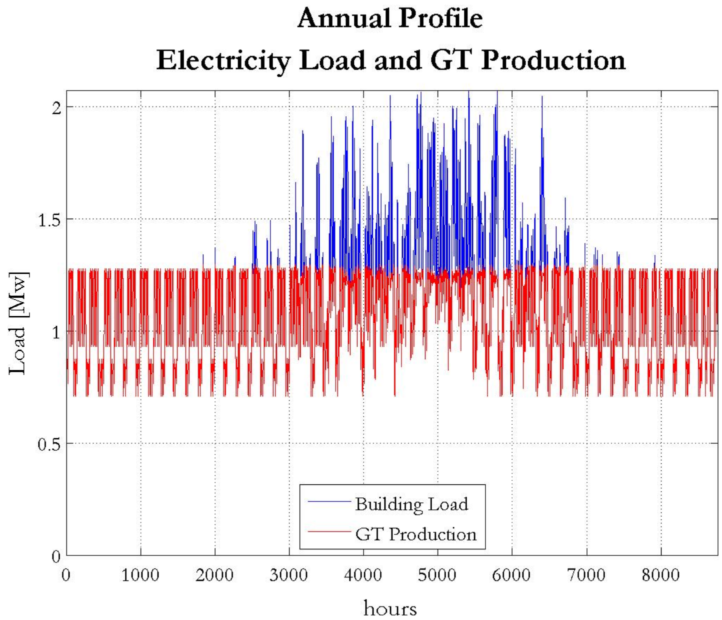

Figure 21: Hourly profile of the electricity production - GT 1300 [kW].

TABLE VIII: MONTHLY ELECTRICITY PRODUCTION FOR ALL THE ANALYZED LAYOUTS - [MWh].

	Base M.	**600**	**700**	**800**	**900**	**1000**	**1100**	**1200**	**1300**
Jan	775	446	521	592	648	695	733	763	775
Feb	700	403	470	535	585	628	662	689	700
Mar	775	446	521	592	648	695	732	762	775
Apr	773	431	503	572	630	680	719	750	767
May	860	441	515	586	651	708	754	792	817
Jun	916	420	490	559	626	687	740	784	820
Jul	1,017	431	503	574	646	714	774	826	870
Aug	1,014	432	505	576	645	709	766	817	862
Sep	861	425	496	564	625	681	727	765	794
Oct	808	445	519	590	653	707	748	781	800
Nov	741	432	504	572	625	668	701	728	740
Dec	775	446	521	592	648	695	733	763	775
Year	10,015	5,200	6,066	6,906	7,630	8,266	8,788	9,220	9,495

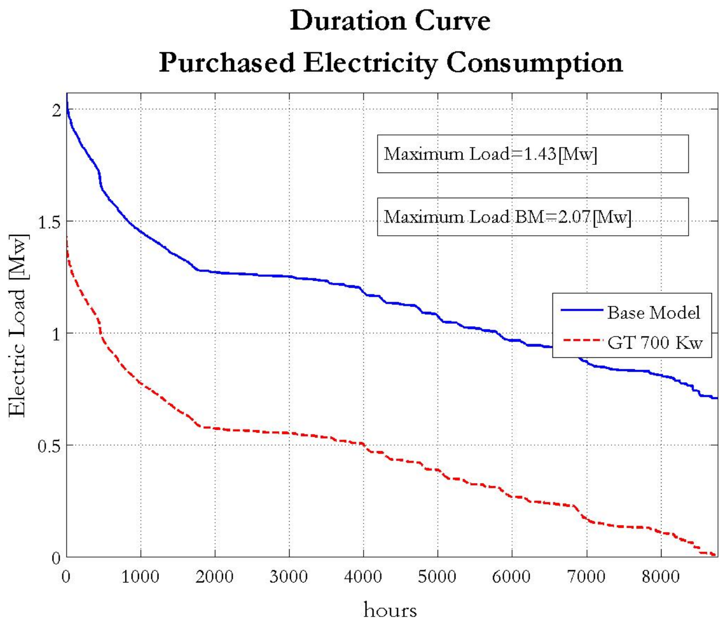

Figure 22: Electric duration curve - GT 700 [kW].

situation usually implies a reduced effectiveness of the economic saving produced by the plant because of the increased investment cost and the ineffective exploitation of the fuel. Moreover, as explained in chapter 2, frequent changes in working condition can cause an increase of the required maintenance action and the connected costs. The estimation of the increased costs is beyond the extent of this work.

3.3.2 Thermal Analysis

The second product obtained by a cogeneration plant is the recoverable heat. The heat is delivered from the gas turbine to the facility by means of hot water. The hot water is produced in a heat exchanger by the utilization of the exhaust gas of the gas turbine. The

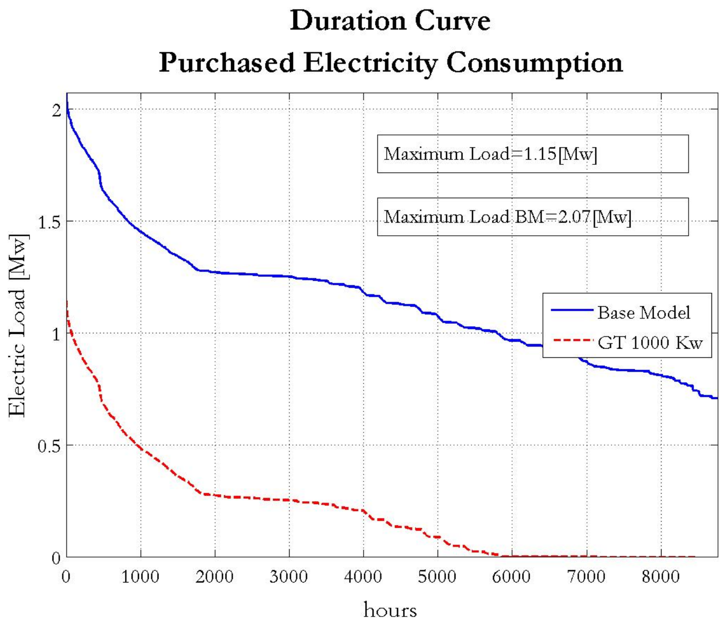

Figure 23: Electric duration curve - GT 1000 [kW].

effects produced by the installation of the cogeneration plant on the energy consumption of the facility, are shown in figure 28, figure 29, and figure 30. The effects of the recovered heat on the fuel consumption of the facility are shown through the variation in the profile of the duration curve for the fuel consumption. The blue and red curve represent the fuel for heating and auxiliary purposes (e.g. kitchen) respectively for the *base model* and cogeneration layout. Once again, although simulation have been performed for sizes from 600 [kW] up to 1300 [kW], the complete data and graphs are available in the appendix, here only the results for the size of 700, 1000 and 1300 [kW] are shown.

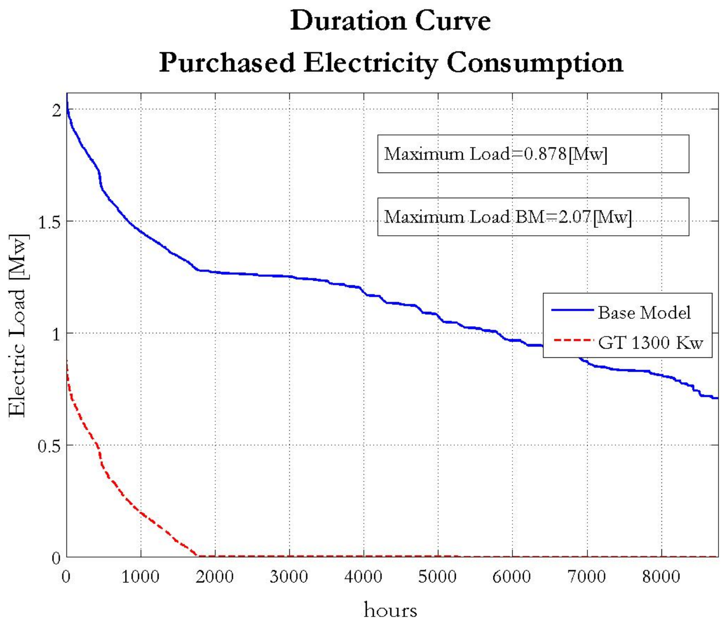

Figure 24: Electric duration curves - GT 1300 [kW].

The effect of the heat recovery are clear, the fuel consumption of the facility is reduced proportionally to the size of the installed prime mover. Increasing the size of the installed gas turbine means increasing the amount of electricity produced. The consequence of a larger amount of electricity produced is a larger amount of recoverable heat available by the exhaust gas. The maximum thermal load required by the *base model* of the facility is 21.24 [MBTU/h], and it is reduced to 11.7, 9.7 and 9 [MBTU/h] for the 700, 1000 and 1300 [kW] gas turbine. The effect of the reduction of fuel consumption on the peak value of the fuel consumption are summarized in Table IX for all the analyzed sizes.

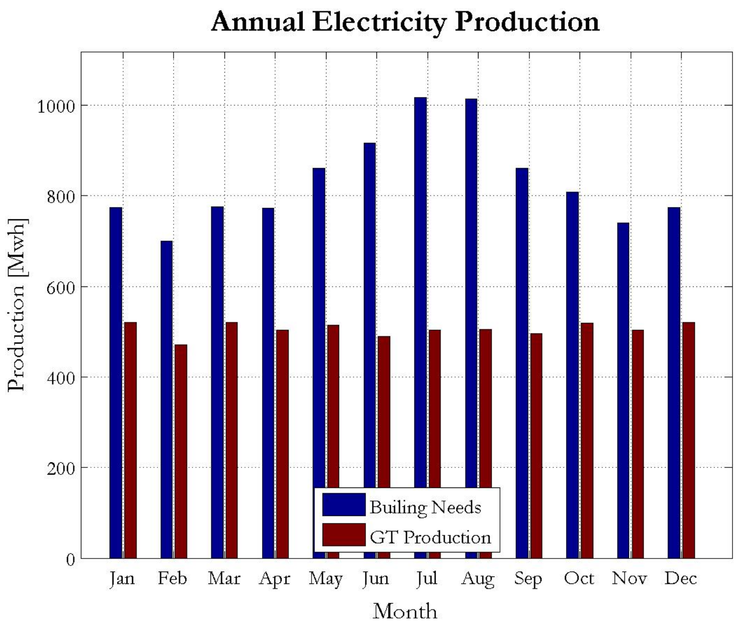

Figure 25: Monthly electricity production - GT 700 [kW].

TABLE IX: FUEL DEMAND PEAK VALUES FOR HEATING AND OTHER PURPOSES.

Size [kW]	**Base M.**	**600**	**700**	**800**	**900**	**1000**	**1100**	**1200**	**1300**
Thermal Load [MBTU/h]	21.24	12.6	11.8	10.8	9.9	9.7	9.5	9.3	9

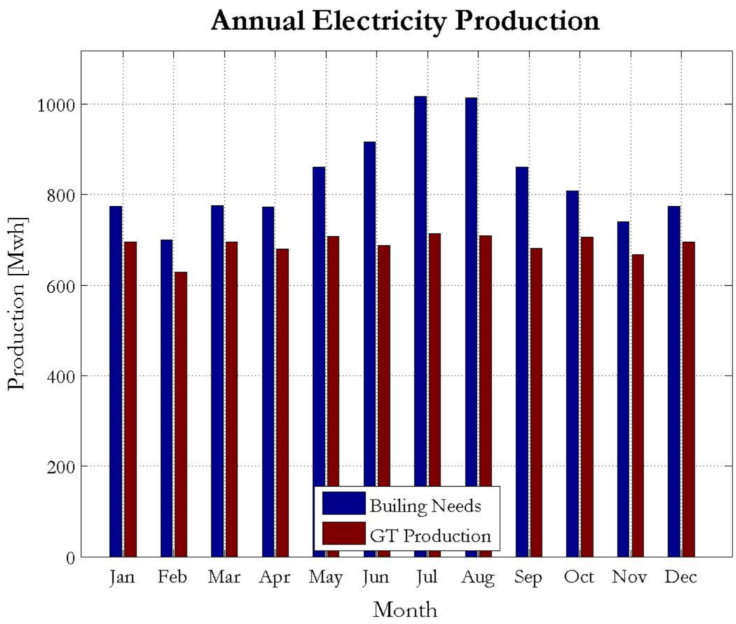

Figure 26: Monthly electricity production - GT 1000 [kW].

The effects produced by the installation of a cogeneration plant on the fuel demand can be seen from the monthly fuel demand for different configuration. The results are shown in figure 31, figure 32, and figure 33 while the complete collection of graphs is available in appendix. What is highlighted in figure 31, figure 32, and figure 33 is how the fuel consumption for heating and other purposes is dramatically reduced by the introduction of the gas turbine recovered heat. Increasing the size of the gas turbine causes a reduction of the fuel consumption, especially during the heating season. However, no changes occur in summer. The steady monthly fuel consumption during summer is due to the needs of facilities such as the kitchen. That amount of fuel cannot be replaced in any way regardless of the installed size of gas turbine. Detailed

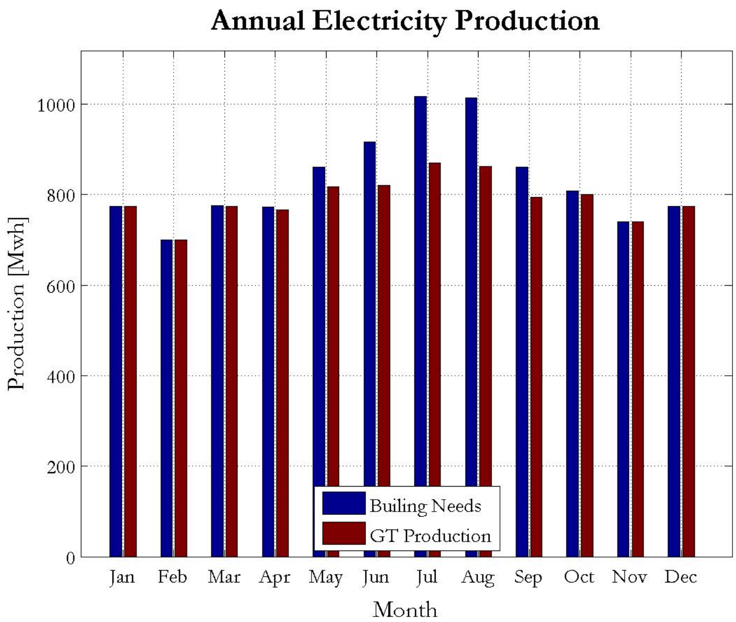

Figure 27: Monthly electricity production - GT 1300 [kW].

information about monthly fuel consumption are reported inTable X for all the analyzed sizes and also for the *base model*.

The presented results in terms of fuel consumption does not take into account the amount of fuel which is needed to feed the gas turbine itself. Although the amount of fuel employed for heating (and other purposes) decrease as the installed gas turbine size increases, the overall fuel consumption of the facility increases accordingly. To take into account the overall fuel consumption of the facility, new duration curves have been produced. The result are shown in figure 34, figure 35, and figure 36 while the graphs for all the other analyzed sizes are available

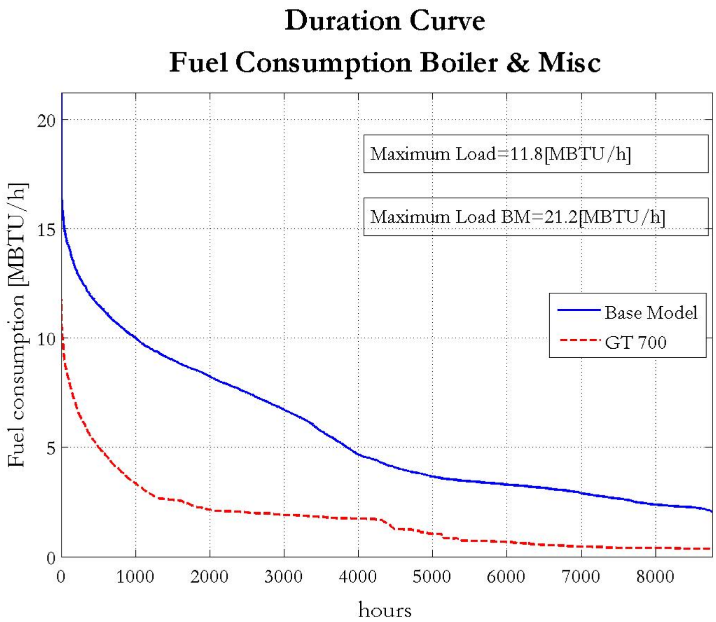

Figure 28: Duration curves of fuel consumption for heating purposes and other consumption - GT 700 [kW].

in appendix. In this case it is possible to see how the overall fuel consumption grows up as the size of the equipment grows up.

Through the year, the heat recovered by the gas turbine is used to satisfy the thermal needs of the building. However, in all those case in which the heat recovered by the gas turbine is not enough to satisfy the thermal needs of the building, the boilers are required to work in order to satisfy the building needs. As the size of the gas turbine increases, the amount of available recoverable heat increases, reducing the amount of fuel burnt in the boilers to meet the thermal load.

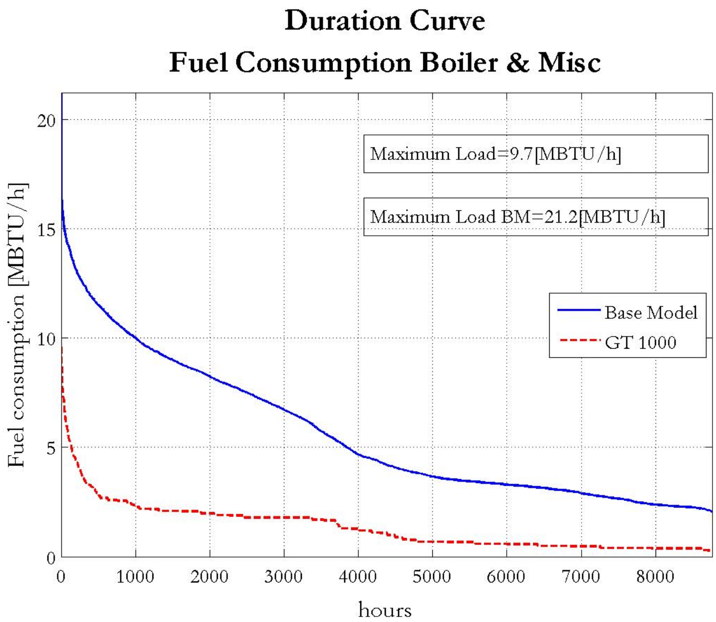

Figure 29: Duration curves of fuel consumption for heating purposes and other consumption - GT 1000 [kW].

The heat available from the gas turbine is not always usable. In all those situations an amount of heat is wasted. Part of the heat produced is wasted through the prime mover. Moreover, the exhaust gas produced by the gas turbine feed an heat exchanger characterized by an efficiency of 80%. Thus, another amount of heat is wasted through the blanket and through the residual thermal energy content of the exhaust gas. Finally, it is possible to deliver the remaining amount of available heat to the hot water loop. However, not always all the available heat is completely exploited. The reasons why this amount of heat is not used by the facility are two. The first one depends on when the heat is produced and when it is requested. Sometimes it can happen that large amount of heat is produced when there is no need by the

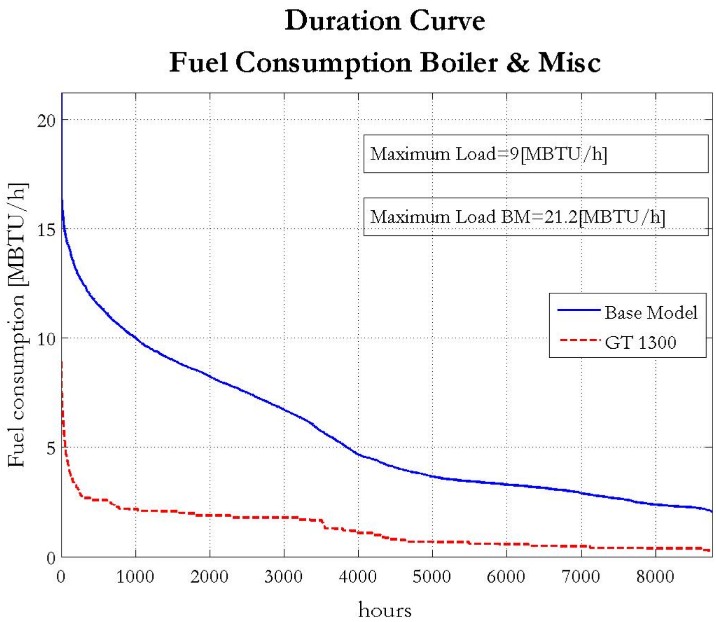

Figure 30: Duration curves of fuel consumption for heating purposes and other consumption - GT 1300 [kW].

facility and vice-versa. The second reason which is the cause of waste of recoverable heat (WRH) is the temperature. Sometimes it can happen that the heat is available at a temperature lower than the required temperature by the thermal user. This situation causes the impossibility to use the recoverable heat and the necessity to use the boiler although a certain amount of thermal energy is still available in the circulating hot water. This phenomenon provides an explanation of why sometimes it is present an amount of WRH, although the need of the facility are not entirely met by the recovered heat.

In order to better understand the dynamics which lie behind the mechanism of heat production, recovery and usage the hour by hour reports are plotted in figure 37, figure 38, and

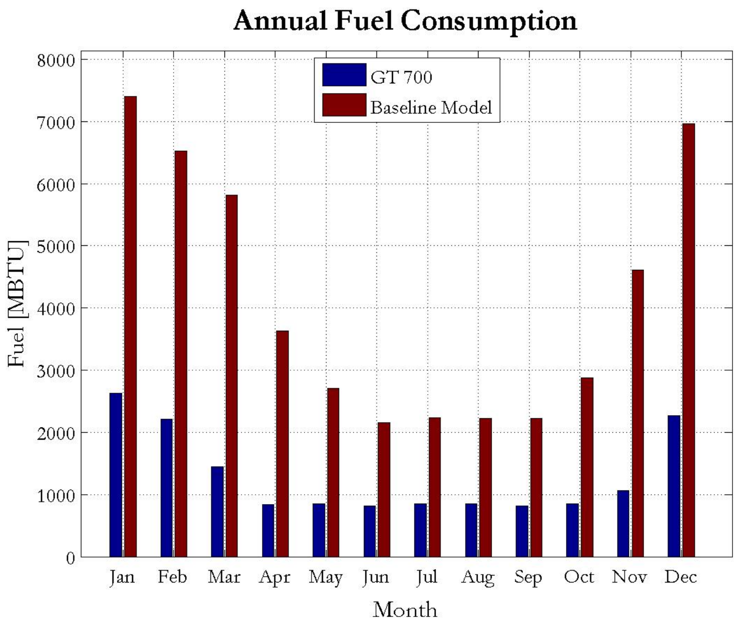

Figure 31: Monthly fuel consumption of the hospital- GT 700 [kW].

figure 39. Although the thermal needs of the building remain the same in all the cases (blue curves), what really changes is the amount of heat recovered by the exhaust (red dashed curves) and the amount of wasted heat(green curves). It is possible to see how the maximum amount of wasted heat occurs during summer when the reduced thermal needs does not correspond to a reduction of the electric needs of the utility.

3.3.3 Efficiency Analysis

Because of the output of two different products (heat and electricity) a specific way to define efficiency has to be adopted. This choice emerges from the different quality of the output products, this difference is identified by both thermodynamics and market logic. In both fields

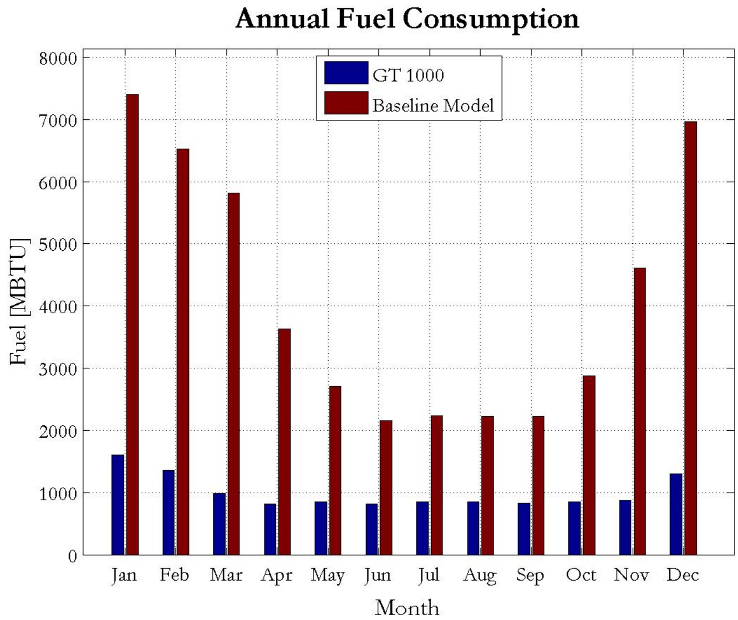

Figure 32: Monthly fuel consumption of the hospital- GT 1000 [kW].

the electricity is generally regarded to have higher value than heat. As a result through the years researchers have proposed several ways to define the cogeneration efficiency [10].

- FERC Efficiency Standard

  The Public Utilities Regulatory Policies Act (1978) defined The FERC efficiency standard to highlight how the value of electricity is higher than the thermal output. To account for these differences in quality the FERC efficiency standard is represented as the ratio of net electric output plus half of the net thermal output to the total fuel used in the CHP system.

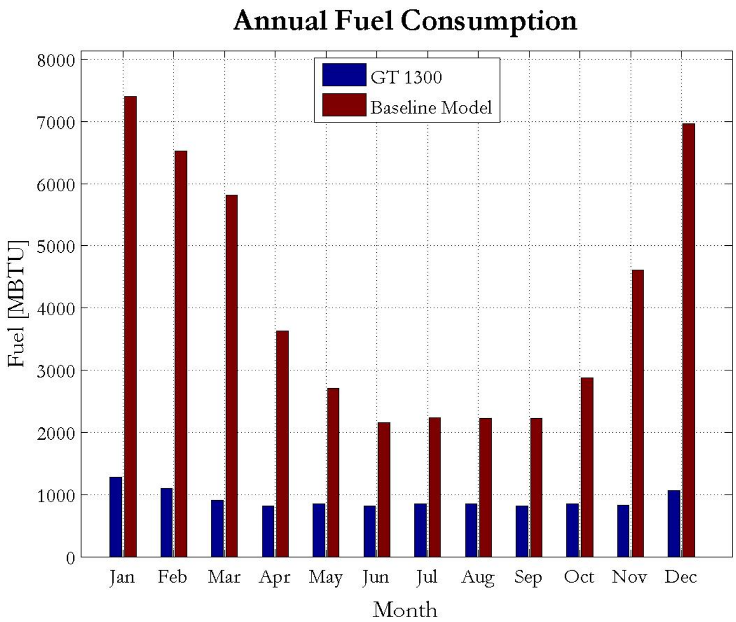

Figure 33: Monthly fuel consumption of the hospital- GT 1300 [kW].

$$\eta_{FERC} = \frac{E_{PM} + Q_{rec.}/2}{F_{PM}} \tag{3.1}$$

- E_{PM} Electrical energy produced;
- $Q_{rec.}$ Thermal energy recovered;
- F_{PM} Prime mover fuel consumption;

- Total CHP System Efficiency

This approach does not take into account the difference, in terms of value, existing between the two products of the CHP system. It defines the efficiency as the ratio of the energy

TABLE X: MONTHLY FUEL CONSUMPTION FOR ALL THE ANALYZED LAYOUTS - [MBTU].

	Base M.	**600**	**700**	**800**	**900**	**1000**	**1100**	**1200**	**1300**
Jan	7,402	3,246	2,626	2,122	1,822	1,603	1,442	1,333	1,273
Feb	6,521	2,741	2,208	1,805	1,545	1,362	1,231	1,143	1,095
Mar	5,812	1,848	1,443	1,183	1,052	988	950	929	909
Apr	3,634	913	844	825	820	822	819	820	821
May	2,708	847	847	847	846	847	846	848	847
Jun	2,157	819	819	818	818	819	820	820	821
Jul	2,232	847	847	848	846	849	848	847	850
Aug	2,227	847	847	846	847	850	847	849	850
Sep	2,223	819	819	819	819	823	818	820	822
Oct	2,877	859	851	847	847	846	844	849	847
Nov	4,609	1,295	1,066	935	887	867	856	844	833
Dec	6,960	2,864	2,266	1,801	1,489	1,301	1,194	1,117	1,064
Year	49,363	17,944	15,483	13,696	12,639	11,976	11,516	11,219	11,033

output (given by the summation of the electric and thermal energy produced.) to the overall amount of energy directly used by the system (fuel consumption).

$$\eta_{CPH} = \frac{E_{PM} + Q_{rec.}}{F_{PM}} \tag{3.2}$$

- E_{PM} Electrical energy produced;
- $Q_{rec.}$ Thermal energy recovered;
- F_{PM} Prime mover fuel consumption;

The overall efficiency of a CHP plant mainly depends on the amount of energy recovered from the turbine exhaust gas. The amount of heat recoverable is essentially a function of

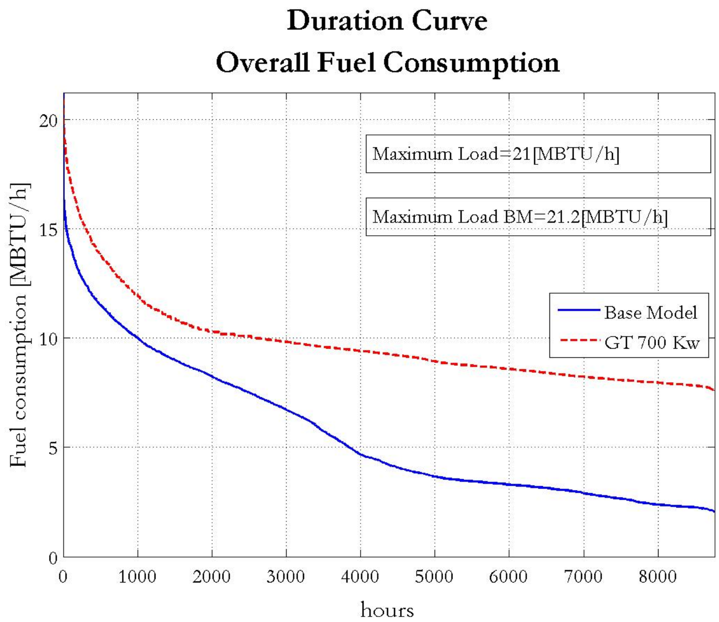

Figure 34: Duration curve of the overall fuel consumption - GT 700 [kW].

the exhaust gas temperature and of the HRSG temperature (temperature of the stack) or in general, if no steam is required, it is a function of the desired temperature of the heated fluid. The first parameter is a function of the inlet gas temperature in the expansion section of the gas turbine and of its pressure ratio. Typical exhaust temperatures are in the range of 850 to 950 [F]. Assuming a fixed HRSG exhaust exit temperature, the higher the turbine exhaust temperature (higher HRSG gas inlet temperature) the greater the recoverable thermal energy, thus the HRSG production increases. In the same way, for the second parameter, the lower the HRSG stack temperature, the greater the amount of energy recoverable by the gas. Increasing the amount of recovered heat, increases the overall efficiency of the system.

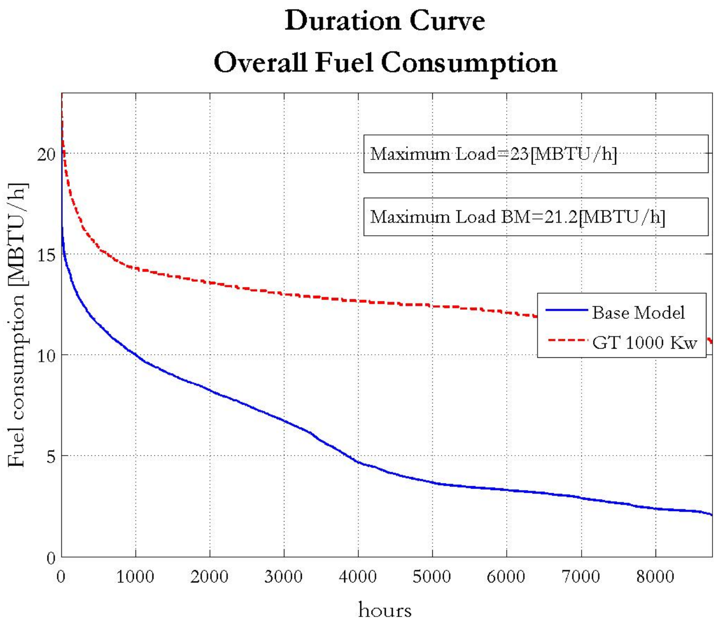

Figure 35: Duration curve of the overall fuel consumption - GT 1000 [kW].

Generally, unfired HRSGs are designed to recover more than 80% of the recoverable heat in the turbine exhaust (the term *Recoverable Heat* represents the maximum energy content recoverable according to the temperature levels of the exchanging heat fluids). Unlike a simple cycle gas turbine, the overall CHP efficiency does not drop dramatically in partial load operation. This is caused by the layout of the system. In fact, the decrease in electric efficiency of the gas turbine at partial load conditions causes a relative increase of the heat available for the recovery system, which may provide a benefit in term of overall efficiency because of the greater amount of heat available. This kind of behavior of the system can be a significant operating

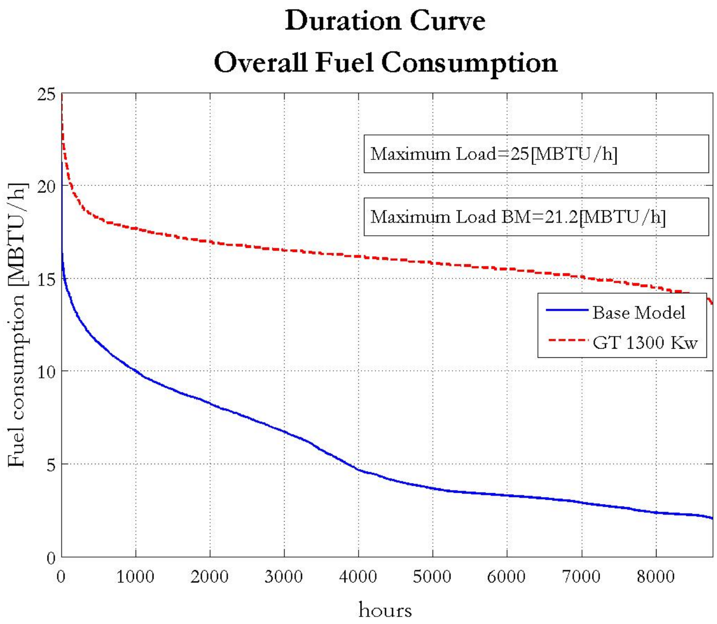

Figure 36: Duration curve of the overall fuel consumption - GT 1300 [kW].

advantage for applications in which the economic benefit are mainly due to the availability of large quantity of thermal energy.

The calculated average efficiency for each layout are reported in Table XI. The average is performed on the whole year and the efficiency is calculated following both the presented approaches. Although the FERC efficiency is lower than the total CHP system efficiency because the lower value appointed to the thermal energy, the common trend is clear. Increasing the size of the plant, prolonged operation at low partial load ratio (PLR) have a negative effect on the efficiency. The PLR is the ratio of the actual power output to the design power of the prime mover.

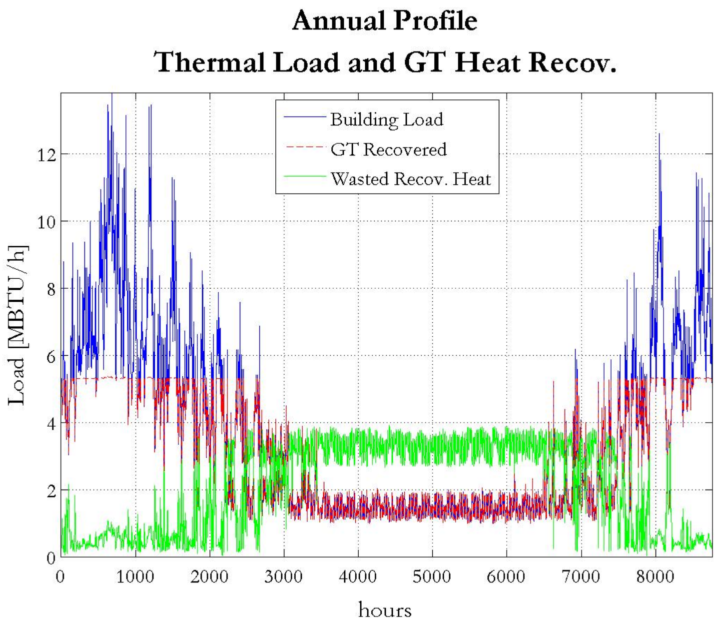

Figure 37: Hourly profile of building thermal needs, recovered heat and WRH - GT 700 [kW].

In the two last columns of Table XI are reported the percentage reduction in source energy consumption (PRSEC). The PRSEC provides a way to estimate the reduction in primary energy source consumption produced by the installation of a CHP plant. The reduction is estimated comparing the consumption of the new layout with the conventional production. The conventional energy production is that one occurring in a generation station connected to the electric grid for producing the electricity. Moreover, also the source energy related to the fuel consumption is taken into account.

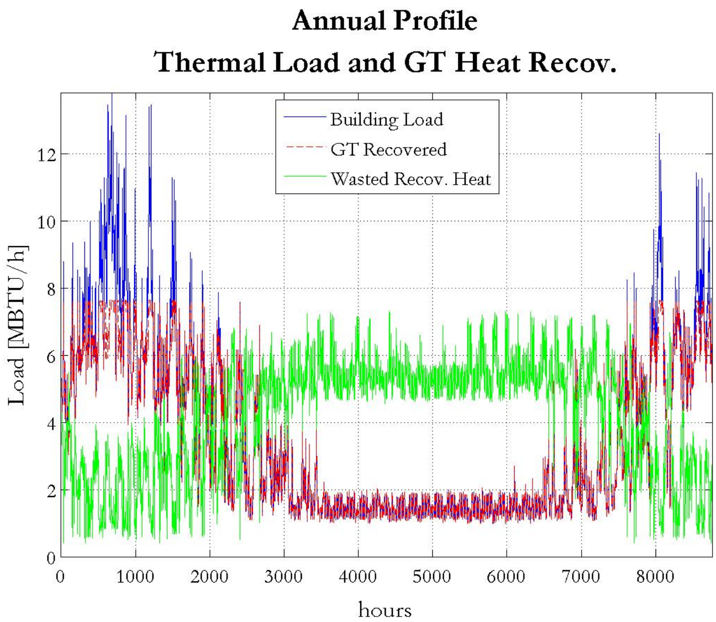

Figure 38: Hourly profile of building thermal needs, recovered heat and WRH - GT 1000 [kW].

The PRSEC formula is Equation 3.3:

$$PRSEC = \frac{SE_{CONV} - SE_{CHP}}{SE_{CONV}} \tag{3.3}$$

$$PRSEC = 1 - \frac{SE_{CHP}}{SE_{CONV}} \tag{3.4}$$

- SE_{CONV} Source energy consumption for conventional production;
- SE_{CHP} Source energy consumption due to CHP installation;

The source energy consumption estimation is performed through the employee of the ANSI/ASHRAE Standard 105-2014: Standard Methods of Determining, Expressing and Compar-

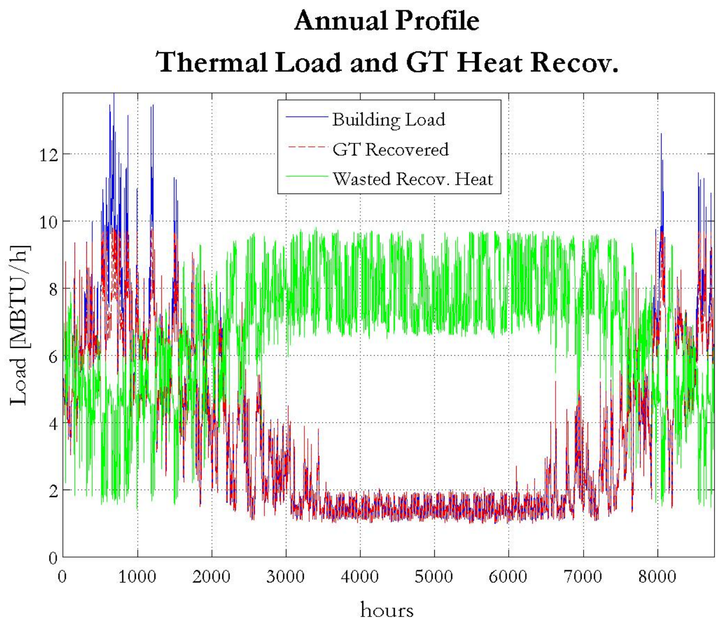

Figure 39: Hourly profile of building thermal needs, recovered heat and WRH - GT 1300 [kW].

ing Building Energy Performance and Greenhouse Gas Emissions [17]. This standard is intended to provide a unique and extensively accepted approach for estimating the energy performance of buildings and the greenhouse gas emissions associated with building operation. The standard includes information on conversion factors that allow the calculation of the source energy consumption and associated greenhouse gas emissions. Several conversion factors are reported, each one of them accounts for a different employed energy source. Knowing the actual energy consumption of the facility, divided by the type of resource, and multiplying each one by the proper factor it is possible the source energy estimation.

The conversion factors depend on where the energy consumptin occurs. Different areas of the country present different conversion factors. This is due to the need for taking into account how the efficiency of production and delivery of the energy changes around the country. The employed technology, the efficiency of the grids, and the region of provision are some of the factors taken into account. Therefore the standards divides the country in 26 subregion. Illinois is part of the region referred as RFCW; in this region the value of the conversion factor of interest are:

- 3.29 for the electricity;
- 1.09 for the natural gas;

The PRSEC index is calculated twice. In the first case the analyzed system is the overall facility, thus all the equipment for the energy supply in it are involved in the analysis. This factor estimates the percentage reduction in source energy consumption of the facility because the installation of a CHP system. Thus, it is influenced not only by the performance of the CHP system itself, but also from the performance of all the other equipment in the system, e.g., boilers and chillers. Moreover, the share of on-site produced energy with respect to the share of purchased energy considerably affects the index. The difference between the analyzed portions of the system is clarified in figure 40. Following this approach a measure of the overall facility performance is obtained and Equation 3.4 becomes:

$$PRSEC = 1 - \frac{[SE_{F.B.} + SE_{F.PM.} + SE_{E.P.}]_{CHP}}{[SE_{F.B.} + SE_{E.P.}]_{CONV}} \tag{3.5}$$

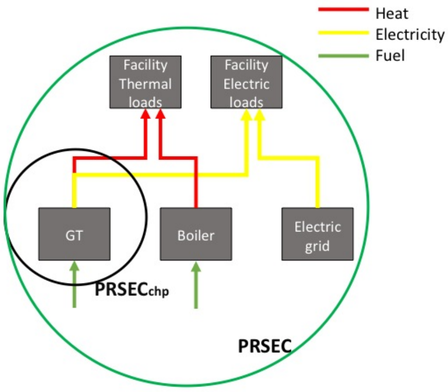

Figure 40: Different portions of the system analyzed with PRSEC index.

$$PRSEC = 1 - \frac{[F_B * AF_{NG} + F_{PM} * AF_{NG} + E_{pur.} * AF_E]_{CHP}}{[F_B * AF_{NG} + E_{pur.} * AF_E]_{CONV}} \tag{3.6}$$

- $SE_{F.B.}$ Source energy associated with fuel for boilers;
- $SE_{F.PM.}$ Source energy associated with fuel for prime mover;
- $SE_{E.P.}$ Source energy associated with electricity purchased;
- F_B Fuel consumption for boilers;
- F_{PM} Fuel consumption for prime mover;
- $E_{pur.}$ Electricity purchased;
- AF_{NG} ASHRAE factor for natural gas;
- AF_E ASHRAE factor for electricity purchased;

The numerator represent the source energy consumption of the facility using a CHP plant where as the denominator is the fuel source energy consumption of the facility without CHP, thus the consumption of the *base model.*

The second approach proposed for applying the PRSEC focuses on a small portion of the system. If only the source energy associated with the CHP plant production is taken into account, the index becomes a measure of the performance of just the CHP plant; instead of being a measure of the whole system performance. In this case, Equation 3.4 is the ratio of the source energy needed by the CHP plant for its operation to the source energy needed for producing the same electrical and thermal output as the CHP system in a conventional plant; or in other words the percentage reduction of source energy consumption per unit of on-site energy produced by the CHP plant. This approach is meant to measure the performance of the CHP system without being affected by the other equipment in the building or by any management logic. This means that the estimated performance is not the one of the facility, but rather a specific feature of the CHP system. Using this approach and using the terms *on-site* to refer to this second approach, Equation 3.4 becomes:

$$PRSEC_{OS} = 1 - \frac{[SE_{F.PM.}]_{CHP}}{[SE_{Q_{rec.}} + SE_{E_{PM}}]_{CONV}} \tag{3.7}$$

$$PRSEC_{OS} = 1 - \frac{[F_{PM} * AF_{NG}]_{CHP}}{[F_B * AF_{NG} + E_{PM} * AF_E]_{CONV}} \tag{3.8}$$

$$PRSEC_{OS} = 1 - \frac{[F_{PM} * AF_{NG}]_{CHP}}{[\frac{Q_{rec.}}{\eta_B} * AF_{NG} + E_{PM} * AF_E]_{CONV}} \tag{3.9}$$

- $Q_{rec.}$ Recovered heat from the prime mover;
- η_B Boiler average efficiency;
- E_{PM} Electricity produced by the prime mover;
- F_{PM} Fuel consumption for the prime mover;
- F_B Boiler fuel consumption to replace the recovered heat $Q_{rec.}$ only;
- $SE_{Q_{rec.}}$ Source energy associated with fuel for boilers, to replace $Q_{rec.}$ only;
- $SE_{F.PM.}$ Source energy associated with fuel for prime mover;
- $SE_{E_{PM}}$ Source energy associated with electricity produced by the gas turbine;
- AF_{NG} ASHRAE factor for natural gas;
- AF_E ASHRAE factor for electricity purchased;

TABLE XI: EFFICIENCY OF THE COGENERATION PLANTS.

Size [kW]	$F_B[MBTU]$	$F_{PM}[MBTU]$	$Q_{rec.}[MBTU]$	$E_{PM}[MWh]$	$E_{pur.}[MWh]$	η_{CHP}	η_{FERC}	$PRSEC$	$PRSEC_{OS}$
600	14,829	59,922	24,787	5,200	4,815	70.9%	50.3%	18.4%	29.1%
700	12,921	69,908	26,707	6,066	3,949	67.8%	48.7%	19.0%	27.0%
800	12,759	79,978	28,101	6,906	3,109	64.6%	47.0%	18.2%	24.7%
900	12,639	90,321	28,917	7,630	2,385	60.8%	44.8%	16.3%	21.2%
1000	11,976	100,585	29,453	8,266	1,750	57.3%	42.7%	14.3%	17.5%
1100	11,516	110,781	29,797	8,788	1,227	53.9%	40.5%	11.5%	13.2%
1200	11,219	120,718	30,038	9,220	795	50.9%	38.5%	8.1%	8.8%
1300	11,033	130,642	30,180	9,495	520	47.9%	36.3%	3.5%	3.5%

In Table XI is shown how the value of the PRSEC reaches a maximum for an installed size of 700 [kW]. This layout results the one ensuring the best reduction in terms of source energy consumption. Differently, the $PRSEC_{OS}$ has a maximum for an installed size of 600 [kW]. The reason of this difference lies once again in the framework of the analysis. Focusing only on the CHP system, the best utilization of the resources occurs when the gas turbine works at full load and the most of the heat is recovered. Although both the 600 and 700 [kW] layouts can ensure full load operation of the gas turbine for all the year, the 600 [kW] show a smaller value of WRH than the other case; this results in a system which works more efficently. However, changing framework and focusing on the whole facility, the PRSEC is higher for the second case because of the higher amount of produced electricity and recovered heat, which can replace the more expensive (in term of source energy) purchase from the grid.

3.4 Economic Analysis

The choice of the best size of gas turbine for CHP purpose is strongly related to the economic evaluation of each of the proposed layouts. Several economic criteria can be adopted to properly size a CHP system; although it is impossible to define the "best" criterion in absolute, an "optimum" can be identified for each individual user. Each user shows a different set of requirements influencing the final choice on the preferred layout. Two possible criteria samples are those applied to a small private facility rather than a large public facility.

The small user is usually more interested in a low investment cost followed by short pay back periods. On the other hand, a large facility having an easy access to economic assets would be more interested on the economic returns produced by the investment over a medium-long period; in this case the net positive value (NPV) of the investment over the plant's life could represent a more interesting way to show the effectiveness of the proposed layout.

Whatever the adopted criterion, it will be strongly influenced by the overall plant costs, which are highly dependent on the size of the prime mover [6]. Therefore finding the optimal size of the prime mover in the CHP framework has a primary role in the analysis.

The cost of generating electricity and heat from a CHP can be classified into capital investment cost, operation and maintenance (O&M) costs and fuel cost. The benefits from the CHP placement can be classified into: economica benefits, power loss reduction and significantly decreasing the expected energy not supplied [18], i.e., through the thermal energy recovered, which is a positive effect in a power system. CHP products can be delivered directly to final users avoiding the associated losses due to transmission. Moreover, for CI, the reliability enhancement obtained through the installation of a CHP system leads to a cost reduction for the final users. This is due to the avoided losses that might be encountered in case of failure of the energy supply system. Not all of these costs and savings can be easily determined, some of them, such as the savings produced through reliability enhancement of the system, can be just approximately estimated. In this analysis, the piece of work concerning reliability is not faced, and the main part about costs analysis is focused on the direct estimation of Investment, fuel and O&M costs. Following the previously mentioned criterion, these costs are taken into account for each system, analyzing their present value and providing an estimation of the overall net present value for each possible layout of the system evaluated over its life.

3.4.1 Utilities Rates

The estimation of the energy utilities costs is a main importance aspect to analyze the economic feasibility of a CHP system. Knowing the rates of the utilities, e.g., electricity and natural gas costs, it is possible to determine the *Base Model* energy costs, the CHP system energy costs and comparing them it is possible to estimate the economic saving produced by the adoption of a specific system layout. The location of the facility is in the Chicago area, which is situated in Illinois and belongs to the US Climate Zone number five. In Illinois, the electricity market is deregulated; thus to collect information about the electricity price the information have been collected from private companies' database. ComEd® is the main electrical utility provider, the information available in its website have been used in this analysis [19]. Moreover, historical information about the average retail price of electricity to ultimate customers have been retrieved from the US energy information administration (EIA) reports published on its website, which are constantly updated [20]. The rates applied by the company depend on the customer profile; three different kind of costumer profiles have been defined by ComEd®: residential, commercial and industrial costumers. The hospital can be regarded as an industrial costumer because of its large consumption in terms of electric energy. The final cost for electricity is the result of the summation of three different contributions:

- The demand charge, which accounts for highest level of electricity supplied (kilowatt [kW]) at one time during the billing period;
- The energy charge, which accounts for the amount of electricity (kilowatt-hours [kWh]) consumed during the billing period. The energy charge is composed by two contributions:

- Energy Distribution Charge, which accounts for the cost of delivery the electricity;
- Energy Charge, which accounts for the cost of generating the electricity;

The final adopted rates for each of the items composing the cost structure are calculates as average of historical values of recent years and are summarized in Table XII.

TABLE XII: ADOPTED ELECTRIC RATES.

Demand Charge	5.8	[$/kW]
Energy Distribution Charge	1.61	[c$/kWh]
Energy Charge	7.22	[c$/kWh]

An historical data collection has been carried out also for the other necessary utility, the fuel. The plant is assumed to be fed by natural gas, which represents one of the best solutions, especially in an urban context, for several reasons. Feeding the plant with natural gas means relying on an affordable price clean energy source, which does not requires storage systems because of the existing distribution network. The information about the rates of this utility have been collected through the reports produced by the US energy information administration (EIA) reports, published on its website[21]. The rate for natural gas is a single value based on the consumption. The retrieved data led to the adoption of the following rate for the Chicago area:

TABLE XIII: ADOPTED FUEL RATES.

NG rate	6.9	[$/1000ft3̂]
	6.5	[$/MBTU]

3.4.2 Investment and O&M Costs

The study has to deal with the estimation of the costs related to the installation and maintenance of the plant. Starting from the investment cost, they are the costs of installing the gas turbine and the related auxiliaries equipment. The costs for the already installed equipment of the *base model*, e.g., the boilers, the chillers and the domestic water heater, are not taken into account because are not considered part of the investment, which is the upgrade from a standard layout to a cogeneration one.

This approach simplifies the analysis but also slightly overestimates the costs. This happens because installing a CHP system, the reduced demand for hot water should result in a reduction of the installed boiler capacity and thus a reduction of the related investment costs.

A detailed analysis about investment costs has been conducted in chapter 2 analyzing the data retrieved in literature and technical spreadsheets [10][11][12][13][14]. These cost are also listed in Table V. The table shows the *Total Pant Cost per net kW* for several sizes of gas turbine. Although the analyzed size range is closer to the size of SOLAR® Saturn 20™ rather than the size of the SOLAR® Taurus 60™, the latter has been adopted for the cost estimation. The reason behind this choice is mainly related to the state of the art about gas turbine. The SOLAR® Saturn 20™ represents an outdated model if compared to the other products by the same manufacturer. Enhancement in performance and an associated reduction of production costs, because of newer and newer employed production techniques, has substantially affected the cost per net kW. Therefore, comparing the information available in Table V with the other information about the average installation costs for a CHP plant retrieved by literature, The SOLAR® Taurus 60™ is assumed to be the model that better represents an estimation of the expected costs. The estimation of 1,314 USD per net kW as investment cost includes not only those related to the gas turbine itself but also the whole plant design, purchase and installation.

The other expected costs are those related to O&M activities. The sources of information about their estimation are the same adopted for the analysis about investment costs [10][11][12][13][14]. The results of the literature review are collected in Table VI in chapter 2. Here are reported the overall cost for O&M activities, which is 0.0074 USD per kWh for the model SOLAR® Taurus 60™. A summary of the simulation outputs for each of the described costs is presented in Table XIV.

TABLE XIV: SUMMARY OF INVESTMENT COST STRUCTURE.

Size [kW]	**600**	**700**	**800**	**900**	**1000**	**1100**	**1200**	**1300**
Investment [$]	788,400	919,800	1,051,200	1,182,600	1,314,000	1,445,400	1,576,800	1,708,200
O&M [$]	38,478	44,891	51,103	56,464	61,166	65,029	68,227	70,264
Natural gas [$]	485,887	538,387	602,794	669,239	731,648	794,928	857,594	920,884
Electricity [$]	499,346	416,216	335,487	264,899	202,176	149,441	104,639	74,040

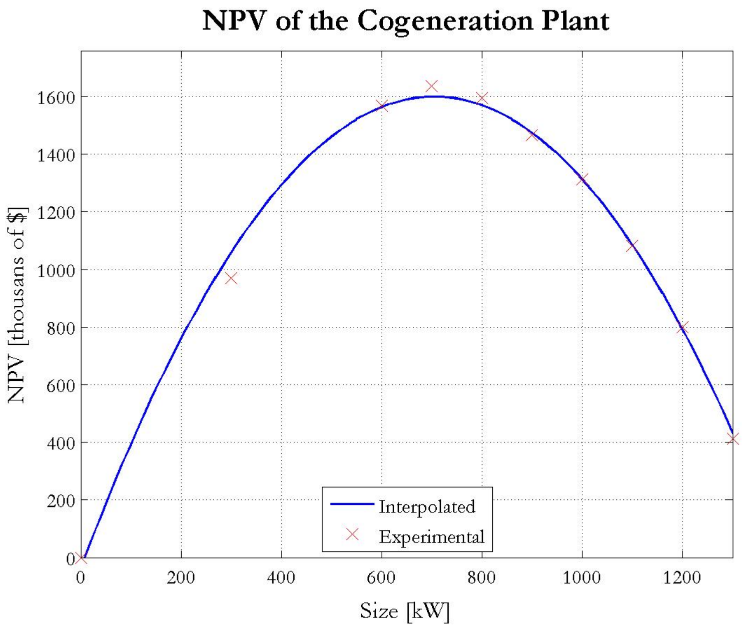

Figure 41: NPV of cogeneration plant.

3.4.3 Results

The obtained results from the economic analysis show the best layout in terms of savings is the one characterized by the installation of a 700 [kW] gas turbine. This result is obtained through an analysis of the NPV for each of the analyzed layout. In order to show the behavior of the NPV for a wider range of sizes, another simulation has been performed for an installed size of 300 [kW]. The NPV has been evaluated over a time period equal to the life of the plant, which has been assumed to be equal to twenty years. The results are shown in figure 41.

In order to completely understand the behavior of the graph two more pieces of information should be provided. The first piece of information concerns the estimated investment costs.

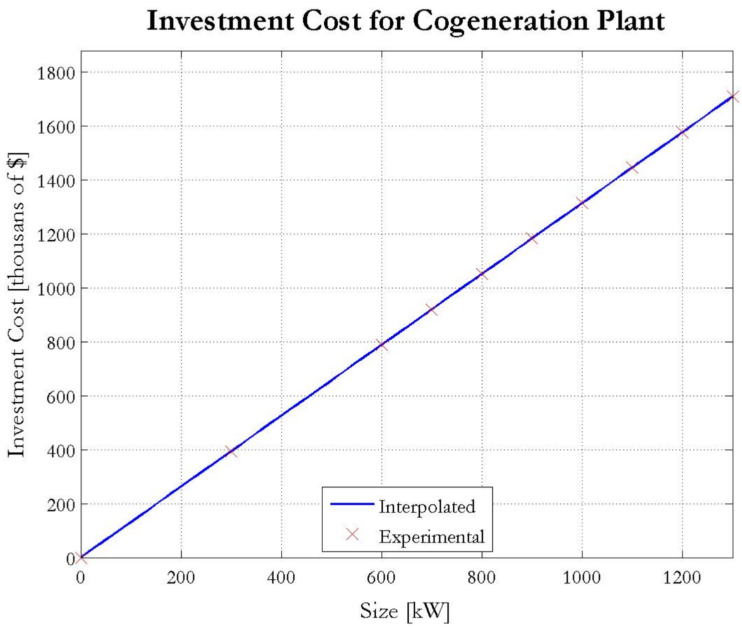

Figure 42: Investment cost for CHP system.

Because of the definition of investment cost as a fixed expense per installed kW, this parameter is monotonically increasing with the size of the gas turbine, figure 42.

Moreover, the annual savings have been evaluated as the difference between the overall management costs of the facility energy supply for the *base model* and the proposed cogeneration layout. The annual management costs are the summation of electricity, natural cost and O&M costs. The *base model* is assumed as a reference to compare the effectiveness of each proposed layout; thus the annual savings with respect to it represent the profits produced by the investment. Looking at figure 43, it is possible to see how the maximum annual savings is reached installing a 800 [kW] gas turbine. This size is the best by not oversize the system, incurring in long partial load operation compromising the production efficiency. The amount of savings produced by the investment like also the investment costs and the NPV for each of the analyzed sizes is reported in Table XV.

TABLE XV: PRINCIPAL ECONOMIC PARAMETERS - COGENERATION.

SIZE [kW]	**600**	**700**	**800**	**900**	**1000**	**1100**	**1200**	**1300**
Investment (1,314 [$/kW])	788,400	919,800	1,051,200	1,182,600	1,314,000	1,445,400	1,576,800	1,708,200
Annual saving [$]	295,303	319,519	329,630	328,412	324,024	309,616	288,554	253,826
NPV [$]	1,568,799	1,636,771	1,595,566	1,466,685	1,313,274	1,082,306	799,840	411,601

Having a more detailed view of the element which determine the NPV value (Investment cost and annual saving), it is possible to understand the shape of the NPV curve. In general the shape of the curve is decreasing for big sizes because of the growing influence of the investments costs, which are not supported by a proportional increase of the produced energy nor a proportional increase of the annual savings. On the other hand the NPV curve has a decreasing shape also reducing the installed size below a certain threshold. This occurs because of the not optimal exploitation of the possibilities of producing energy offered by the facility. As example, the 600[kW] layout results in a plant working at full load for the whole year, however, increasing the size to 700 [kW] an increase of the produced energy without any compromise in terms of efficiency, because the equipment will still work always at full load. The maximum value of

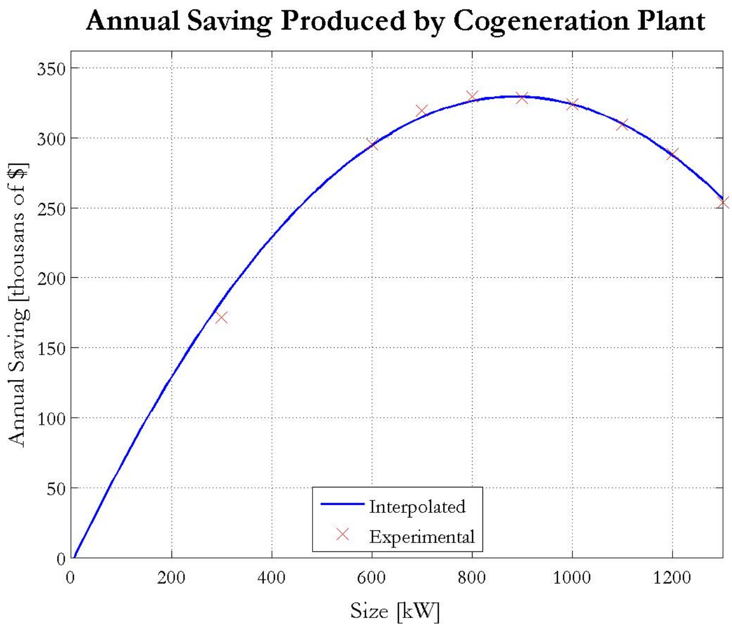

Figure 43: Annual savings for CHP system.

annual savings occurs for the size of 800 [kW], however the higher investment costs does not result in the best size. On the contrary, the 700 [kW] layout is the best size because of the best balance between the low investment cost, which are smaller than the 800 [kW] model, and the annual saving produced.

CHAPTER 4

CHILLER TECHNOLOGIES

Thermodynamics defines heat as that kind of energy which flows from a system to another one at a different temperature. The second principle of thermodynamics explains how this flow of energy takes place naturally only from the system at the higher temperature toward the system at the lower temperature. Chilling a system means remove energy from the system itself through a process which let the energy, under the form of heat, move toward another system at a higher temperature than the initial one. Having this in mind, we can easily understand that is not possible to keep a system, e.g., the spaces inside a building, at a temperature lower than the external environment, unless a device which works in the opposite way of the natural heat flow is used.

In the field of heating, ventilation and air conditioning of buildings (HVAC systems) one of the most popular device used to manage the temperature in buildings, during cooling operations at least, is the chiller. A chiller is a device which performs a thermodynamic cycle whose result is removing heat from a fluid (usually water) and thus decreasing its temperature. This result is made possible thanks to the energy usage of the equipment, therefore the second principle of thermodynamics is not violated. The chilled water is used to cool down the temperature of the supply air of the building's air conditioning system through heat exchangers. Several kinds of equipment, exploiting different technologies, are nowadays available in the market, this analysis will focus on two big families of equipment classified according the thermodynamic cycle performed:

- Vapor compression chiller:
- Absorption chiller:

4.1 Vapor Compression Chiller

The refrigeration cycle is the thermodynamic process which lies at the base of the cooling process and the vapor compression cycle is the most widley applied technology in the field of refrigeration. This kind of equipment represent the preferential choice in case of medium-large size HVAC systems, food preservation processes, chemical plants and automotive air-conditioning. The real thermodynamic cycle performed by the equipment can be approximated by the reverse Rankine's cycle. A representation is depicted in figure 44; figure (a) is the representation on the pressure-enthalpy graph of the cycle, instead figure (b) is the representation of the same cycle on the temperature-entropy graph. A chiller performs the process using four key components:

- Compressor
- Condenser
- Expansion device
- Evaporator

The scheme of the system, depicting how the components are connected, is reported in figure 45, in this figure the same numbers of figure 44 are used to reference the corresponding

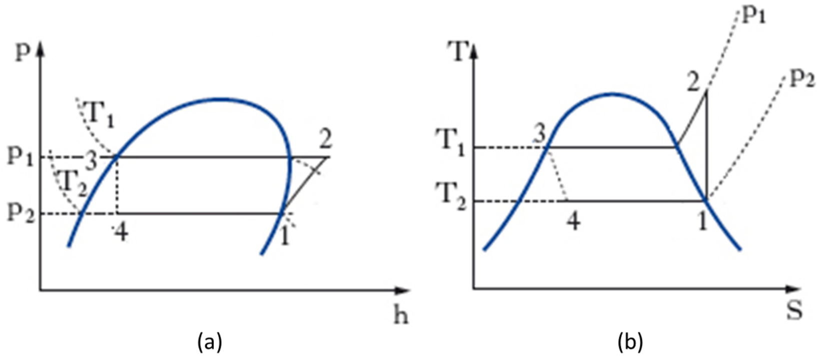

Figure 44: Reverse Rankine's cycle.

points either in the scheme of the plant and in the graphical representation of the thermodynamic process.

The gaseous refrigerant, coming from the evaporator, is compressed through a compressor, obtaining an overheated gas. The overheated gas, which is at a temperature higher than the external one, releases heat toward the external environment. This energy discharge allows the gas to condense in an heat exchanger thus called condenser. When the refrigerant comes out from the condenser it is a saturated liquid. The fluid now passes through the expansion valve. This component causes a pressure drop and let the evaporation process of the fluid start. The following component encountered by the fluid is the evaporator. The pressure level in such component allows the phase change to occur at a temperature lower than the environment's one, thus the energy required by the process is obtained removing heat from the environment, which

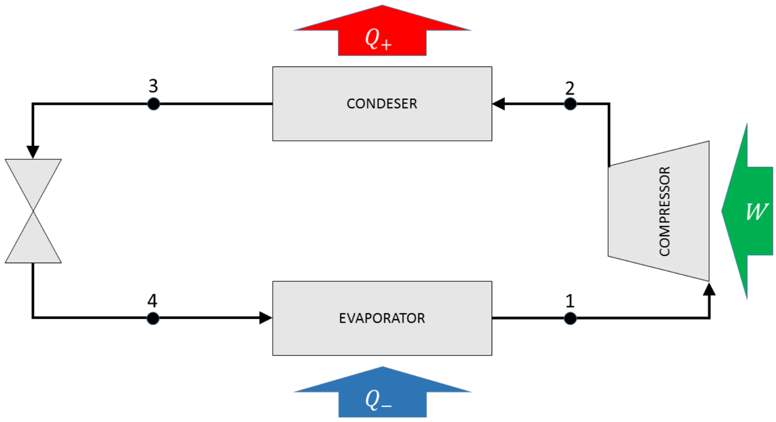

Figure 45: Schematic representation of a vapor compression device.

requires to be refrigerated. The vapor produced is ready to enter the compressor, starting the cycle again. The parameter used to characterize the performance of any refrigerating device is the Coefficient Of Performance (COP). This parameter characterizes the efficiency of the equipment or in other words it provides a measure of how well the energy provided to the device is used, i.e., taking into account that the final goal is the cooling effect. The exact definition of the COP is the following:

$$COP = \frac{Q_-}{W} \tag{4.1}$$

- Q_- Amount of heat removed by the lower temperature environment;
- W Amount of work to perform the cycle.

4.2 Absorption Chiller

Whatever the thermodynamic cycle used, the heat removed from the cooling water by the chiller in the evaporator is used to let the refrigerant undergoes a phase change from liquid to vapor. Because the equipment has to perform a continuous operation it is necessary to bring the vapor back to the liquid phase. An absorption chiller performs this action relying on a thermochemical process rather than the traditional vapor cycle which relies on the compressor. There are two fluids involved in this thermochemical process: the refrigerant and the absorbent. The most important feature of this couple of substances is the high chemical affinity, the main consequence of this property is that one substance dissolves easily in the other one. The capability of the absorber to absorb the refrigerant depends on the concentration of the two substances in the mixture made by both of them. As a consequence the absorption capability decreases when the absorption process takes place. This happens because a higher and higher percentage of refrigerant is dissolved in the mixture. In order to restore the absorbing capability of the mixture it is necessary to boil it and distill the mixture recovering the refrigerant. Letting the mixture boil is an easy way to distill a mixture which has a high concentration of absorber and thus a restored absorbing capability. Over the years only two couples of substances have been used with a wide approval in commercial applications. The first couple is the one made by lithium bromide and water (H_2O—$LiBr$), in this arrangement the water is the refrigerant and the lithium bromide behaves as absorber. The second widespread couple is the one made by ammonia and water (H_2O—NH_3), the absorber in this case is the water and instead the

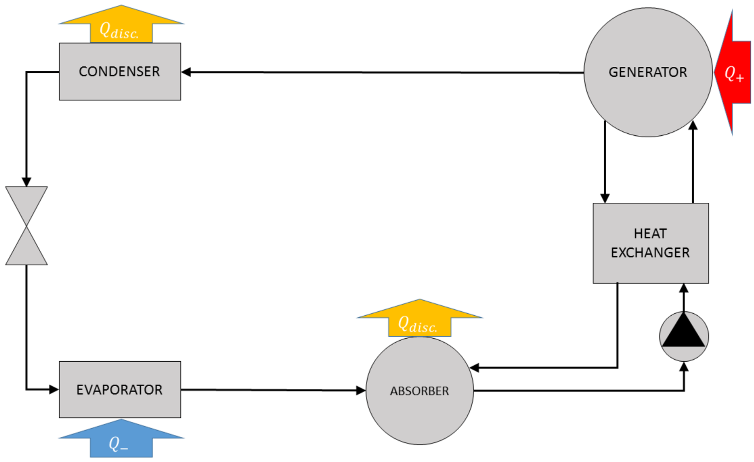

Figure 46: Schematic representation of an absorption chiller.

ammonia is the refrigerant substance. Under a thermodynamic point of view, the refrigerating cycle works using three different thermal sources at three different temperatures:

- The low temperature source is the environment which needs to be refrigerated (in the heat pump arrangement the outdoor environment is the coldest source);
- The intermediate temperature source is the external environment in which the heat is discharged (in the heat pump arrangement the indoor environment is the intermediate temperature source);
- The high temperature source is the one which provides the heat to the refrigerating cycle (it is commonly represented by a burner or a hot fluid which transfers heat from an external source);

The device is constituted by a low pressure side and a high pressure side. The low pressure side is composed by the absorber and the evaporator. Looking at figure 46 as a reference: in the evaporator it is possible to find the mixture with a high amount of refrigerant, here the refrigerant evaporate to remove the heat from the low temperature source. The evaporated refrigerant is absorbed by the mixture which is in the absorber and which is rich of absorbent. This is a direct consequence of the fact that the refrigerant in the mixture has a value of surface tension which is lower than the value of pressure in the evaporator. This capability to remove the evaporated refrigerant from the environment allows the evaporation of more and more refrigerant without any change in the value of pressure in the evaporator. An increase in the pressure of the evaporator would have the undesired effect to interrupt the absorption process of the refrigerant. On the other hand the increasing content of refrigerant in the mixture (thus a low value of concentration of the mixture) has to be countered. This goal is achieved using a pump to remove the mixture formed in the absorber and to move it to another part of the equipment to properly treat it. The goal of the pump is not only to move the mixture against the pressure losses of the circuit but also to rise up the pressure of the mixture to the maximum level of the whole process. The pump release the mixture in the generator. The high pressure side of the equipment is thus constituted by the generator and the condenser. The generator is the component where heat is provided from the outside source to let the evaporation process of the refrigerant take place. As said before, the external source of heat can be a combustion process which takes place in a burner (Direct fired equipment), or as an option could be used heat from an external source such as the waste heat from a cogeneration prime mover. The gaseous refrigerant produced in the generator is than condensed releasing heat to the intermediate temperature source, which is the external environment in the refrigerator arrangement. After the condensation process takes place, the fluid is expanded in an expansion valve. During this process, the fluid reduce its pressure and it is headed to the evaporator, the cycle is thus completed.

Considering the whole equipment, the refrigerant is not the only fluid which undergoes a passage through an expansion valve. Indeed the mixture rich of absorber, which is distilled in the generator, undergoes the same process as the refrigerant in a different valve. This mixture has to pass through another expansion valve to come back to the absorber and bring the correct concentration back in the absorber itself. So it is clear at this point how the equipment is divided under the point of view of pressure values. Two environments at two different temperature are required to let the equipment work. The high pressure side of the equipment is constituted by the condenser and the generator (the high pressure let the refrigerant undergo a phase change at a temperature which is higher than the one of the surrounding), on the other hand the low pressure side of the equipment is constituted by the absorber and the evaporator (the low pressure let the refrigerant undergo a phase change at a temperature which is lower than the one of the surrounding).

In order to enhance the performance of the absorption chiller a heat exchanger is commonly used. It is used to preheat the low concentration mixture which comes from the absorber and which is directed to the generator. This process is possible thanks to the heat available from the hot high concentration mixture which comes out from the generator. It is obvious how this process enhance the performance of the equipment reducing the amount of heat required to distill the mixture in the generator. Another important consequence of the introduction of the heat exchanger is the reduction in the reduced amount of heat which has to be removed by the absorber, because of the reduced temperature of the high concentration mixture which go inside the component. The absorber is always equipped with a cooling circuit (usually it is the same circuit which removes the heat from the condenser) to remove the heat form the evaporation process, the heat produced during the mixing (exothermic process) and the heat from the overheated mixture from the generator.

4.2.1 Performance Analysis

The performances of this kind of equipment is evaluated in the same way as the other refrigerating equipment, using the coefficient of performance (COP). Although its definition is not always the same throughout the literature and the technical files provided by companies, for this kind of equipment two different value of the COP has to be defined. The first one is the thermal COP, which is defined as:

$$COP_T = \frac{Q_-}{Q_+} \tag{4.2}$$

- Q_- Amount of heat removed by the low temperature source;
- Q_+ Amount of heat provided to the generator;

The second one is the electric COP, which is defined as:

$$COP_T = \frac{Q_-}{Q_+} \tag{4.3}$$

- Q_- Amount of heat removed by the low temperature source;
- Q_+ Amount of work to perform the cycle;

In an absorption chiller the most of the work is required, under the form of electricity consumption, by the pump for recirculating the mixture. Typical values of the thermal COP for a single effect equipment ranges between $0.6 - 0.8$.

Higher values of COP are achieved using double effect absorption chillers. In a double effect absorption chiller the generator is divided into two different sections: the high pressure section of the generator and the low pressure section. In the high pressure side, the external heat is used to distill the low concentration mixture, this process allows to separate the evaporated refrigerant and the liquid mixture which is rich of absorber. The steam is sent to the low pressure side of the steam generator. The pressure level in this environment allows the steam production at a lower value of temperature, so it is possible to use the steam produced in the high pressure side as heat source for the process. This more sophisticated equipment can work at higher efficiency, typical value of the thermal COP is around $1.1 - 1.35$. Although the value of the COP is higher than the single effect equipment, the technical requirements of the double effect absorption chiller has to be taken into account. This kind of chiller has to be fed with a higher temperature heat with respect to the single effect absorption chiller. Analyzing the health care facility thermal needs, the gas turbine exhaust temperature and the higher investment costs, it has been chosen to adopt a single stage absorption chiller as the most feasible and profitable solution.

It is worth noticing that the values of COP of an absorption chiller are much lower than those obtained by a traditional vapor compression chiller. However, this does not represent a big practical issue. The reason lies in the fact that the energy source employed to run the equipment is not a valuable one. The absorption chiller requires thermal energy at a relatively low temperature level, which is, under a thermodynamic point of view (and usually also under an economical point of view) less valuable with respect to the electric energy required to run the traditional vapor compression chillers. The main advantages provided by this technology are:

- The possibility to recover waste heat from other processes;
- The use of refrigerants which are not harmful to the environment and the atmospheric ozone (water);
- The high value of reliability provided by an equipment which has few moving components;
- The long operational life which is even longer than 20 years for the not direct combustion equipment;
- The very low amount of noise and vibrations during the operational phase;
- The reduced consumption of electricity, which is an important feature in all the situations where continuity in operation is a key factor;
- The good performance in partial load operation.

Moreover, the low electricity consumption is an important feature, also in the direct flame arrangement, in all those situations where the electrical grid is not available or it is too expansive to create a connection. Changing point of view and looking at the technologies from a wider perspective, it is clear how this technology, whatever the type of power supply, could represent an interesting opportunity to reduce the constantly increasing summer load peaks of the electricity demand. With this mind it would be interesting to look at this technology as a way to reduce the problems in delivering energy; this is what usually happen during summer months when the grid is usually overloaded. Furthermore the increasing usage of gas in summer months could provide a compensation to the peak of gas usage in winter months. Flattening the consumption profiles would optimize the production and the efforts in terms of logistics to produce and deliver these resources. Obviously absorption chillers are not free of disadvantages. First of all the higher cost with respect to a vapor compression equipment of the same size and also another important feature is the low value of COP (despite of the previously made observations). An additional drawback, which gives a contribution to the high plant cost, is connected to the need of keep the absorber internal temperature always under control. This is usually made using cooling towers for the absorber cooling system. This issue rises in case the mixture employed in the plant is H_2O—$LiBr$ because lithium bromide deposits are possible as well as crystallization phenomena.

4.2.2 Crystallization

The crystallization is a phenomenon which can occur in the absorption chiller using H_2O—$LiBr$ as a working fluid. The crystallization of lithium bromide occurs in the generator when too high concentration of lithium bromide are reached (i.e. when the temperature of the generator is raised up too much). The deposition of lithium bromide in solid state causes the formation of a layer in the internal surfaces reducing performance because of the reduced capability to exchange heat. Over time, this phenomenon leads to the complete stop of the equipment when the most of the salt in the circulation loops of the equipment is in a solid state causing the choking of the pipes. The leading causes could be:

- Air infiltration in the equipment due to leakages;
- Too low condenser temperature;
- Overload of the equipment or too high generator temperature;
- Sudden and prolonged stop of the equipment;
- Ineffective maintenance.

To avoid this deleterious phenomenon modern absorption chillers are equipped with sensor and dedicated actuators which allow to avoid this phenomenon recirculating the working fluid and changing operative parameters.

4.3 Off-Design Condition

An analysis of off-design condition is of utmost importance for the absorption chiller. This is due to the key position performed by this component in the layout of a trigeneration system.

The absorption chiller is controlled by the waste heat obtained by the prime mover of the plant, which in turn is driven by the electric load profile required by the user. The whole system is governed by the electric demand, which shows a variable profile through the year. Taking this into account, it is obvious how it is important to know the off-design behavior of the absorption chiller to analyze the performances of the trigeneration system and to provide a continuous cold supply to the facility. The analysis is performed analyzing the most important variable parameters and comparing the information available in literature with the forecast performance provided by the absorption chiller model implemented in eQuest®.

4.3.1 Chilled Water Temperature

One of the important parameters in the management of an absorption chiller is the temperature of the chilled water (CWT). The parameter of interest is always the thermal COP and what it is important to know is how it changes with the change in the temperature level of chilled water required by the user. De Vega shows through experimental measures the effect of the changes in CWT on the thermal COP [22]. The result is the decrease of the COP when the CWT is decreased. The variation in the evaporator temperature, which in turn represent the variation in CWT (if all the other parameters are kept constant), has a strong effect on performance. This is showed in the analysis done, indeed a CWT variation from 285 [K] to 275 [K] can cause a reduction of COP around 21%. The measures are taken at a constant condenser temperature and at a constant generator temperature.

The same trend is forecast by the model of the absorption chiller available on eQuest®. The model provides the results in terms of the capacity percentage that is the ratio between

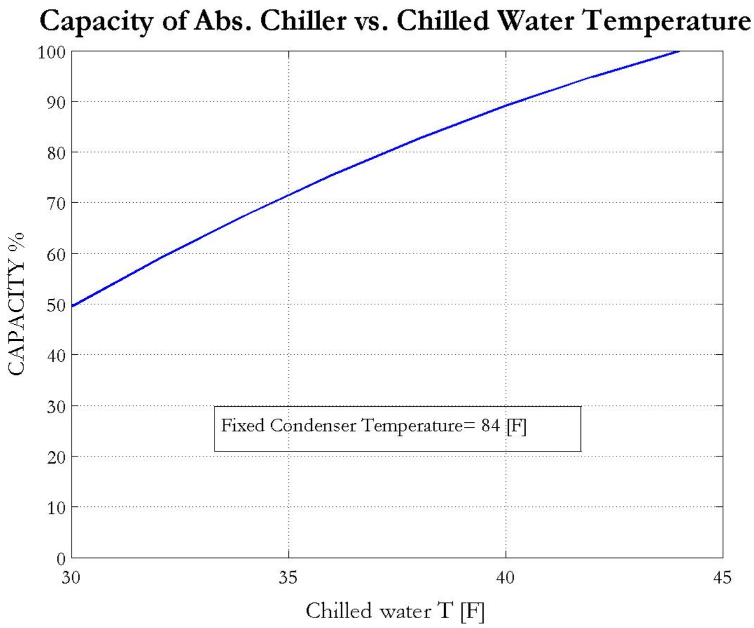

Figure 47: Capacity of absorption chiller vs. chilled water temperature (eQuest Model).

the real cooling capacity and the cooling capacity in design condition. Being all the other parameters kept constant the variation in capacity is connected to the variation of the thermal COP. So it is possible to use this analysis as an analysis on the behavior of the thermal COP. The representation of the eQuest® model results is provided in figure 47. The curve shows how a reduction of CWT produces a reduction of the cooling capacity (and thus in thermal COP). Although the trend is the expected one, comparing the off-design performances of this model whit the experimental values obtained by De Vega is highlighted is how efficiency forecast by the model degrades faster.

4.3.2 Condenser Temperature

The effect of condenser temperature, which can be approximated by De Vega's cooling water inlet temperature [22], on performances can be seen as the direct result of a variation in the outdoor temperature. This is strictly true for the air cooled equipment and it is also true for a water cooled equipment under the assumption of constant rejected thermal power of the water cooling system. As it is shown in De Vega's work, the effect of condenser temperature variation, has a strong influence on the thermal COP and on the evaporator heat transfer (which represents a measure of the cooling capacity). The measurements has been made at a constant evaporator temperature and at a constant generator temperature. Increasing the condenser temperature produces deleterious effects on both the thermal COP and the cooling capacity of the absorption chiller. The work made by De Vega shows how variations of the condenser temperature between 298 [K] and 313 [K] produce a reduction in thermal COP up to 20% and a reduction of the cooling capacity up to 50% for the tested equipment. The lower is the temperature of the generator, the higher is the relative effect on chiller performances. Such behavior is the same for the eQuest® model, a curve about performances in off-design condition is provided in figure 48 and figure 49.

4.3.3 The Generator Temperature

Only qualitative information are provided about the effects of generator temperature changes because of the particularity of the case studied. The layout of trigeneration system has some constant features which constitute a restriction in the possible operation of the equipment itself. One of those features is the direct link between the prime mover from which the heat is recovered

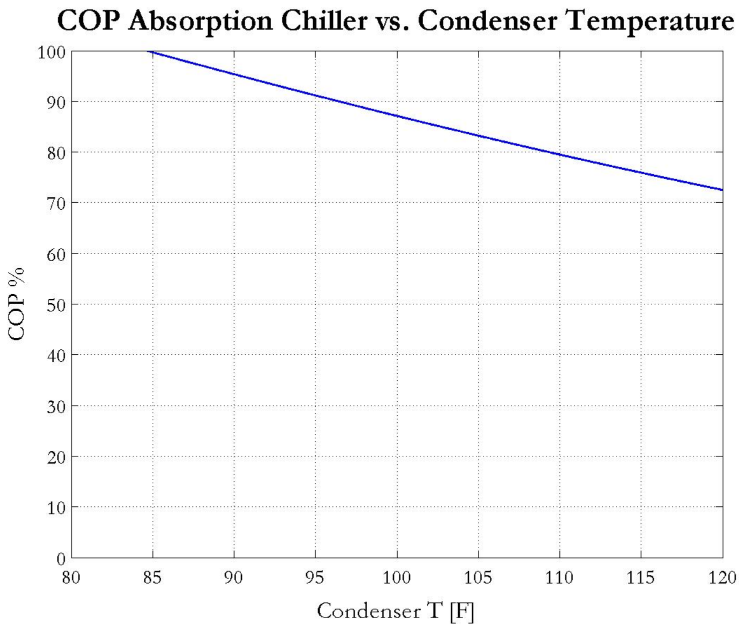

Figure 48: COP absorption chiller vs. condenser temperature (eQuest Model).

and the absorption chiller where the heat is employed. The most important resource in terms of recoverable heat, whatever the prime mover employed is, is constituted by the exhaust gas. During operation the temperature of the exhaust gas is a roughly constant parameter. On one hand this feature ensures a reliable source of heat, but on the other hand it results in a substantially fixed feeding temperature of the generator of the absorption chiller. Having this in mind, it is obvious the reason why no extensive analysis is performed on the effect of the variation of this parameter on the performance of the chiller. Despite of everything few key information are reported. The equipment performances increase directly with the temperature of the generator, although the effects are less pronounced than those caused by

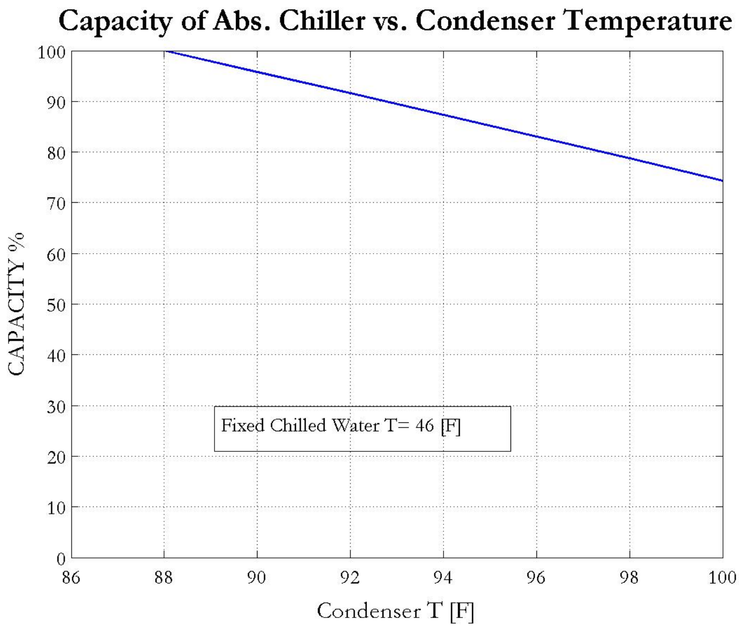

Figure 49: Capacity of absorption chiller vs. condenser temperature (eQuest Model).

the condenser temperature variation or the evaporator temperature variation, i.e., which is the CWT. Increasing the temperature of the generator the mass flow rate of the refrigerant circulating increases, because of the enhanced heat transfer and thus the higher amount of evaporated refrigerant. The higher generator temperature causes also other consequences, such as the increase of the condenser pressure (because of the larger amount of vapor produced). This results in a higher temperature at the condenser; this is the reason why in case of large value of outdoor temperature, an increase in the generator temperature is required to let the equipment work without compromising the heat exchange. Usually the generator temperature is a key factor in the design process because from this parameter depends the concentration of lithium bromide in the generator and the possibility of crystallization phenomenon to occur.

4.3.4 Partial Load Ratio

The last parameter studied in this analysis is the partial load ratio. The importance of the effect of a reduced cooling load on performance has a big importance on the effectiveness of the solution proposed to satisfy the cooling load of the health care facility. The reason lies in the fact that during the cooling season, especially at the beginning and at the end of the season, the equipment has to satisfy a reduced cooling load if compared with the design size of the equipment. This happens because the equipment is sized starting from the information on the maximum amount of recoverable heat, i.e., the availability of the energy resource, from the prime mover and not on the average value of the requested cooling capacity through the year. The chiller is oversized with respect to the real cooling needs in some period of the year, thus the equipment has to work at very low cooling load. In other words, defining the partial load ratio as the ratio of the real cooling capacity to the design capacity, at very low value of PLR. If the chiller does not show good performances in such condition, the proposed solution could become a not feasible one. The performance curve provided by eQuest® and reported in figure 50, represents an unacceptable solution because of the very poor performance in off-design conditions. The model was probably developed a long time ago, resulting in a very old and inefficient kind of equipment compared to the newer available in the market. This strict judgment is due to the sudden drop in performance at partial cooling load which represents an

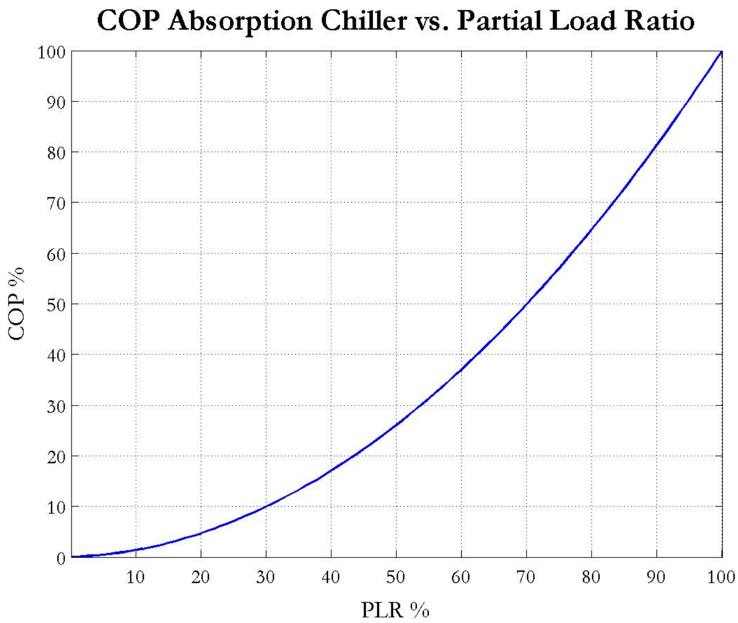

Figure 50: COP absorption chiller vs. partial load ratio (eQuest Model).

unrealistic situation for the latest generation of absorption chillers, which instead have one of their strength point in partial load performances.

4.3.5 Chiller Behavior in Off-Design Condition

The behavior in terms of performance of the absorption chiller is the result of the management of several parameters such as the cooling capacity, the generator temperature, the condenser temperature and the evaporator temperature. If one of those parameters changes, all the other parameters have to change during the operation in order to meet the required load. Usually the CWT is a fixed parameter which depends on the requirement fixed by final user, i.e., the coils of the HVAC system. The same consideration counts also for cooling capacity. However, the chilled water temperature is fixed during operation rather than the cooling capacity, which is the target to follow. The condenser temperature is an unplanned variable depending on the external temperature (it is not taken into account the management of the cooling system which can change its working condition in order to keep constant the condenser temperature) and the only real possibility to manage the system lies in the management of the generator temperature.

In order to better understand the way in which the absorption chiller works an example is provided analyzing the performance of the equipment studied by De Vega [22]. The following analysis is possible for any kind of absorption chiller in all those situations in which the off-design performance curves are available. Starting from the charts provided by the author the following situation is analyzed. The absorption chiller is assumed to provide 7 [kW] cooling capacity producing chilled water at 286 [K]. This situation, looking at the curves, could be achieved feeding the chiller with hot water at 358 [K] if the cooling system of the equipment can keep the condenser at 308 [K]. But if the condenser temperature rises up to 313 [K], in order to meet the load (in terms of both cooling capacity and temperature) the generator has to be kept at a higher temperature than the initial case, in the specific case the value is 370 [K]. Unfortunately, it is not always possible to manage the temperature of the generator, this is true when the generator is fed by the recovered heat provided by an independent equipment, e.g., trigeneration systems. When the generator temperature is a constant value and the condenser temperature is raised up, the result is a reduced cooling capacity. Analyzing the performance of the equipment studied by De Vega when the generator temperature is 373 [K], the chilled water temperature is always 286 [K] and the condenser temperature is raised up to 313 [K], the final result is a reduction of the cooling capacity to 3 [kW]. The final consideration about the absorption chiller seems to be extremely positive because it seems that any external condition can be managed by the equipment. This is not true at all because of the previously mentioned crystallization phenomenon.

4.4 Absorption Chiller Model Improvement

Although the models comparison between the eQuest® model and the one referring to the equipment studied by De Vega has shown in most of the cases a good correspondence about the overall qualitative behavior of the equipment, the model is not good enough in terms of quantitative values of forecast COP and capacity in off-design condition if compared with the current equipment available on the market. The eQuest® piece of software suffers the obsolescence of some of the models available in its database, which is updated to the early releases. Nowadays technology and manufacturer have made great enhancement to this kind of equipment, especially because of the growing interest in this technology by the market. For example, the introduction of a variable speed pump to recirculate the mixture is one of the solutions for improving the performance in partial load conditions. This improvement allows the equipment to operate at high values of COP in off-design condition also for very low value of PLR, placing this kind of technology in a preferential position compared to other solutions when unstable cooling loads have to be satisfied. Thus a new model of absorption chiller is developed for the eQuest® piece of software starting from the specifications of an equipment produced by YORK®. The analyzed equipment is the MILLENNIUM YIA™ Single-Effect

Absorption Chillers, an absorption chiller produced to satisfy cooling loads from 420 [kW] to 4840 [kW]. All the performance curves are built starting from the manufacturer specification provided in the technical data sheet of the manufacturer [23][24]. The piece of software requires the mathematical definition of seven curves to properly produce a model of a single stage absorption chiller.The required curves can be reduced to five in the case studied, under some simplifying assumptions which will not effect the effectiveness of the proposed model.

- COP percentage vs the condenser temperature;
- COP percentage vs the chilled water temperature;
- COP percentage vs the partial load ratio;
- Capacity percentage vs the condenser temperature;
- Capacity percentage vs the chilled water temperature.

4.4.1 Chilled Water Temperature

As explained in the previous passage the effect of changes in CWT have a relevant effect on the performance of the absorption chiller if compared with other parameters. The manufacturer does not provide in its specification direct information on how the thermal COP changes with the CWT, thus the curve about the COP is built starting from other information provided by YORK®. The first information directly available from the producer is the behavior of the cooling capacity with the CWT. Starting from the experimental points obtained by the manufacturer, an interpolation is performed to obtain the mathematical definition of the curve. The result is presented in figure 51 and the definition obtained provides an estimation of the

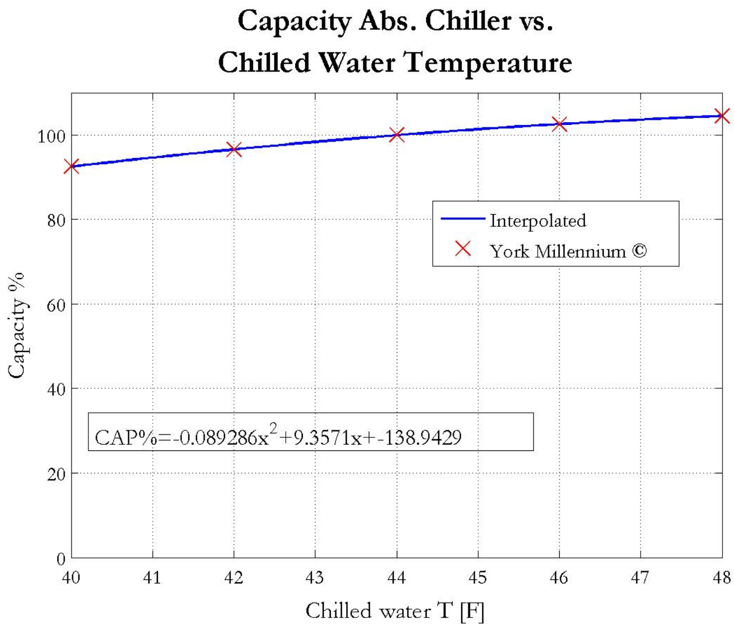

Figure 51: Capacity absorption chiller vs. chilled water temperature.

percentage of cooling capacity available with respect to the design capacity if the temperature is expressed in Fahrenheit degree.

$$Cap\% = -0.0893x^2 + 9.3571x - 138.943 \tag{4.4}$$

The 100% of capacity, which represent the design capacity, is provided at 44 [F] chilled water temperature and 85 [F] condenser temperature. They represent the ARI 550/590 standard to evaluate the performance of chillers [25]. Because of this, in this analysis the operative condition point defined by ARI 550/590 standard (44 [F] CWT and 85 [F] Condenser T.) has been adopted as a reference point to normalize the percentage performance of the equipment. In the figure 52

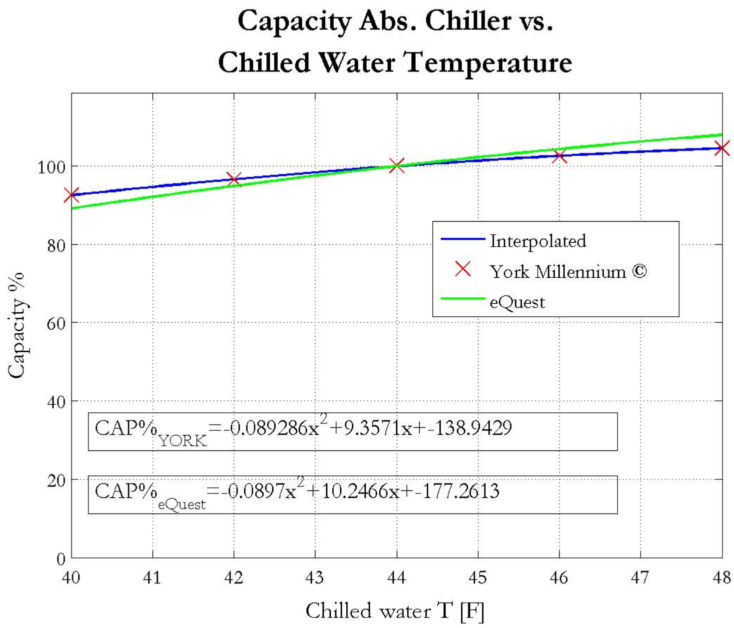

Figure 52: Capacity absorption chiller vs. chilled water temperature.

is proposed the comparison the new proposed trend and the default model available on eQuest®. The latter shows a steeper curve, resulting in a more sensible dependence on CWT variation. The eQuest® model is described by Equation 4.5.

$$Cap\% = -0.089x^2 + 10.247x - 177.261 \tag{4.5}$$

The second important information provided by YORK® is about the variation of fuel consumption according to changes in CWT. The meaning of the word fuel consumption has to be interpreted as the thermal energy consumption of the equipment, regardless of how this heat is produced, e.g., hot water, steam or direct flame device. Once again, starting from the

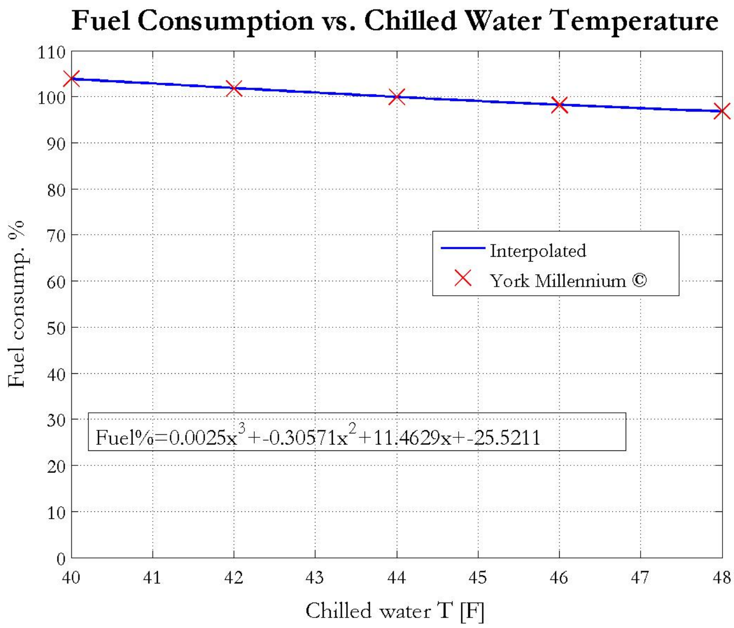

Figure 53: Fuel consumption vs. chilled water temperature.

experimental points obtained by the manufacturer, an interpolation is performed to obtain the mathematical definition of the curve, the result is plotted in figure 53.

$$FuelC.\% = 0.0025x^3 - 0.306x^2 + 11.463x - 25.521 \tag{4.6}$$

The last important parameters to define the performance of an absorption chiller in off-design condition is the trend of the COP due to variation of CWT. These information are not directly provided by the manufacturer, thus through some hypothesis those value are obtained. The COP percentage is defined as the ratio of the real COP in specified condition and the

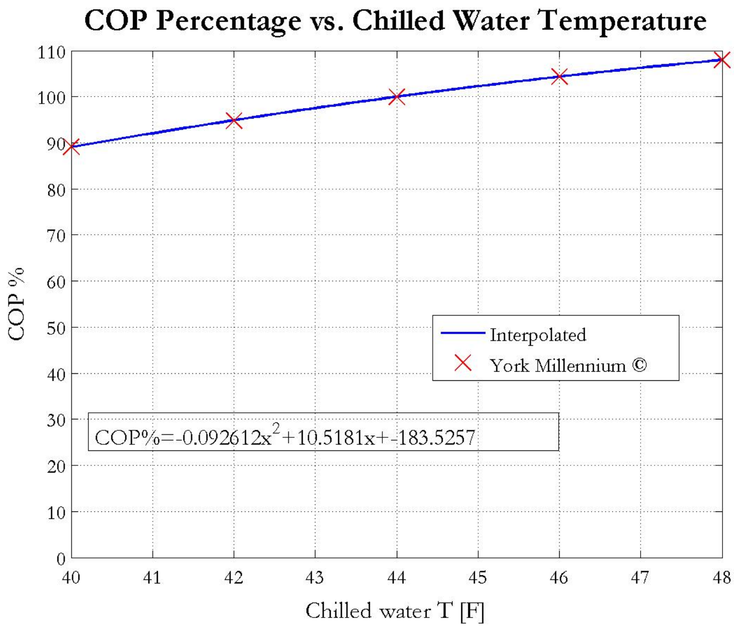

Figure 54: COP percentage vs. chilled water temperature.

design value. Through some algebra it is possible to show as it is equivalent to the ratio of the percentage variation in cooling capacity to the percentage variation in fuel consumption.

$$COP\% = \frac{COP}{COP_{des}} = \frac{\frac{Cooling\ Capacity}{Fuel\ Cons.}}{COP_{des}} = \frac{\frac{(Cooling\ Capacity)_{des} \cdot Capac.\%}{(Fuel\ Cons.)_{des} \cdot FuelCons.\%}}{COP_{des}} = \tag{4.7}$$

$$COP\% = \frac{COP_{des}\frac{Capac.\%}{FuelCons.\%}}{COP_{des}} = \frac{Capac.\%}{FuelCons.\%} \tag{4.8}$$

Thus is demonstrated how the required information about the COP percentage variation can be obtained as the ratio of the previously analyzed experimental points. The result is shown in figure 54.

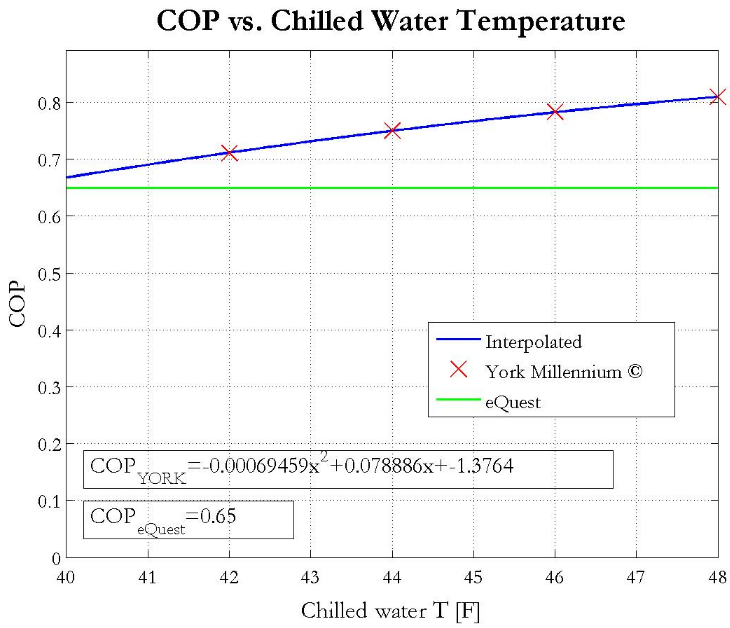

Figure 55: COP percentage vs. chilled water temperature.

$$COP = -0.093x^2 + 10.518x - 183.526 \tag{4.9}$$

Comparing the model produced in this study with the default model available in eQuest®, what is highlighted is how this second model does not take into account the effect of CWT variations on COP. Looking at figure 55, it is possible to see how the replacement of a flat curve with the new model provides better performance for the absorption chiller. The equation describing this behavior is:

$$COP = 0.65 \tag{4.10}$$

Although a complete analysis about the importance of CWT effects is provided, further assumption is made to simplify the eQuest® model. In the case studied , but this is not a general assumption, the plant requires CWT always at the same temperature of 44 [F]. This is a constrained parameter set using the options provided by eQuest®. Because of this situation the model will never experience the necessity to evaluate performances at different values of CWT other than 44 [F]. Starting from this assumption the other performance curves are normalized to obtain 100% of cooling capacity and COP at the design condition (ARI 550/590), while the curves produced about chilled water temperature are omitted during the implementation on the software, setting a constant value in the required part of the code.

4.4.2 Condenser Temperature

In order to evaluate the performance changes due to the effect of the condenser temperature, the analysis start from figure 56, provided by YORK®. The chart shows the relation between the energy input, which is a synonym of the term fuel consumption, requested by the equipment and the cooling capacity produced at several condenser temperatures. The implied assumptions is about the chilled water temperature which is kept constant at 44 [F] (the design value). The chart provide information for PLR higher than 10%, this is the minimum ratio of the cooling capacity which can be satisfied by the equipment. Starting from figure 56 and fixing the value of the partial load ratio it is possible to produce a curve which describes the behavior of the thermal COP at several condenser temperatures. As usual, at each experimental point the thermal COP percentage is evaluated as the ratio of the actual capacity divided by the actual

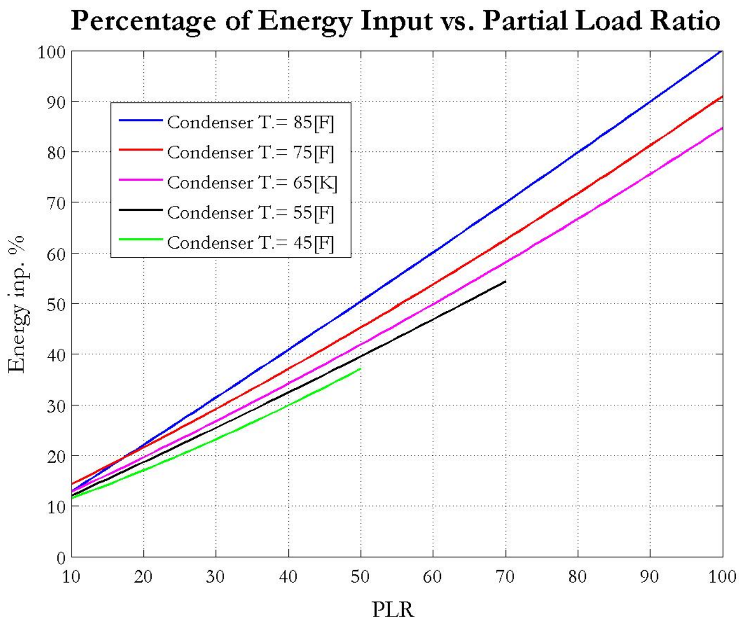

Figure 56: Percentage of energy input vs. partial load ratio.

heat request, as seen in Equation 4.9 for the COP percentage. The result for a partial load ratio of 90% is reported in figure 57.

$$COP\% = -9.77E - 4x^3 + 0.22x^2 - 16.79x + 565.48 \tag{4.11}$$

Comparing the previous result with the performance of the default model in eQuest®, is possible to see how the new correlation offers the possibility to operate at higher COP whetever the external temperature (and thus the condenser temperature) is. The result is depicted in figure 58

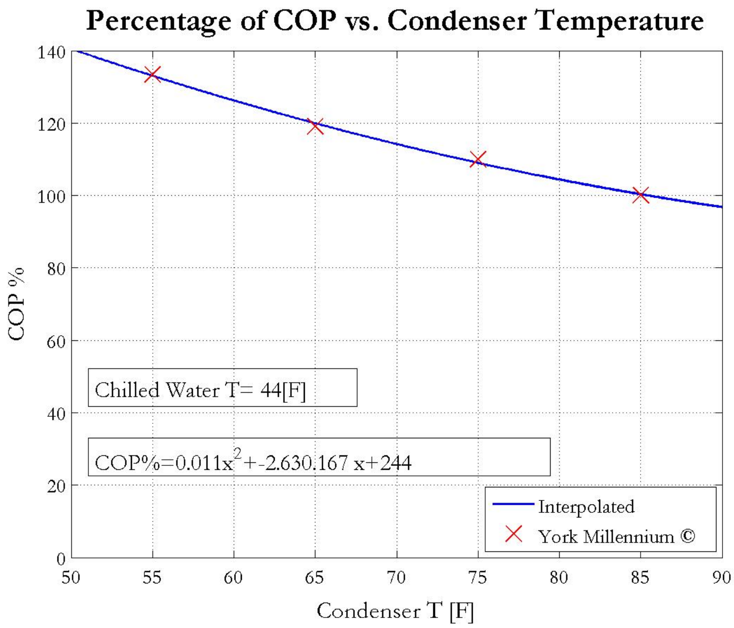

Figure 57: Percentage of COP vs. condenser temperature.

Proceeding with the same approach used to produce the graph in figure 57, it is possible to obtain a graph where the relation between the cooling capacity and the condenser temperature is shown. The curves in figure 59 represent several values of the percentage energy input and the implied assumption is always the constant value of the CWT, which is 44 [F]. The design capacity is reached at full load condition (red curve), for a condenser temperature of 85 [F], according to the ARI standard [25]. The experimental points are fitted to obtain the forecast performance of the equipment within the possible range of condenser temperature.

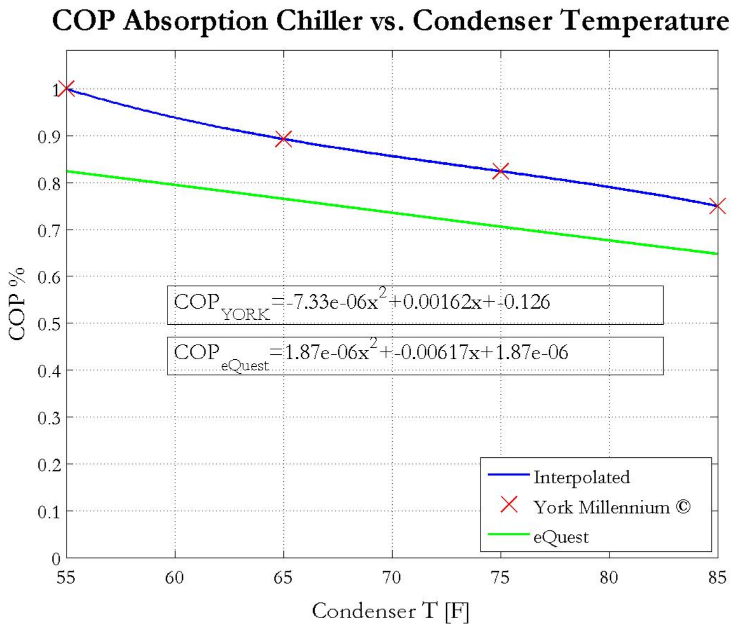

Figure 58: COP vs. condenser temperature.

4.4.3 Partial Load Ratio

As explained in the previous paragraph big improvements are expected for a new generation equipment with respect to the forecast performance available on eQuest®. Once again starting from the experimental measures and for different values of the condenser temperature the COP percentage is estimated and the result are shown in figure 60. The mathematical definition proposed refers to the standard condenser temperature of 85 [F].

$$COP\% = -3.36E - 5x^2 - 0.0049x + 0.578 \tag{4.12}$$

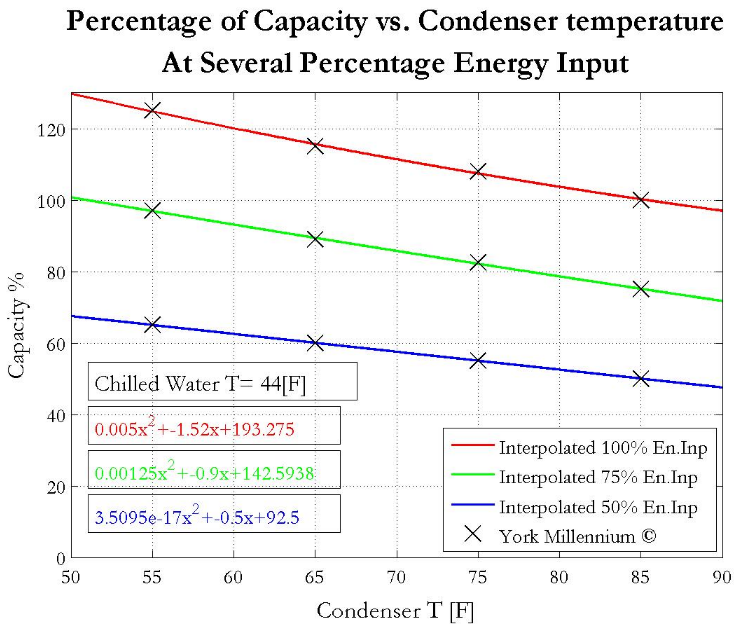

Figure 59: Percentage of capacity vs. condenser temperature at several percentage energy input

If compared with the graph about partial load performance of figure 60, the improvements are extremely clear and confirm the assumption on the obsolescence of the default model available on eQuest® and the need to produce a newer one. In figure 61 is proposed a comparison between the new model and the previous one. The new model provides better off-design performance than the other. The latter does not reflect the forecast good performance of the absorption chiller at low PLR. Its behavior is described by Equation 4.13

$$COP\% = 6.226E - 5x^2 + 0.00028x + 3.26E - 5 \tag{4.13}$$

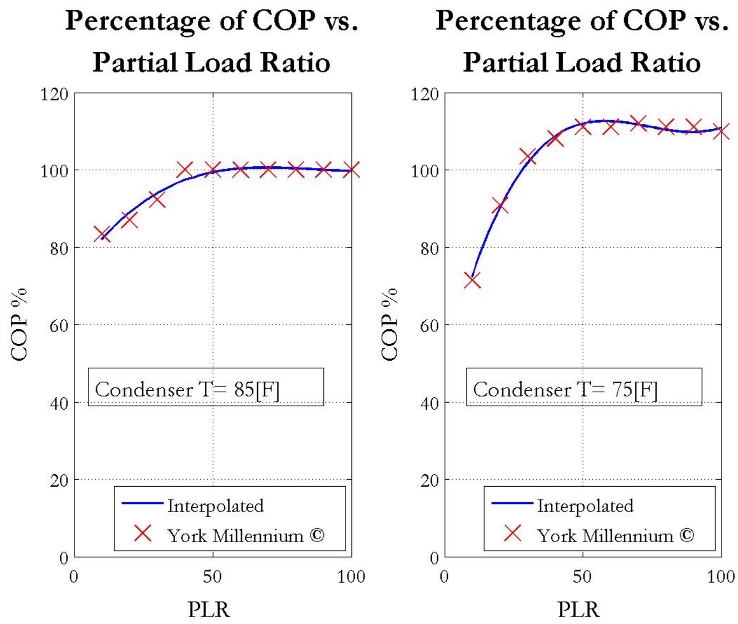

Figure 60: Percentage of COP vs. partial load ratio

4.4.4 Conclusion

The implementation on eQuest® of the MILLENNIUM YIA™ Single-Effect Absorption Chiller model provides a big enhancement to the capability of the software to effectively simulate the performance of a trigeneration system made by up-to-date components. The importance of the exact evaluation of the performances of this component lies in its key position in the system, this component links the energy production system (through the recoverable heat) with the cooling system of the building. Increasing the complexity and also the costs of the whole plant it is important to have the best up-to-date model to estimate the maximum possible

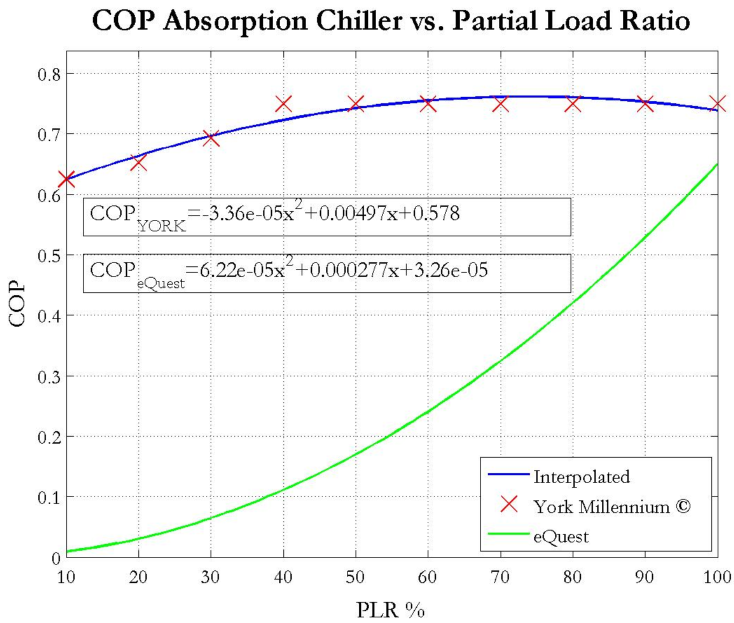

Figure 61: COP vs. partial load ratio

production of the device to properly analyze the economical feasibility of the trigeneration plant.

CHAPTER 5

TRIGENERATION

In trigeneration field, fossil fuel is used for the production of electricity while thermal energy is recovered from the prime mover. The thermal energy recovered has the dual purpose to satisfy the heat demand of the facility and to be used in an absorption chiller to satisfy the cooling load of the facility through the production of chilled water. Although the most of the research carried out on trigeneration have been produced in the last years, the increasing interest in this field is the clear result of the undeniable highlighted advantages of using trigeneration to satisfy the energy demand of final users [26]. The suitable facilities for installing a trigeneration system are basically the same previously described referring to the possible users of a cogeneration system, with the additional feature of cold demand.

5.1 An Overview

The efficiency of electricity generation processes varies widely with the employed technology. However, despite of the technology adopted, the average production efficiency of conventional power plants, based on single prime movers, usually does not exceed the 40%. In a traditional coal plant, for example,only about 27-32% of the fuel's energy content is delivered in the form of electricity to the electrical grid. Improvement in applied technology allows power plants, known as integrated gasification combined cycle (IGCC), to reach efficiency levels above 60%[27]. Compared with the single production of electricity, the trigeneration technology allows the

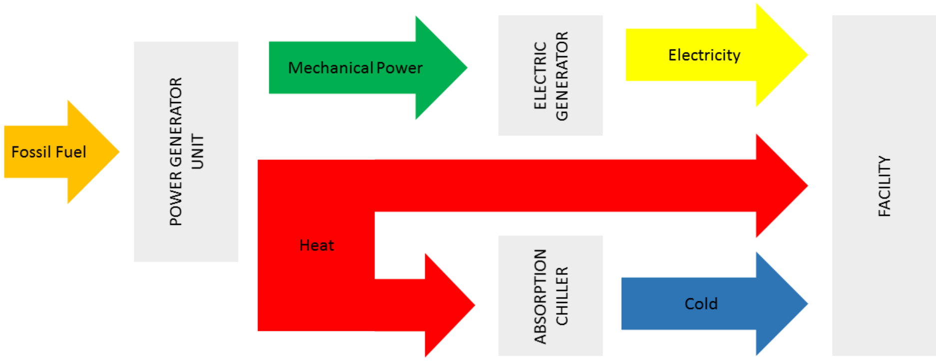

Figure 62: Logical scheme of fuel energy content exploitation.

overall efficiency of the plant to increases because of the better usage of the energy content of the fuel, figure 62. The recovery of the waste heat, through the direct utilization (cogeneration) or through the utilization as primary source in an absorption cycle (trigeneration), allows the generation plants to reach efficiency as high as 85% [26].

In a trigeneration plant the recovered energy from a generation unit, such as a gas turbine, is used to drive both the heating and cooling systems of the facility, which represents the thermal energy loads for the plant. Therefore, because of the better usage of the primary energy source, the installation of such a plant causes an improvement of the overall efficiency of the energy supply side and a reduction of the overall amount of pollutants discharged into the environment, because of the reduction in the primary energy sources usage.

In theory, cogeneration and trigeneration systems can be designed to exploit any kind of primary energy resource. These solutions are nowadays ready to be profitably employed in the market, having the background of a growing amount of well known research and real applications. The most common solutions can be classified according the following classes based on the primary energy source:

- trigeneration/cogeneration systems based on fossil fuels;
- trigeneration/cogeneration systems based on solar energy;
- trigeneration/cogeneration systems based on bio-fuels;

However, although an increased interest on all these system is shown by the research and the market, fossil fuels based systems represent the most developed and profitable kind of trigeneration system. Despite of the adopted system, some common advantages provided by all of the previously described classes of trigeneration systems are:

- Reduction of the primary energy cost;
- Reduction of the plant management cost;
- Reduced sensitivity to the primary energy cost fluctuation;
- Reduction of the fossil fuel consumption;
- Increased reliability of the energy supply;

As explained for cogeneration systems, the last benefit provided by on-site power generation is the increased reliability of the energy supply. Especially for CI, which are users that cannot suffer an energy supply interruption without catastrophic consequences, this asset represents a profitable way to increase reliability, rather than incurring in the costs increase caused by the over sizing of the emergency backup system.

5.1.1 Layout

A scheme depicting the principal elements constituting a trigeneration plant is shown in figure 62. The system's principal units are four. The first one is the power generation unit. Examples of commonly adopted prime mover are reciprocating engines, steam and gas turbine. The prime mover is connected to the second element constituting the system, which is the electric generator. The last two elements are those meant to satisfy the heating and cooling load. The heating load is satisfied by an heat exchanger to recover the heat from the exhaust gas of the prime mover and produce hot water. In some cases, when the thermal need is represented by the demand of steam, a heat recovery steam generator (HRSG) is installed. The system always encompasses a backup boiler, to satisfy the thermal needs whenever recovered heat is not available. Finally, the cooling load of the facility is satisfied by the installation of an absorption chiller. The overall layout of the system entails, like for the heating system, added of cooling capacity through the traditional electric chiller.

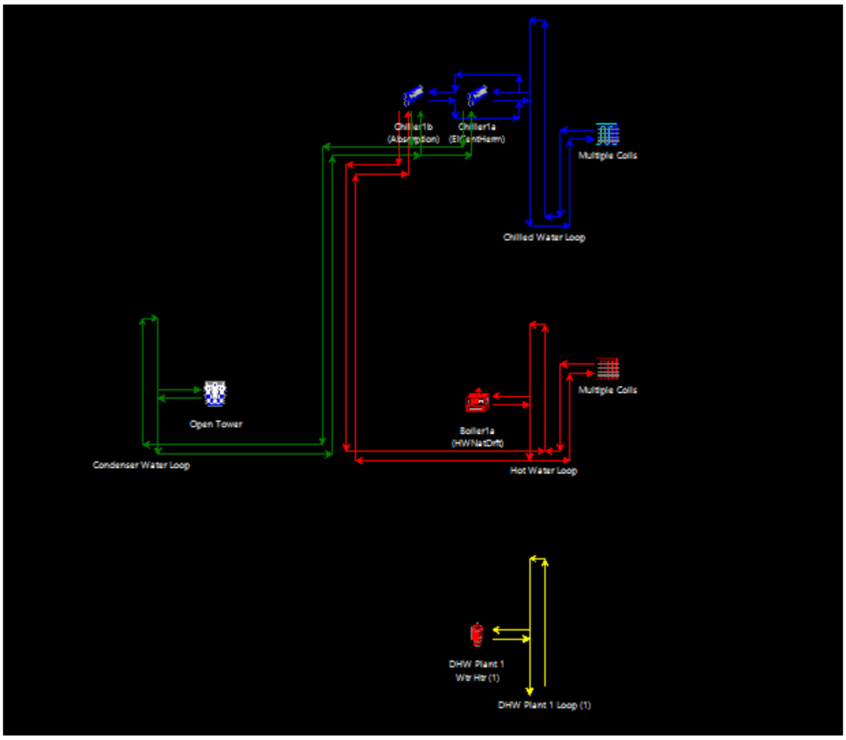

Figure 63: Layout of the trigeneration plant - prime mover is not depicted in eQuest® scheme.

The scheme of the analyzed layout is reported in figure 63 as it is shown on eQuest®; the picture does not provide information about the installed prime mover. The new interesting feature is the presence of a second chiller, the absorption chiller, which is connected to the hot water loop (red line). The hot water loop is where the recovered heat is discharged and from where the chiller is fed. The production process in a trigeneration plant consists of few consequential passages. The fuel is burnt in the power generation unit, producing mechanical power as output of the process. The mechanical power, available as shaft power, drives the electric generator producing electricity. Necessarily, the production of mechanical power goes with the occurrence of losses constituted by waste heat. Using the same nomenclature as in chapter 3 *recoverable heat*, which includes the thermal energy content of exhaust gas, lubrication oil, and jacket water is partially recovered to meet the cooling and heating demand of the facility; the *recoverable heat* becomes *recovered heat* if it is exploited by the user. The amount of heat unused becomes *wasted recoverable heat*. The cooling effect is usually obtained via a single effect absorption chiller, even though other solutions such as reversible heat pumps, and adsorption equipment represent feasible layouts.

The efficiency of the overall system is strongly affected by the efficiency of each element constituting the system and by the efficient interaction of the connected components. Thus, the proper sizing of each component is the result of the perfect integration of all those components. Being all the elements connected to each other, the proper operation of the system is ensured by the correct relative sizing of each component with respect to the other one and with respect to the load of the facility.

5.1.2 Background for Plant Realization

The target of the design phase is the choice of a layout ensuring the best results in terms of energy savings, which obviously have an immediate reflection on the economical benefits of plant operation. Although a good design is the first issue to ensure the proper economical operation of the plant, to reach a real highly efficient and economic trigeneration system some other conditions are required. The system is really sensitive to the influence of some external factors, such as the price ratio between primary energy resources (fuel cost and electricity cost).

IEA performed an analysis to highlight some of the optimal conditions necessary to ensure the existence of a background for the realization of a trigeneration plant [15]. The proposed criteria accounts for the importance of the relative price of primary energy resources; the ratio should be higher than 2.5. Moreover, in order to ensure a reasonable pay back time of the investment the demand of cold and heat should last for more than the 60% of the year. Shorter period of thermal energy recover could not produce enough energy benefits to justify the higher investment cost due to the more complex layout of the trigeneration plant with respect to a traditional layout.

This target is achievable, for example, in all those facilities needing a small constant thermal load through the year. In some facilities, such as in residential buildings, heat and cold demands represent two alternative requests occurring in different periods of the year. Conversely, in some commercial and industrial facilities the heat and cold demand is not necessarily split during the year, because of production needs or air conditioning special requests, i.e., some buildings requires air cooling also during winter because of big internal loads. These factors affect the demand profile of the facility and thus the design choices since the early design phases. In case the constant load is not available, it could be artificially created installing a thermal storage.

The function of a thermal storage is to shave the peaks of thermal demand, converting an unsteady demand in a more smooth one; the new profile of thermal demand will have a value which is the average of the original fluctuating demand. The installation of a thermal storage as a subsystem of a trigeneration plant could represent a simple way to improve the economic benefits produced by the plant.

The IEA also advice that to promote the best result in energy efficiency, the location of the plant with respect to the facility is important. The on-site generation benefits could vanish by too high cost for piping and by unavoidable energy losses due to the transportation of thermal energy for long distance. This is the reason why the site of the plant has to be as close as possible to the facility representing the final user.

5.2 Trigeneration System, Sizing Procedure

Starting from the analyzed layout of the cogeneration plant, the next step necessary to further improve the energy efficiency of the health care facility is the introduction of an absorption chiller to supply the cold demand. One of the key factor ensuring to the health care facility the optimal exploitation of the potentiality of a trigeneration plant is constituted by the disjunction of the heat and cold demand through the year. As it is shown in figure 64 the most of the cold demand is located during summer. In this period the heat demand by the facility reduces basically to just the heat needed to satisfy the domestic hot water demand. This feature of the thermal profiles of the health care facility causes the existence of a large amount of wasted heat during the summer months, in case a cogeneration plant is installed. This amount of extra heat can efficaciously be employed for the satisfaction of the cold demand through the presence of the absorption chiller, creating the necessary background for the design of a trigeneration system.

In the previous analysis several sizes of gas turbine have been simulated in order to get a wide range of data on the most important parameters characterizing the behavior of the system. These data allowed the development of a parametric analysis of the plant aimed at determining

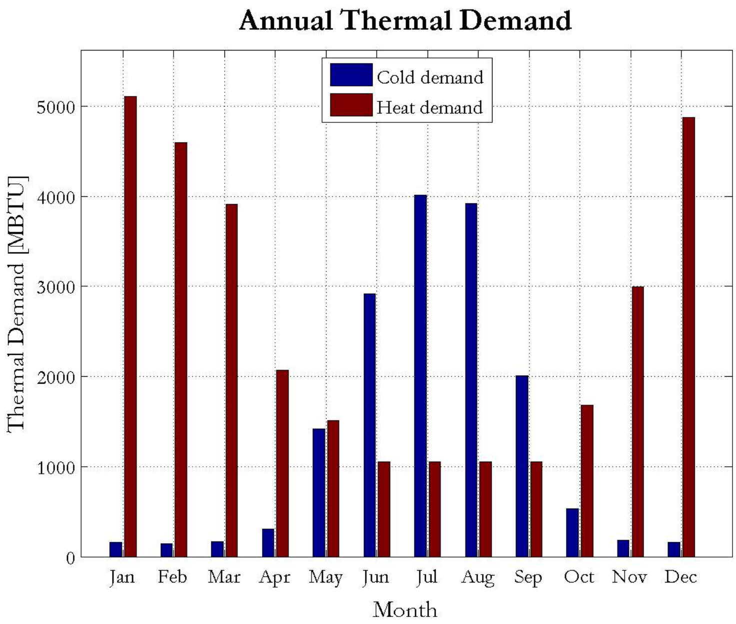

Figure 64: Thermal energy demand demand of the facility.

the size of the gas turbine. For each of the sizes of gas turbine, ranging from 600 [kW] up to 1300 [kW], the annual profile of the WRH was analyzed (figure 37,figure 38, and figure 39); the complete results are available in appendix). The hourly load profile of the WRH provides the information necessary to properly size the absorption chiller. Indeed, having information on the average amount of this resource during the summer month and also knowing the relation existing between the cooling capacity and the heat consumption at full load condition for the absorption chiller, it is possible to estimate the proper size of the equipment. Knowing that at full load condition the thermal COP of the equipment is around $0.7-0.8$, depending on outdoor condition, this implies that having 100 [kW] of WRH it is possible to install an equipment with a cooling capacity of about $70 \div 80$ [kW]. In figure 65, figure 66, and figure 65 the effects of the integration in the layout of the plant of the absorption chiller are depicted for some of the analyzed sizes (all the produced graphs, showing the result of all the analyzed sizes, are reported in appendix).

The results of these simulations show two different but interconnected effects on the behavior of the plant. At first glance, for all the cases, the reduction of the WRH (green line) is clear, this trend is opposed to the marked increase of the amount of recovered heat from the gas turbine (red dashed line). This change in the shape of the thermal profiles is due only to the installation of the absorption chiller.

Unfortunately the choice of the proper size of the absorption chiller is not a straight forward procedure. Because of the fluctuation of the WRH profile, the choice of the absorption chiller is a crucial issue. The fluctuation are the result of the combination of two different conditions. The first one is the unsteady profile of the electricity demand, which causes variations in the gas turbine production and thus variations of the exhaust gas production (*recoverable heat*); the second one is the unsteady profile of the heat demand by the facility. The difference between these two unsteady profile results in the oscillating profile of the WRH, which is the difference between the *recoverable* and the *recovered* heat. Moreover a second order phenomenon conditioning the sizing phase of the absorption chiller is caused by the changes occurring in the electric demand profile. This phenomenon is further analyzed in section 5.3.

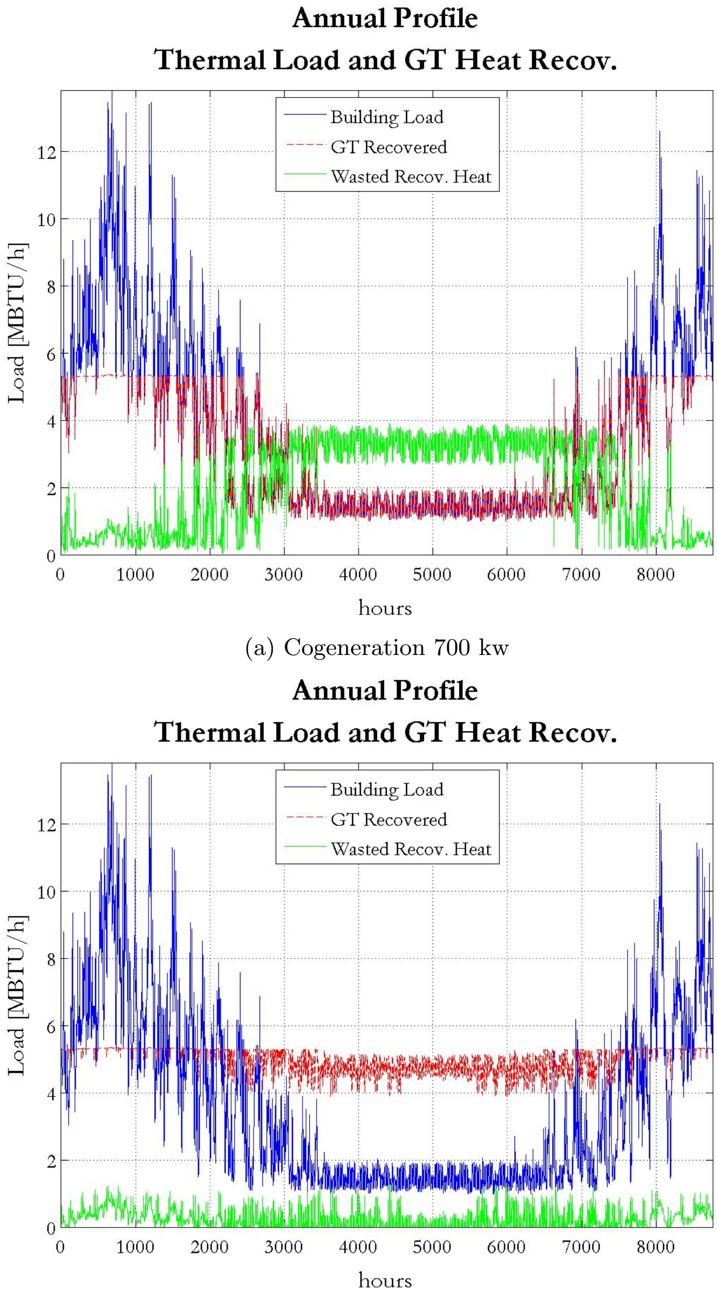

(a) Cogeneration 700 kw

(b) Trigeneration 700 kw

Figure 65: Wasted recoverable heat profiles comparison - 700 [kW].

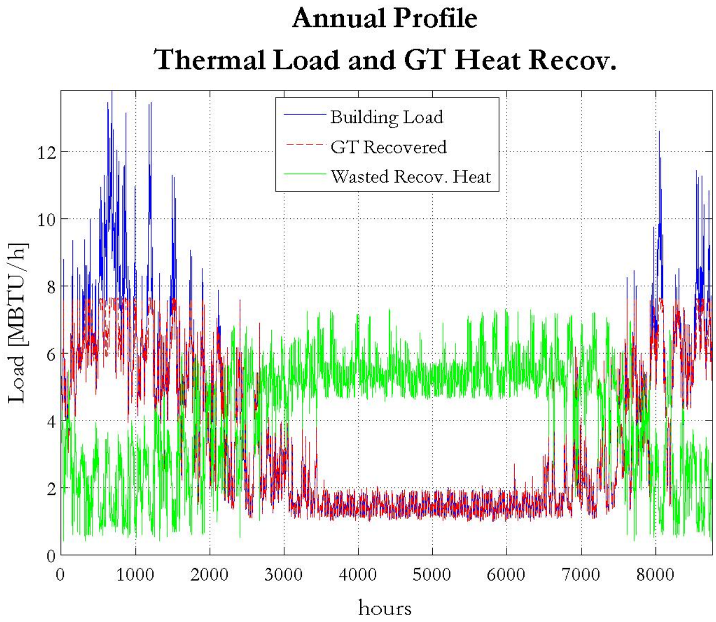

(a) Cogeneration 1000 kw

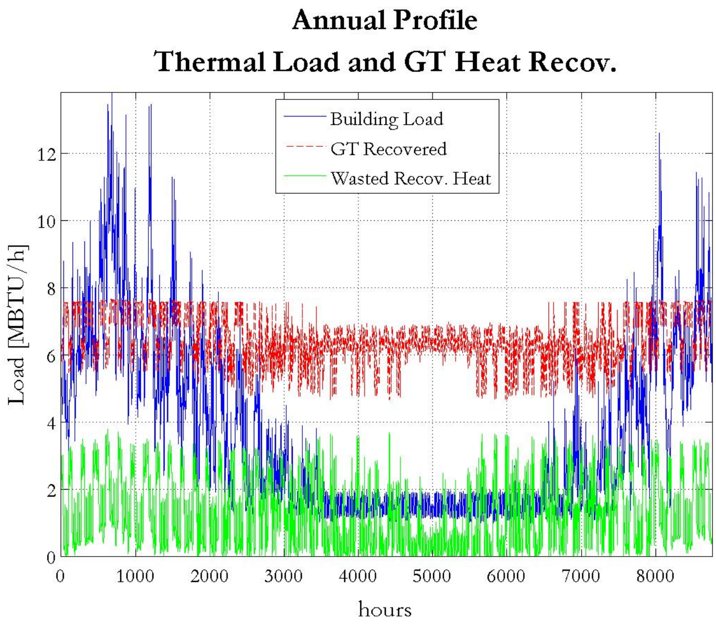

(b) Trigeneration 1000 kw

Figure 66: Wasted recoverable heat profiles comparison - 1000 [kW].

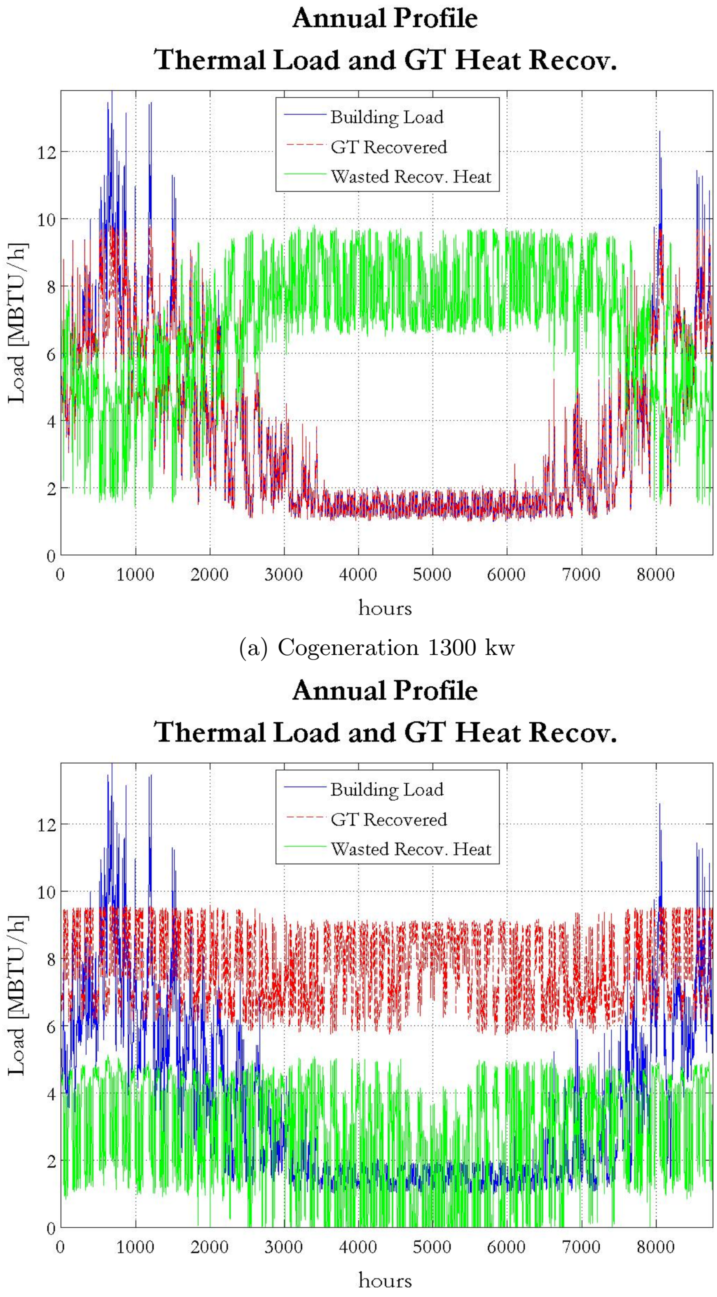

(a) Cogeneration 1300 kw

(b) Trigeneration 1300 kw

Figure 67: Wasted recoverable heat profiles comparison - 1300 [kW].

5.2.1 Management of the Unsteady WRH Profile

eQuest® cannot set rules for the usage of the *recoverable heat* and cannot split the thermal demand according the component constituting the thermal load. In other words, eQuest® cannot satisfy different simultaneous loads using specified energy sources for each one of them. Thus, whenever the absorption chiller requires a thermal power higher than the amount of *recoverable heat* available at that moment from the gas turbines, eQuest® manages this situation following the same procedure. The first action is to exploit the whole amount of *recoverable heat* from the prime mover, the second action is to switch the boilers on to satisfy the residual thermal demand. This second action, the direct firing of natural gas to produce hot water for feeding an absorption chiller, is not acceptable under the point of view of the optimal exploitation of the energy resources.

As an example, consider a situation in which 100 units of energy in fuel form are available. Firing them in a 80% efficient natural gas boiler produces 80 units of energy in the form of hot water. Finally, using the hot water in an absorption chiller characterized by a thermal COP equal to 0.8, 64 units of chilled water are produced. A more reasonable approach consider the possibility to use the fuel for electricity production purposes at an average efficiency of 0.27 and then the usage of the electricity to drive a traditional electric chiller. Using the latter approach, from 100 units of energy in fuel form it is possible to obtain 27 units of energy in form of electricity. In a modern industrial chiller characterized by an electric COP of 4.0, 27 units of electricity are transformed in 108 units of chilled water [28]. This quick analysis provides an estimation of how the direct firing of fuel for feeding an absorption chiller could be around 40% less efficient than the employ of a traditional electric industrial chiller.

This undesired production chain of the cooling effect, combined with the impossibility to properly manage the heat production and distribution through the plant, lead to strict requirements for the sizing of the absorption chiller. A possible way to overcome this disadvantage could be the the introduction of a thermal storage, rather than any change in the simulation process. The flattening of the peaks of the availability of WRH caused by the installation of a thermal storage in the heat recovery side of the plant, can provide a more smooth source of energy for the proper operation of the absorption chiller. In this way it would be avoided the previously mentioned improper exploitation of the primary energy sources, it would be allowed the full exploitation of the WRH and would occur an increase of the installed absorption chiller size.

5.2.2 Iterative Approach

One of the suggested procedure to overcome the problem of the proper exploitation of energy resources and to ensure the optimal sizing of the absorption chiller is not straight forward. The approach is an iterative process which lead to the definition of the optimal size of the absorption chiller through several simulations of the system. Starting from the evaluation of the average amount of WRH available (see figure 65, figure 66, and figure 65) and taking into account the efficiency of the absorption chiller, a first evaluation of the optimal size is made. The following step in the sizing procedure is the simulation of the new layout of the system, which encompasses the first evaluated size of absorption chiller. The simulations highlights if in some period of the year the WRH is null. In those cases, also analyzing the change in the overall fuel consumption of the health care facility, the occurrence of the direct firing of fuel to feed the absorption chiller is detected.

In a trigeneration system, the installation of an absorption chiller should not have any influence on the overall fuel consumption of the facility, because the absorption chiller should be driven only by a recovered resource, without any other direct fuel consumption. A marked change in fuel consumption highlight the opposite situation. Consequently, whenever this event occurs, a reduction of the installed size of the absorption chiller, and thus a reduction of its heat consumption, is preferred to avoid the undesired manage of the resources. The reduction of the installed size has not to be too large. If this happens, the opposite undesired situation occurs, which is highlighted by a too high availability of WRH. The availability of a large amount of WRH represents an inefficient exploitation of the resources. In those cases an increase of the proposed size of the absorption chiller is done. The whole sizing procedure is an iterative process, which consist in the simulation of the plant, the analysis of the WRH profile and the re-sizing of the equipment seeking the optimal size.

5.2.3 Double Simulation Approach

Another approach has also been used to solve the problem of the management of the resources. It artificially tries to overcome the problem running two times the same analyzed case. The first run on eQuest® is a simulation of the trigeneration system in which the cooling system is not operating; the second one, on the other hand, is a simulation performed interrupting the operation of the boilers. The final data used for the post process are produced mixing the output data of the previous simulations. The first data are used to describe the winter season, when the cooling demand is close to zero and a huge amount of heat is requested by the facility. The second data are used to describe the behavior of the plant in summer season. Also in real practice, during summer the heating system of buildings is not working and conversely during winter the cooling system is not operating. Using this approach the problem of the direct firing of fuel in boilers to satisfy the thermal needs of the absorption chiller is completely avoided. Despite this, the interruption of cooling system operations cannot ensure the proper management of the correct temperature in some areas of the building. Some area of the health care facility, e.g., operating theater, needs air conditioning throughout the whole year. Conversely, the opposite situation can occur during summer, when the cooling system relies on the proper operation of the re-heat coils. This situation not ensure the reliability of the obtained output data in therms of energy needs of the facility. Although the proposed solution seems to be feasible in theory, it was not applied because of the specific features of the case study.

5.2.4 Final Results

In Table XVI the data collected applying the iterative approach through this phase of study are reported. It is not possible to provide an exact value of the average WRH because, as said before, fluctuating value of this resources occurs through the cooling period. This fact lead to the choice of providing, rather than a value, a range of variation of the thermal power available as WRH during the cooling season.

This fluctuation are higher for the last case examined, the one with a 1300 [kW] gas turbine installed. The reason of this wider range is connected to the increased fluctuation of the *recoverable heat* from the gas turbine, which increases because of the increased production of the gas turbine. The increased installed electric capacity allows the prime mover to better meet the electric demand of the facility; unfortunately this also causes the continuous change of operating point due to the necessity of the gas turbine to follow the electric demand profile. A highly fluctuating electricity production causes a highly fluctuating WRH profile. This phenomenon is less marked when the installed electric capacity is lower. A smaller equipment works on average in a more steady way, causing a reduced amount of fluctuation in the *recoverable heat* profile. When the installed electric capacity is reduced, the fluctuation are mainly due to the fluctuation of the heat demand of the facility; the fluctuation of the heat demand is the summation of the daily cycle of the domestic hot water demand and of the amount of heat requested by the re-heat coils of the cooling system.

Starting from the result derived by the analysis of the cogeneration layout of the plant (chapter 3), a range of WRH availability is defined. In the following step a range of possible absorption chiller sizes is estimated through information about thermal COP in design condition, as it has been previously explained. Finally the iterative approach has been applied changing the size of the chiller within the range of possible ones.

The proper size is estimated trying to keep as low as possible the fuel usage to feed the absorption chiller. The increase of the fuel usage for boilers operation due to the installation of the chiller has been kept below the 1.47%, which is an acceptable value in order to avoid the under sizing of the equipment. All the data are collected in Table XVI, where also the final adopted size is reported. The installed sizes are usually closer to the lower value of the proposed sizes range than to the larger.

TABLE XVI: ESTIMATED AND INSTALLED ABSORPTION CHILLER SIZES.

Size [kW]	**WRH Availability (min / max) [MBTU/h]**	**Est. Chiller Cap. (min / max) [MBTU/h]**	**Installed Chiller Cap. [MBTU/h]**	**Installed Chiller Cap. [tons]**
600	2.0 / 3.0	1.6 / 2.4	1.8	150
700	2.7 / 3.7	2.2 / 3.0	2.7	225
800	3.6 / 4.4	2.9 / 3.5	3.2	267
900	4.0 / 5.0	3.2 / 4.0	3.6	300
1000	4.9 / 5.8	3.9 / 4.6	4.0	333
1100	5.6 / 6.6	4.5 / 5.3	4.5	375
1200	6.0 / 7.0	4.8 / 5.6	5.0	417
1300	7.0 / 9.0	5.6 / 7.2	5.8	483

5.3 The Effect of Trigeneration on the Energy Demand

The changes caused by the upgrade of a cogeneration plant into a trigeneration plant affect mainly the electric demand profile of the health care facility. Part of the cooling load is satisfied by the absorption chiller, reducing the load for the traditional electric chillers and thus causing the reduction of the electrical power request during summer; this is also the period of the year when the highest electric demand occurs. The effect produced can be seen in figure 68,figure 69, and figure 70 where the duration curves for the trigeneration plant are compared with the duration curves of the cogeneration layout. All the graphs, showing the results for all the studied sizes, are available in appendix. Furthermore, to provide a synthetic presentation of the results obtained for each of the analyzed plant layouts, the collected data are reported in Table XVII.

TABLE XVII: EFFECTS OF ABSORPTION CHILLER INSTALLATION ON ELECTRIC PEAK DEMAND.

Size [kW]	**600**	**700**	**800**	**900**	**1000**	**1100**	**1200**	**1300**
Absorption chiller size [tons]	150	225	250	300	333	367	416	483
Electric peak demand Cogeneration [MW]	1.52	1.43	1.34	1.25	1.15	1.06	0.97	0.88
Electric peak demand Trigeneration [MW]	1.44	1.33	1.23	1.13	1.03	0.93	0.83	0.6
Percentage reduction	5.3	7.0	8.2	9.6	10.4	12.3	14.4	31.8

Analyzing the data presented in Table XVII, the principal conclusion is about the magnitude of the reduction in the peak demand. Increasing the size of the installed gas turbine increases the WRH. This allows the possibility to install bigger and bigger absorption chillers in terms of cooling capacity. The larger the installed absorption chiller the larger is the percentage reduction of the maximum demand of electricity. This reflects the reduction of the cooling capacity provided by electrical chillers.

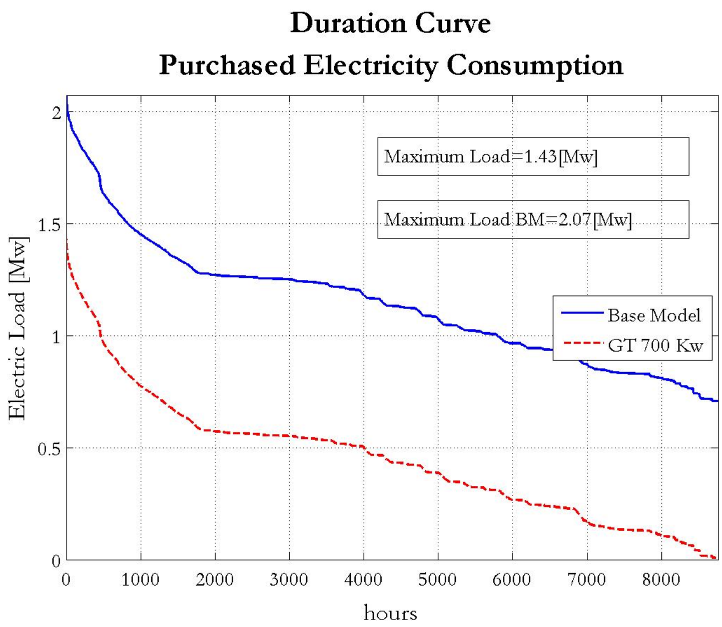

(a) Cogeneration 700 kw

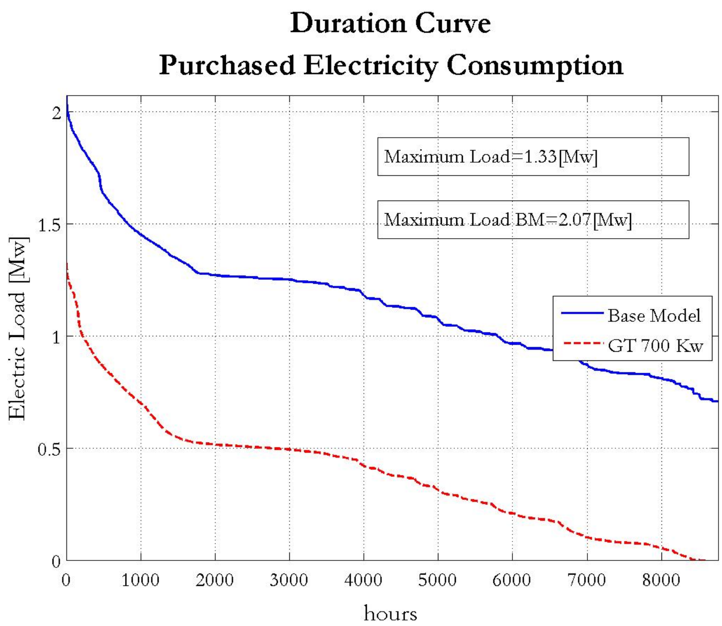

(b) Trigeneration 700 kw

Figure 68: Electric duration curve - 700 [kW].

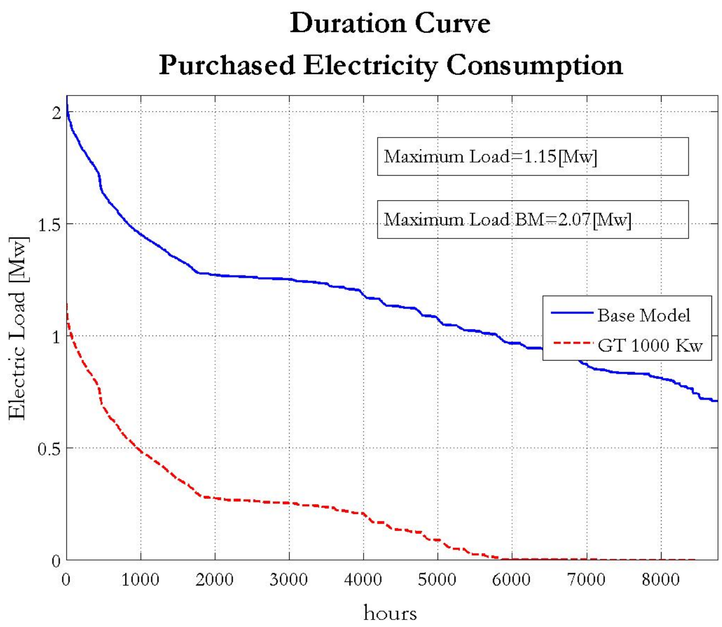

(a) Cogeneration 1000 kw

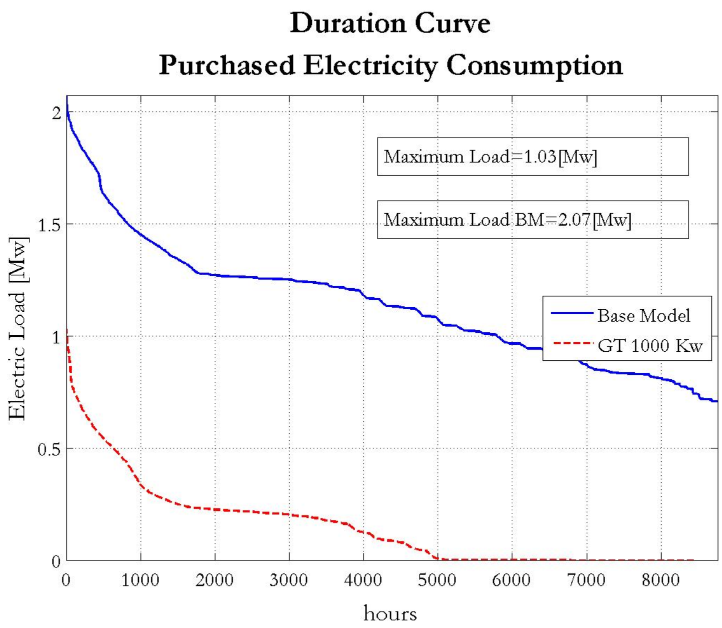

(b) Trigeneration 1000 kw

Figure 69: Electric duration curve - 1000 [kW].

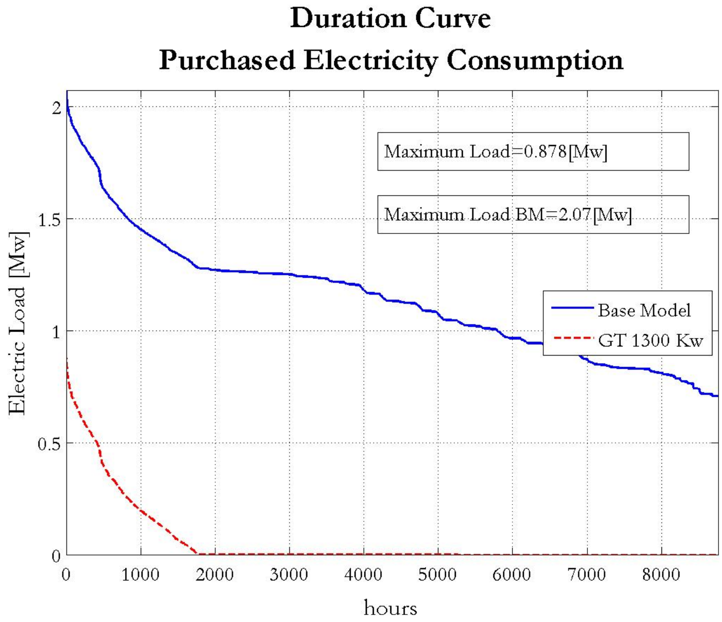

(a) Cogeneration 1300 kw

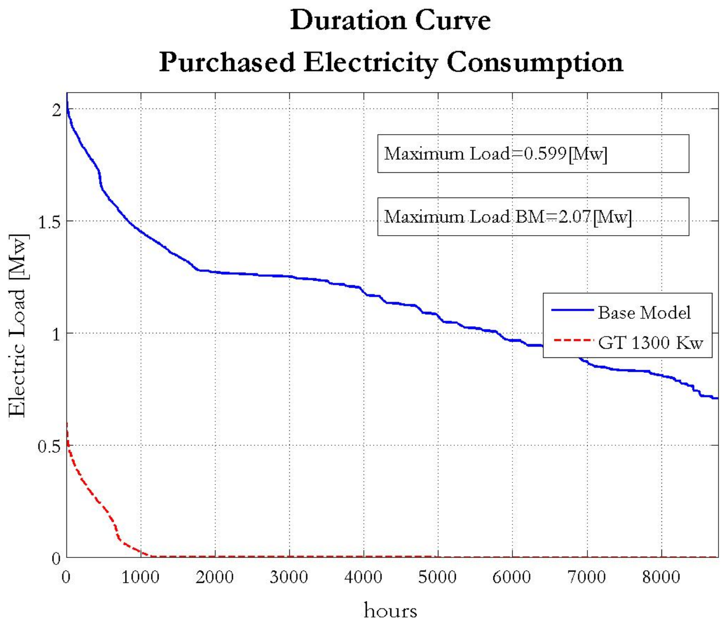

(b) Trigeneration 1300 kw

Figure 70: Electric duration curve - 1300 [kW].

The reduction of the electric demand has a side effect, whose magnitude is directly proportional to both the size of the gas turbine and the size of the absorption chiller. Especially for the larger gas turbines, the reduction of the electric demand causes a change in their operating conditions, i.e., gas turbines working at lower PLR than the cogeneration cases. This effect does not exist for gas turbines having a size well below the minimum value of the electric power demand. In these conditions the reduced power demand does not affect the PLR, resulting in equipment always working at full load. This phenomenon result in a degradation of the efficiency of the gas turbines for the first case and in just a reduction of the purchased electricity in the second case.

Moreover, in all the cases in which the reduction of the electric demand causes a change of the operating point of the gas turbine another phenomenon occurs. It is well known how the efficiency dramatically reduces in partial load condition with respect to the full load condition for this kind of equipment. Thus, on the one hand the reduction in the electric power output causes a reduction of the *recoverable heat* with a consequent reduction of the primary resource for the absorption chiller. On the other hand the reduction in efficiency contrasts the reduction of *recoverable heat*, increases the fraction of input fuel wasted under the form of heat. These concurrent and opposing effects increase the need to perform multiple simulation of the layout of the plant in order to determine the optimal size of the absorption chiller.

In order to better understand the advantages produced by the installation of an absorption chiller on the reduction of the electric demand, the hourly profiles are reported for some of the analyzed sizes and a comparison is shown with the hourly profile of the cogeneration layout in figure 71,figure 72, and figure 73. At first glance it is possible to see how an overall small reduction of the value of the electric demand occurs through the whole year, without any significant difference among the analyzed layout. What really changes, increasing the size of the absorption chiller, is the shape and the value of the peaks occurring during the summer season. The effect of the reduction are proportional to the size of the installed absorption chiller, thus are much more marked for the 1300 [kW] layout rather than for the 700 [kW]. The results for the other analyzed layout are collected in the appendix.

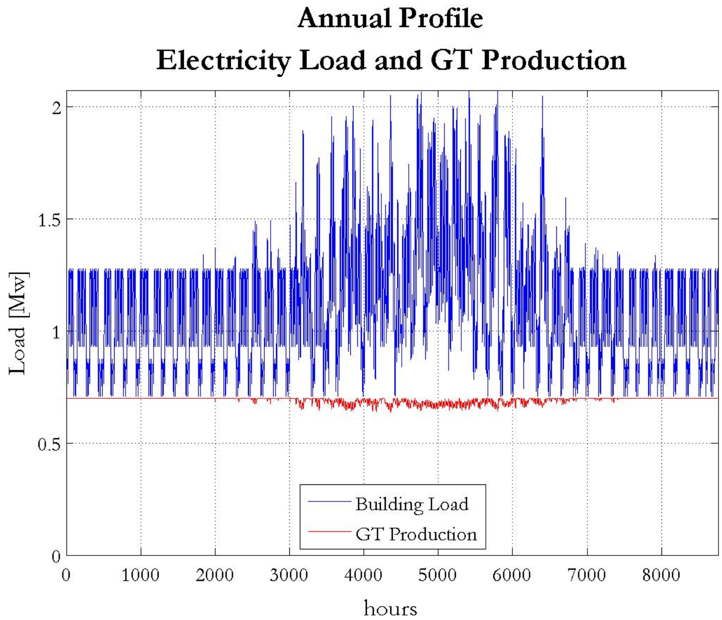

(a) Cogeneration 700 kw

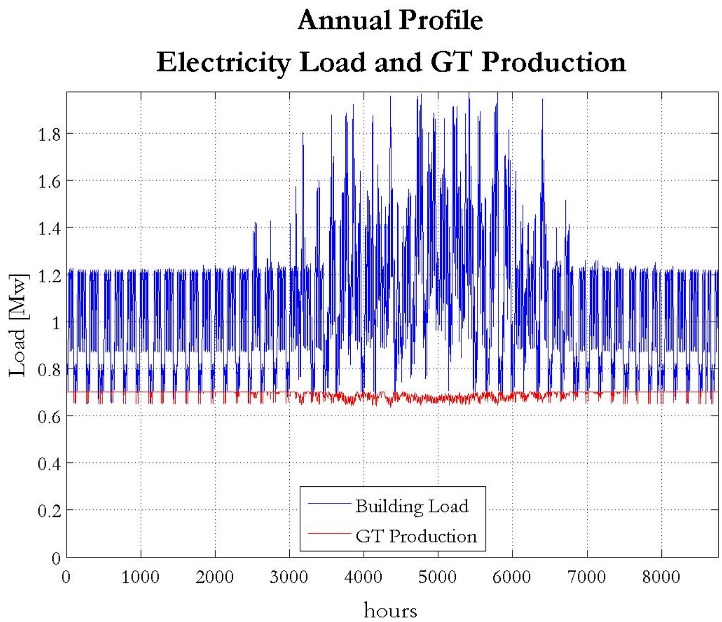

(b) Trigeneration 700 kw

Figure 71: Hourly profile of the electric demand - 700 [kW].

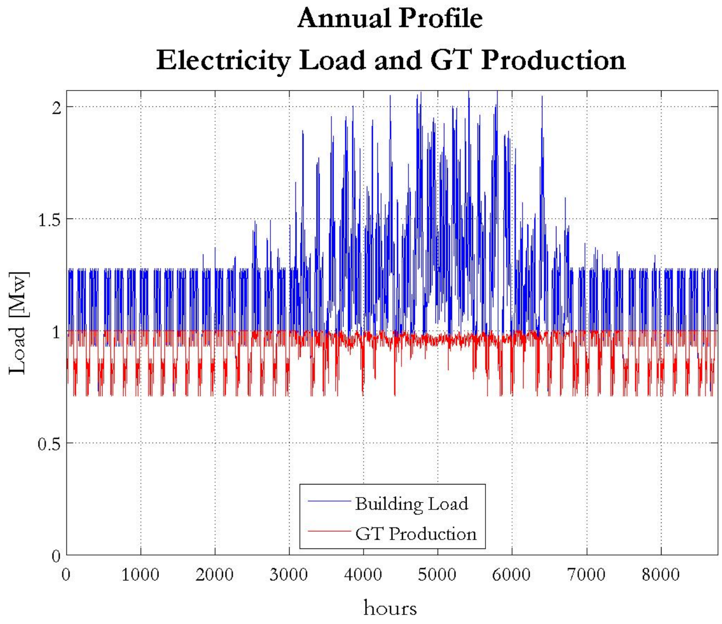

(a) Cogeneration 1000 kw

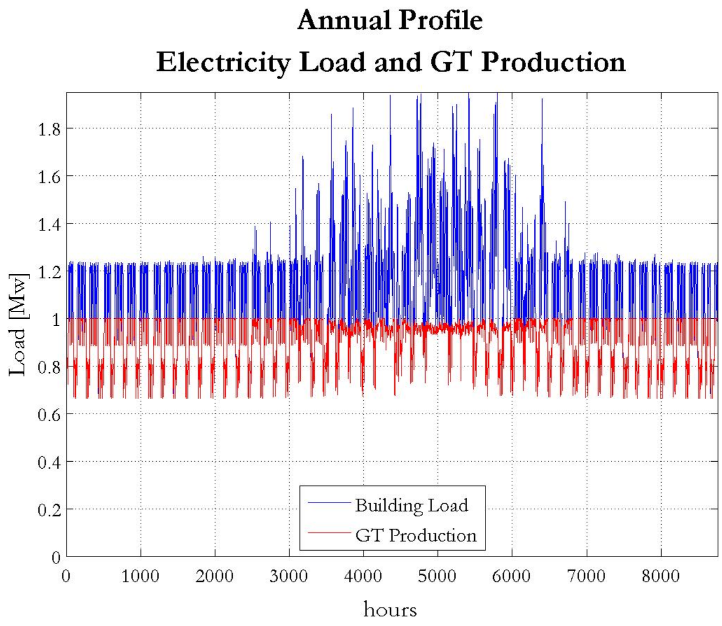

(b) Trigeneration 1000 kw

Figure 72: Hourly profile of the electric demand - 1000 [kW].

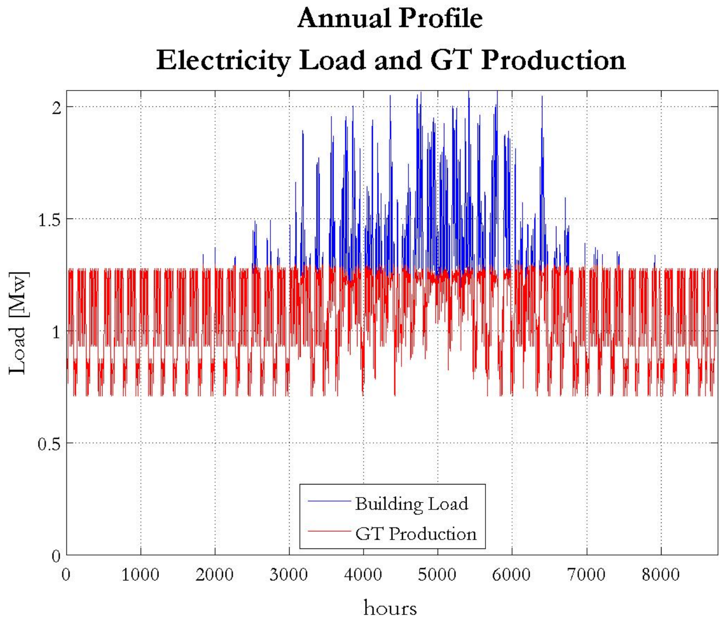

(a) Cogeneration 1300 kw

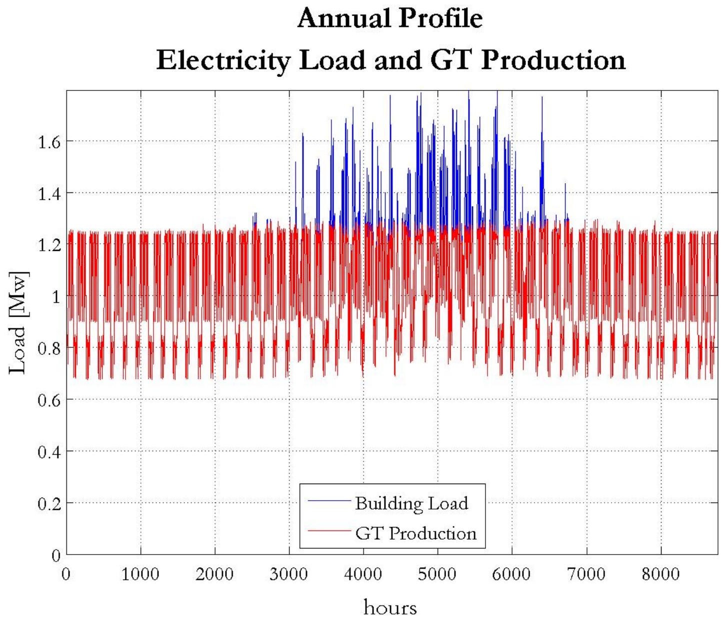

(b) Trigeneration 1300 kw

Figure 73: Hourly profile of the electric demand - 1300 [kW].

5.4 The Improvements in Energy Efficiency

The final purpose of the realization of technologically advanced plant to satisfy the energy needs of a building is to ensure improvements in energy efficiency, which allow the reduction of the primary energy resources consumption. The main effect on the primary resources consumption, caused by the realization of a trigeneration system rather than a cogeneration one, is the reduction of the overall amount of electricity needed by the facility. In order to quantify the electric savings achieved for the proposed layouts, the electricity produced and purchased by the facility throughout the whole year are calculated. The results are than summarized in Table XVIII. Some important features have to be highlighted.

First of all, it is easy to see how the overall amount of electricity needed by the health care facility is a constant value for the cogeneration system and a decreasing value for the trigeneration one, because of the positive influence of the absorption chiller.

The second important result is the almost constant values of the amount of electricity produced by the gas turbines of small sizes. Only for layouts with an installed electrical power higher than 900 [kW] it is possible to recognize a substantial reduction in the overall production due to the increased effect of the reduced electricity demand. This effect is maximum for the 1300 [kW] layout, where the reduction approaches 354 [MWh] per year.

The final interesting effect on the annual electric balance is represented by the reduction of the amount of electricity purchased by the external grid; although it has the same decreasing trend both for the cogeneration and the trigeneration plant, it always shows a smaller value in the second case. This information represent the key factor of the energy and thus economic savings produced by the upgraded system.

TABLE XVIII: ELECTRICITY PRODUCED AND PURCHASED FOR THE ANALYZED LAYOUTS - [MWh].

Size [kW]	**COGENERATION**			**TRIGENERATION**		
	Produced	**Purchased**	**Total**	**Produced**	**Purchased**	**Total**
600	5,200	4,815	10,015	5,200	4,225	9,425
700	6,066	3,949	10,015	6,059	3,361	9,420
800	6,906	3,109	10,015	6,847	2,533	9,379
900	7,630	2,385	10,015	7,517	1,851	9,368
1000	8,266	1,750	10,015	8,081	1,284	9,365
1100	8,788	1,227	10,015	8,552	809	9,361
1200	9,220	795	10,015	8,941	412	9,352
1300	9,495	520	10,015	9,141	209	9,349

Concerning the fuel consumption balance, the system is mainly meant to improve the energy exploitation of the already existing fuel consumption, rather than cause its increase or decrease. Despite this, the reduction in the electricity production by the gas turbine shown in Table XVIII, has the benefit to reduce the gas turbine fuel consumption, although the effect is quite moderate because of the usually contemporary decrease of the efficiency. The most relevant effects can be seen in the larger sizes, both in terms of gas turbine size and absorption chiller cooling capacity. The results are collected in Table XIX. The gas turbine fuel consumption is reduced with respect to the cogeneration layout, although the effect does not appear for the 600 [kW] gas turbine, whose electricity production is not affected by the presence of the absorption chiller and by its effects on the electric demand. The profiles for the 600 [kW] gas turbine production are available in appendix.

Analyzing the changes in the overall fuel consumption, which takes into account both the fuel used for the electricity production and the fuel used to run the boilers and other equipment, the positive effects of the reduction in fuel consumption by the gas turbine are still present.

Deeply analyzing the results, the reduction in the overall fuel consumption does not occur for the 600 [kW] and 700 [kW], where an increase in the overall fuel consumption is seen. This result is the consequence of the undesired, but moderate, direct firing of fuel for feeding the absorption chiller to meet the increased thermal needs of the facility due to the absorption chiller. The effect is present also for the other sizes, but it is disguised by the marked reduction in the gas turbines fuel consumption. Although this occurrence could be fixed by reducing the installed size of absorption chiller, being the maximum percentage increase in the fuel consumption for boiler operation smaller than 1.47%, the effects are so limited to be considered negligible. Moreover, a further reduction of the absorption chiller cooling capacity installed would have a too marked negative effect on the effectiveness of the absorption system for those sizes. This is the reason leading to the acceptance of this very small inefficiency.

It is interesting to analyze the effect of the upgrade from a cogeneration layout to a trigeneration one on the exploitation of the *recoverable heat* produced by the gas turbine. The trends of the monthly overall thermal needs of the building (which does not include the heat request of

TABLE XIX: FUEL CONSUMPTION FOR THE ANALYZED LAYOUTS - [MBTU].

	Cogeneration		**Trigeneration**	
Size [kW]	**Fuel Gas Turbine**	**Overall Fuel consumption**	**Fuel Gas Turbine**	**Overall Fuel consumption**
600	59,922	74,752	59,922	75,865
700	69,908	82,829	69,807	83,199
800	79,978	92,738	79,195	91,900
900	90,321	102,960	88,695	101,312
1000	100,585	112,561	97,938	109,832
1100	110,781	122,297	107,405	119,132
1200	120,718	131,938	116,717	128,468
1300	130,642	141,675	125,562	136,916

the absorption chiller), the monthly *recovered heat* by the gas turbine and the monthly amount of WRH are depicted in figure 74, figure 75, and figure 76 for several sizes. What the graphs show is the amount, on a monthly base, of the exploitation of the thermal resources compared to the thermal needs of the building. The best usage of the resources occurs for the smaller sizes, because of the easy sizing of the absorption chiller due to the reduced fluctuation of the WRH (see figure 65, figure 66, and figure 65). However, this has not been possible for the larger installed sizes. The highly fluctuating WRH profile has not allowed the best heat recovery, this effect is highlighted in figure 76, where the monthly amount of WRH it is not as small as the other cases.

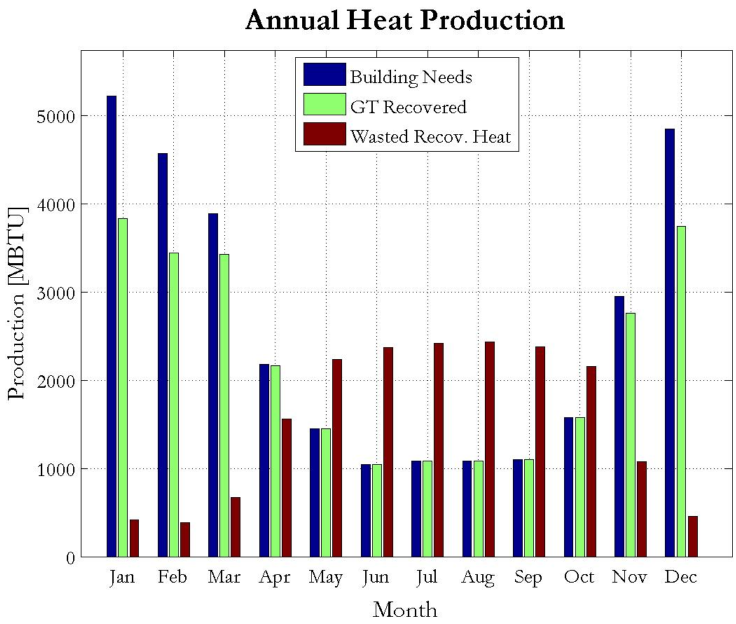

(a) Cogeneration 700 kw

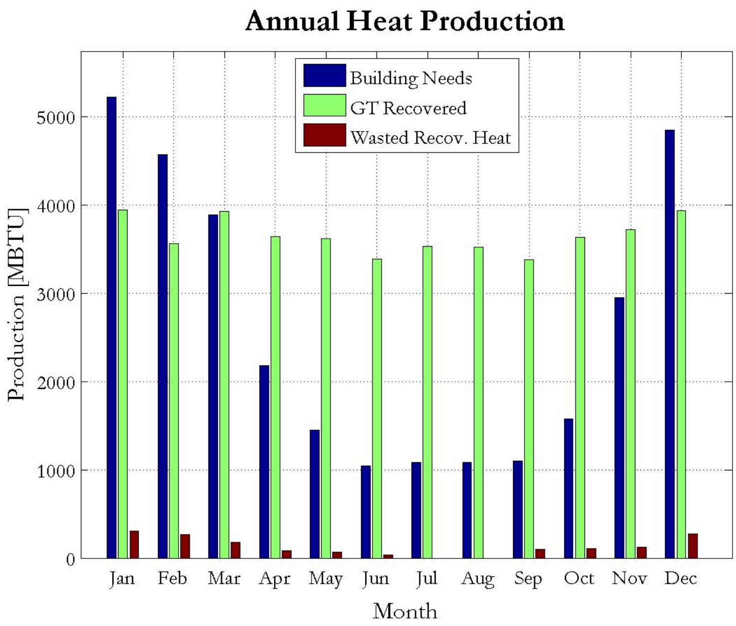

(b) Trigeneration 700 kw

Figure 74: Usage of the recoverable heat from the gas turbine - 700 [kW].

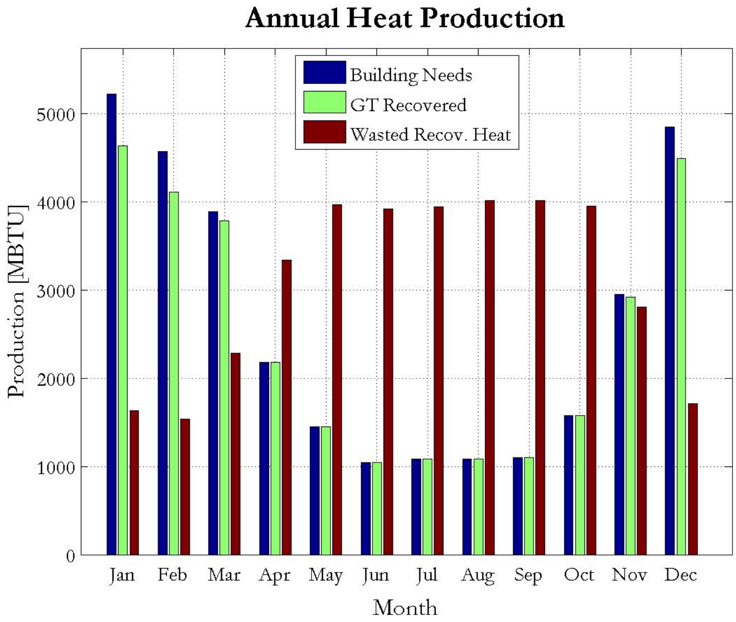

(a) Cogeneration 1000 kw

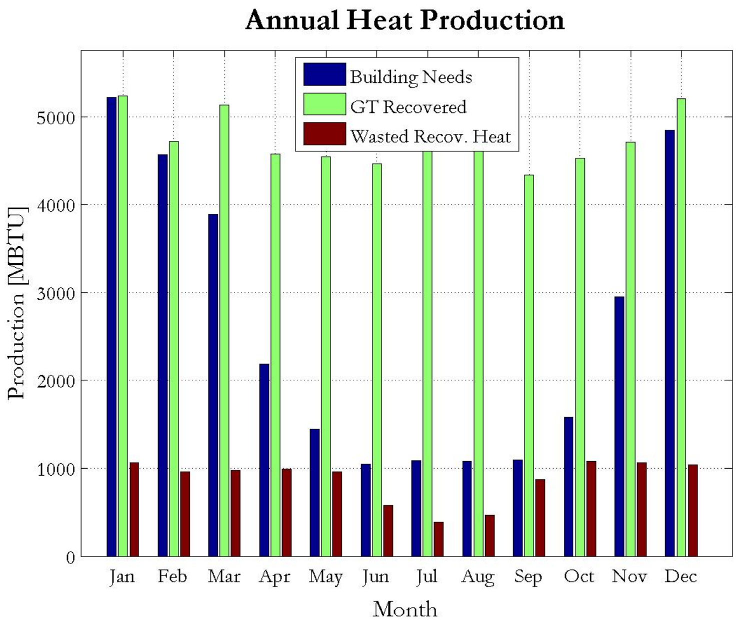

(b) Trigeneration 1000 kw

Figure 75: Usage of the recoverable heat from the gas turbine - 1000 [kW].

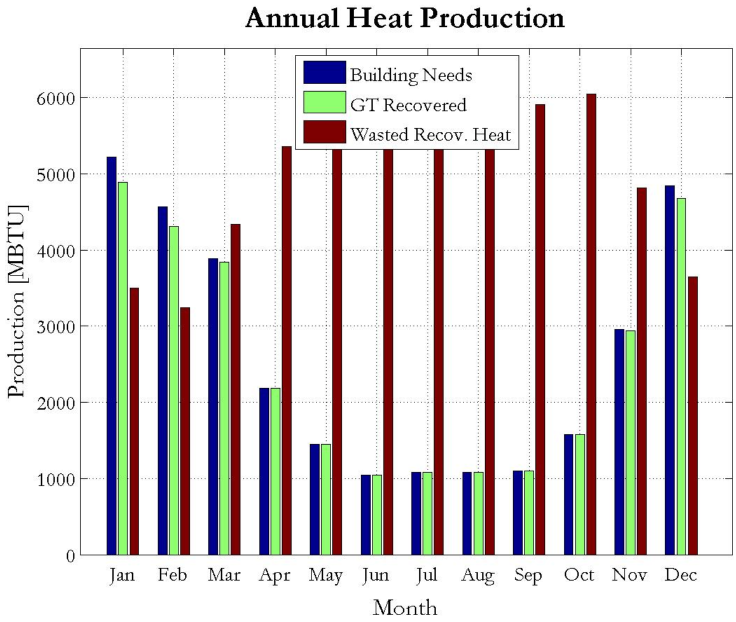

(a) Cogeneration 1300 kw

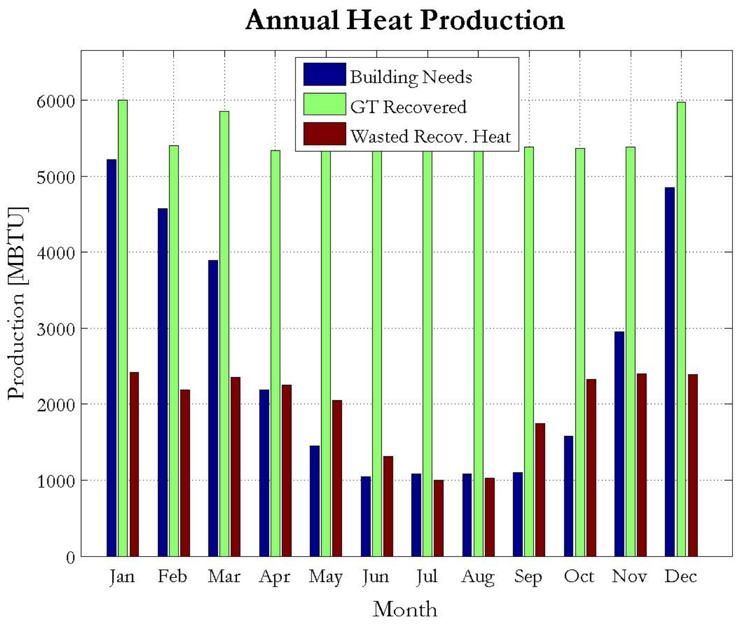

(b) Trigeneration 1300 kw

Figure 76: Usage of the recoverable heat from the gas turbine - 1300 [kW].

5.4.1 Efficiency Analysis

It is necessary to define the efficiency of a system to properly estimate its performance regardless of the result obtained in absolute terms. Following the same approach proposed in chapter 3 for the definition of the efficiency of a cogeneration plant, the same calculation are repeated also for a trigeneration plant. However, the previously proposed approaches (see Equation 3.1,Equation 3.2, and Equation 3.3) do not take into account the benefit regarding the reduction of the electrical demand produced by the trigeneration plant because of the alternative cold production.

Analyzing Equation 3.2, it is possible to enclose in the term at the numerator Q_{rec}, the amount of heat delivered to the absorption chiller. This approach shows an increase of the efficiency if compared with that of the cogeneretion layout. However this increase in efficiency does not properly reflect the real improvement realized in the plant. Better results are provided applying the PRSEC index. The definition of the index does not change with respect to Equation 3.6 to include the effect of the absorption chiller. What occurs is a reduction of the consumption of fuel for the gas turbine and a reduction of the purchased electricity; these effects directly affect also the associated source energy.

Changes occur in the second approach to the PRSEC evaluation, which has been defined as $PRSEC_{OS}$. Among the products of the plant has to be included also the cold production. Starting from Equation 3.4:

$$PRSEC_{OS} = 1 - \frac{[SE_{F.PM.}]_{CHP}}{[SE_{Q_{rec.}} + SE_{E_{PM}} + SE_{Q_{abs.}}]_{CONV}} \tag{5.1}$$

$$PRSEC_{OS} = 1 - \frac{[F_{PM} * AF_{NG}]_{CHP}}{[F_B * AF_{NG} + E_{PM} * AF_E + E_{abs.} * AF_E]_{CONV}} \tag{5.2}$$

$$PRSEC_{OS} = 1 - \frac{[F_{PM} * AF_{NG}]_{CHP}}{[\frac{Q_{rec.}}{\eta_B} * AF_{NG} + E_{PM} * AF_E + \frac{Q_{abs.}}{COP} * AF_E]_{CONV}} \tag{5.3}$$

- $Q_{rec.}$ Recovered heat from the prime mover (not for absorption chiller);
- $Q_{abs.}$ Cooling load satisfied by the absorption chiller;
- η_B Boiler average efficiency;
- COP Average COP of an electric chiller;
- E_{PM} Electricity produced by the prime mover;
- $E_{abs.}$ Electricity to produce $Q_{abs.}$ in an electric chiller;
- F_{PM} Fuel consumption for the prime mover;
- F_B Boiler fuel consumption to replace the recovered heat $Q_{rec.}$;
- $SE_{Qrec.}$ Source energy associated with fuel for boilers, to replace $Q_{rec.}$;
- $SE_{F.PM.}$ Source energy associated with fuel for prime mover;
- $SE_{E_{PM}}$ Source energy associated with electricity produced by the gas turbine;
- AF_{NG} ASHRAE factor for natural gas;
- AF_E ASHRAE factor for electricity purchased;

The term $SE_{Q_{abs.}}$ accounts for the source energy used in a electric chiller to replace the absorption chiller operation. It is evaluated analyzing the cold production of the absorption chiller and dividing it by the average COP of an electric chiller; the COP has to be chosen in a range of $3-4$ the equipment. In this way the avoided electricity consumption is estimated and using the conversion factor by ASHRAE it is possible to account for the source energy consumption avoided. The results are collected in Table XX.

TABLE XX: EFFICIENCY OF TRIGENERATION PLANTS.

Size [kW]	$F_B[MBTU]$	$F_{PM}[MBTU]$	$Q_{rec.}[MBTU]$	$E_{PM}[MWh]$	$E_{pur.}[MWh]$	η_{CHP}	$PRSEC$	$PRSEC_{OS}$
600	15,942	59,922	24,779	5,200	4,225	73.6%	21.7%	33.8%
700	13,393	69,807	26,768	6,066	3,361	70.3%	22.6%	31.5%
800	12,706	79,195	28,099	6,906	2,533	67.2%	22.7%	29.4%
900	12,617	88,695	28,914	7,630	1,851	63.6%	21.0%	26.2%
1000	11,894	97,938	29,450	8,266	1,284	60.1%	19.3%	22.7%
1100	11,726	107,405	29,793	8,788	809	56.7%	16.4%	18.6%
1200	11,751	116,717	30,035	9,220	412	53.6%	12.9%	14.4%
1300	11,354	125,562	30,177	9,495	209	50.5%	8.8%	9.4%

What Table XX shows is how the efficiency of a trigeneration plant is higher than the separate production of the energy products needed by the facility. The efficiency of the plant decreases due to increasing the size of the installed gas turbine because of two factors: the gas turbine operation at low PLR and the incomplete recover of the WRH for highly fluctuating profiles. Making a comparison with Table XI it is possible to recognize how the efficiency for a trigeneration plant is always larger than a cogeneration plant. The analysis of the PRSEC better accounts for the real energy savings produced by the trigeneration system. The percentage reduction in source energy consumption reaches a peak for an installed size of 800 [kW]; however, making a comparison with the results obtained for the cogeneration system and reported in Table XI, the bigger improvements are reached for the larger installed sizes. In these cases the PRSEC is almost double the correspondent value for the cogeneration layout. This occurs for the increasing influence of the absorption chiller benefits produced for bigger installed sizes. Similar consideration can be produced for the $PRSEC_{OS}$. However, like in the trigeneration layout, the maximum of the $PRSEC_{OS}$ occurs for the smaller sizes. This is the consequence of having a system working at full load for the most of the time with reduced fluctuation of the WRH and of the gas turbine production; these factors allows higher efficiency to be reached.

5.5 Economic Analysis

The approach to the economic analysis of a trigeneration plant is the same as the one for a cogeneration plant, carried out in section 3.4. The economic parameters of interest are: the investment cost, the fuel cost, the O&M costs, and the economic savings obtained. Most of the previous information can be obtained analyzing the data presented in Table XIX and Table XVIII. Moreover, to carry out the analysis the following assumptions are adopted:

- The utility rates for energy resources are the same as those adopted for the cogeneration plant analysis;
- The investment and O&M costs for the management of the gas turbine are the same as those adopted for the cogeneration plant analysis;

- The reference point for the estimation of the economic savings obtained is the *base model* of the facility;
- The estimation of the O&M costs for the absorption chiller operation are neglected. It is assumed that they are comparable to the O&M costs of a traditional chiller;

For the sake of clarity, the last proposed assumption is a consequence of the adopted approach to the economic analysis. The analysis is not aimed to estimate the overall cost of the realization and management of the energy plant for the health care facility. Its purpose is rather estimating the economical benefits produced by the upgrade of the standard plant. Thus, only the differential costs between the different layouts are taken into account. Assuming the same O&M costs for an absorption chiller and a traditional electric chiller, this difference in layout has not to be reported in the economic analysis.

On the contrary, investment cost for the absorption chiller has to be evaluated. These information have been retrieved from the material provided by TRANE® in its website [29]. The company provides detailed information about the installation costs of its equipment. Only information about investment cost have been collected, because differential cost for piping and wiring between the two types of chillers is neglected. The information are summarized in Table XXI

The analyzed chiller sizes range from 150 to 483 [tons], thus the related costs are 250 [$/ton] for the traditional chiller and 350 [$/ton] for the absorption chiller. Concerning the electric chillers, the smaller installed equipment does not position inside the size range for which the

TABLE XXI: CHILLER INSTALLATION COSTS.

Type		Size [tons]	Cost [$/ton]
Centrifugal		200 to 600	250
		600 to 1400	240
Absorption	1 - stage	90 to 1600	350
	2 - stage	350 - 1000	500

cost estimation proposed by TRANE® works. However, being the only case and also being its size really close to lower limit of the range, the cost estimation has been adopted anyway.

As said before, the goal of this analysis is the estimation of the benefits and differential costs produced by the installation of an upgraded system, rather than a traditional one. The installation of an absorption chiller of a certain size avoid the installation of a tradition electric chiller of the same size. Thus, concerning the installation cost, the interesting parameter is the cost difference between two alternative solutions rather than their absolute cost.

5.5.1 Results

The preferential criterion to estimate the effectiveness of the proposed layouts is the analysis of the NPV values of the investments over their duration, which correspond to the life of the plant (twenty years). Thus, starting from the data collected in section 5.4 the NPV calculation is performed and the results are reported in figure 77.

The graph shows a maximum of 2,057,036.13 USD occurring for an installed size of 800 [kW]. The graph shows also a trend-line interpolating the experimental points, whose range is from 0 to 1300 [kW]. However, it has not been possible to perform intermediate simulations

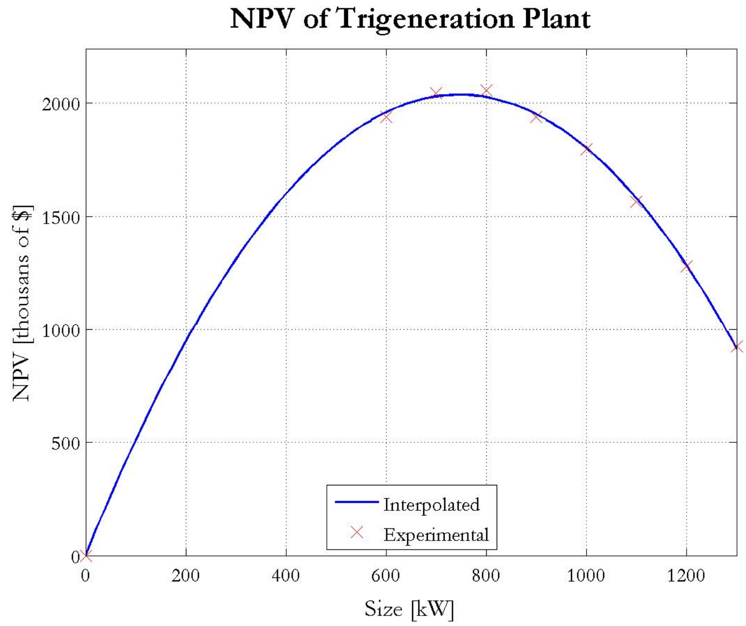

Figure 77: NPV of trigeneration plant.

to further prove the forecast shape of the curve. Simulations performed for sizes smaller than 600 [kw] show a dramatic increase of the fuel consumption due to the frequent unavailability of *recoverable heat*. This situation does not allow the proper simulation of a trigeneration plant. Moreover, for sizes smaller than 600 [kW] the corresponding optimal size of absorption chiller results is quite small; in this case also the cost estimation about the investment costs becomes unrealistic, reducing the reliability of the information obtained.

The NPV assessment is strictly connected to the estimation of the cash-flows of the investment. These are represented by the initial investment cost and the subsequent annual savings produced by each analyzed layout.

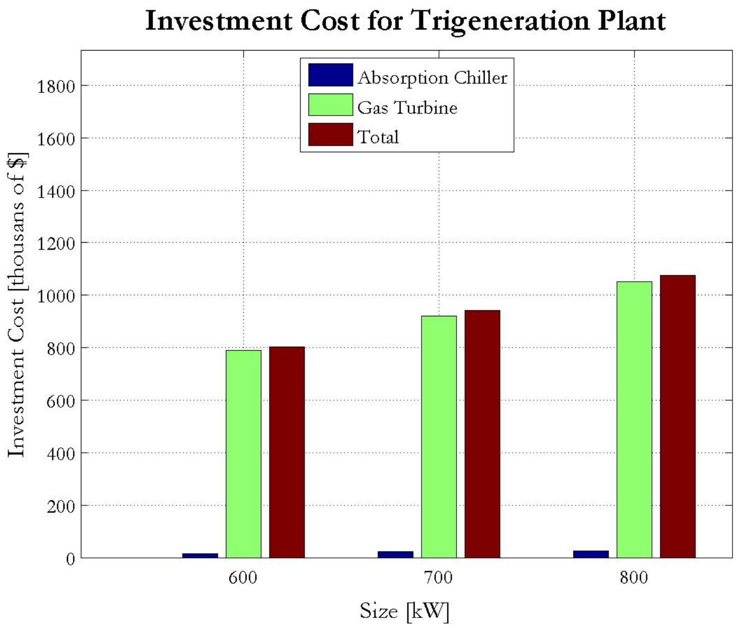

Figure 78: Investment costs of trigeneration plant.

The investment costs are reported in figure 78. The cost is split into the two components constituting it: the investment cost for the gas turbine and the investment cost for the absorption chiller. The former is two orders of magnitude larger than the latter, which thus has a reduced impact on the investment itself. The overall investment cost, are thus roughly linear, being controlled by the gas turbine investment cost.

Finally, figure 79 depicts the behavior of the annual saving produced by the investment. These savings are evaluated as the difference in fuel and O&M costs between the *base line* model of the plant and the trigeneration layout. The maximum is achieved for an installed size of 900 [kW] and is equal to 393,066 USD, although in the range between 800 and 1000 [kW] the

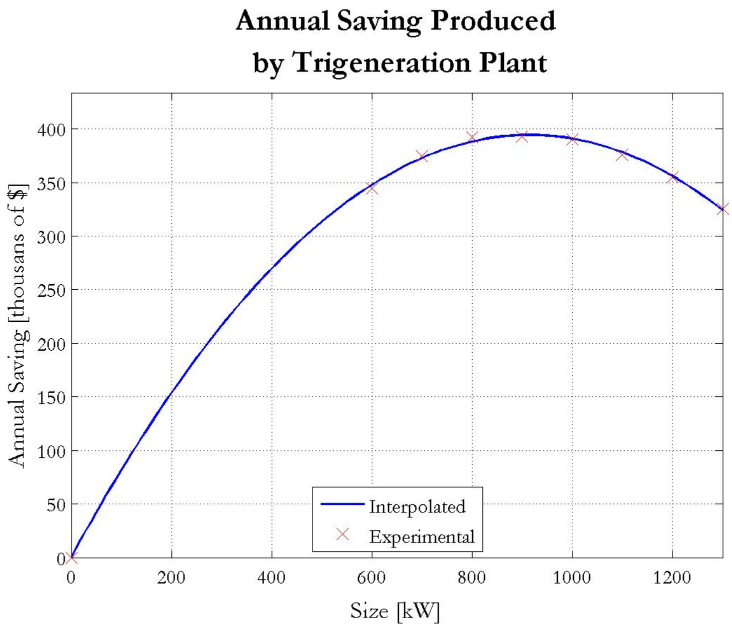

Figure 79: Annual savings of trigeneration plant.

curve is almost flat. This plateau has not to be misunderstood, the absorption chillers always provide increasing economic benefits as the installed sizes. However, these benefit are frustrated by the gas turbine efficiency reduction. Making a comparison with the annual savings profile for cogeneration plant (see figure 43) highlights how the maximum in annual savings occurs for a size of 800 [kW]; further increase of the installed size of gas turbine cause a steep savings decrease. The important economic parameters are summarized in Table XXII for all the analyzed sizes.

The 800 [kW] layout results the best system from a economic point of view because offers roughly the same annual savings of the bigger sizes at a reduced investment cost. It is the result of a compromise between the benefits produced by the gas turbine, which show a maximum for

TABLE XXII: PRINCIPAL ECONOMIC PARAMETERS - TRIGENERATION [USD].

Size [kW]	**600**	**700**	**800**	**900**	**1000**	**1100**	**1200**	**1300**
Investment Cost	803,400	942,300	1,076,200	1,212,600	1,347,300	1,482,100	1,618,400	1,756,500
Annual Savings	344,765	374,690	392,191	393,066	390,535	376,084	355,320	325,716
NPV	1,937,981	2,043,318	2,057,036	1,939,812	1,797,767	1,563,378	1,278,762	924,091

smaller sizes, and the benefits produced by the cold production through the absorption chiller, which offer the best effectiveness for larger sizes.

CHAPTER 6

CONCLUSION

The present study addressed the complex decision-making process regarding the design of the energy supply system of a health care facility.

This problem has been faced through the simulation on eQuest® of the design addressed by ASHRAE Standard 90.1 [7] [8]. The choice of referring to ASHRAE Standard 90.1 is due to the possibility to study a building that should be as similar as possible to an average US health care facility. The proper simulation of the building on eQuest® has required the revision of some of its default parameters. The adopted improvements consisted of: installation of pre-heat coils in the HVAC system, oversizing of certain heat exchangers, and increase of the maximum air temperature difference through the heat exchangers. These actions led to the proper management of the thermal loads in all the areas of the facility, ensuring the design temperature throughout it.

The improved accuracy in the simulation of the building provides a higher reliability of the output data concerning the estimation of the facility energy demand. *Base model* is the term used for referring to this initial layout of the energy supply system, which encompasses natural gas boilers for the heat production, electric chillers for the cold production, and the direct connection to the external electric grid for satisfying the electricity demand.

The obtained results are the profiles of the electric and thermal energy demand for the whole year. Moreover, the annual electrical consumption of the *base model* is 10,015 [MWh] and the overall fuel consumption is 49,363 [MBTU]. Other important retrieved information regard the peak demand of these resources, which are the parameters of interest for sizing the equipments. The maximum electrical demand occurs in summer, when the cooling need of the facility plays a fundamental role; its value is 2.07 [MW]. Conversely, the maximum fuel consumption occurs in winter because of the large heating load. The maximum value of the fuel demand is 21.24 [MBTU/h].

In order to enhance the energy efficiency of the facility, the study of a cogeneration system has been performed as an intermediate step towards the analysis of a trigeneration layout. The upgrade from the plant *base model* to the cogeneration plant is realized through the installation of a gas turbine, as prime mover, and a heat recovery generator for the hot water production.

The prime mover is the core of the plant, it is important to revise it, in order to provide reliable results. Thus, before the simulation of the cogeneration plant, information about the performances of modern gas turbine systems have been collected from manufacturers. This work highlighted how the default model of gas turbines on eQuest® is obsolete if compared with modern systems. Starting from the data provided by SOLAR® about its turbine named Centaur 40™, a new model has been developed. The obtained achievements can be summarized in an increased full-load efficiency, from 18.96% to 28.73%, and in a better behavior in off-design condition, which is no longer affected by a dramatic efficiency decrease.

Several gas turbine sizes have been simulated, ranging from 600 to 1300 [kW]. The analysis allowed to estimate the changes in energy demand profiles caused by each layout of the system. Increasing the size of the installed gas turbine an increase of the fuel consumption is experienced, although a reduction of the fuel consumption for heating purposes occurrs. Simultaneously, increasing the gas turbine size, a reduction of the amount of electricity purchased from the external grid is observed, because of the increased on-site electricity production.

The study highlights how these trends have different behaviors, thus the increase in fuel consumption is not always concurrent with a proportional reduction of the purchased electricity. This situation allows to maximize the benefits produced by the plant emprovement.

The definition of the gas turbine optimal size has been possible thanks to the analysis of economic benefits produced by each layout. The NPV for each system is calculated taking into account the initial investment cost associated with the plant realization and the produced annual savings; the latter are evaluated as the differential annual management cost between the *base model* and the analyzed cogeneration layout.

The best system size encompasses a 700 [kW] gas turbine. It provides the highest NPV value over the life of the plant; this value is of 1,636,771 USD.

The results obtained by tha analysis of the cogeneration layouts are not only necessary to perform the economic analysis, but also to assess the feasibility of a trigeneration system. Analyzing the information about the amount of *wasted recoverable heat* available for each layout, it has been possible to determine the optimal sizes of absorption chiller. Two different approaches have been proposed for the sizing procedure: the iterative and the double simulation approach. However, only the former has been extensively applied, because it provides a higher reliability of the simulation output.

Absorption chillers with sizes ranging from 150 to 483 [tons] have been installed in different plant layouts. The larger the size of the installed gas turbine, the larger that of the proposed absorption chiller.

The post process of each simulation output data has allowed the evaluation of the improvement provided by the upgrade to a trigeneration layout. The principal effect produced by the installation of the absorption chiller is the reduction of the electric demand throughout the whole year, especially in summer, when the highest cold demand is encountered. The overall electric consumption suffers a reduction which is proportional to the installed sizes of absorption chiller. The reduction percentage of the electric consumption ranges from 5.9% to 6.7% for the larger size.

Moreover, a deep analysis of the fuel consumption data shows two sides effects of the installation of an absorption chiller. First of all, the fuel consumption due to the gas turbine feeding does not experience as large of a reduction as the electric production, because of the partialization of most of the gas turbines. Secondly, the analysis has detected an undesired but unavoidable consumption of natural gas for the direct feeding of the absorption chillers. This situation causes an increase of the overall fuel consumption for boilers operation. Multiple simulations have been performed to proper size the absorption chiller and to keep this amount of extra fuel as low as possible, even though it has not been possible to completely eliminate it. This situation has been accepted as a reasonable drawback compared to the benefits produced by the absorption chiller; especially because the maximum percentage increase of the fuel for boilers has been lower than 1.47%, if compared to the overall fuel consumption of the facility.

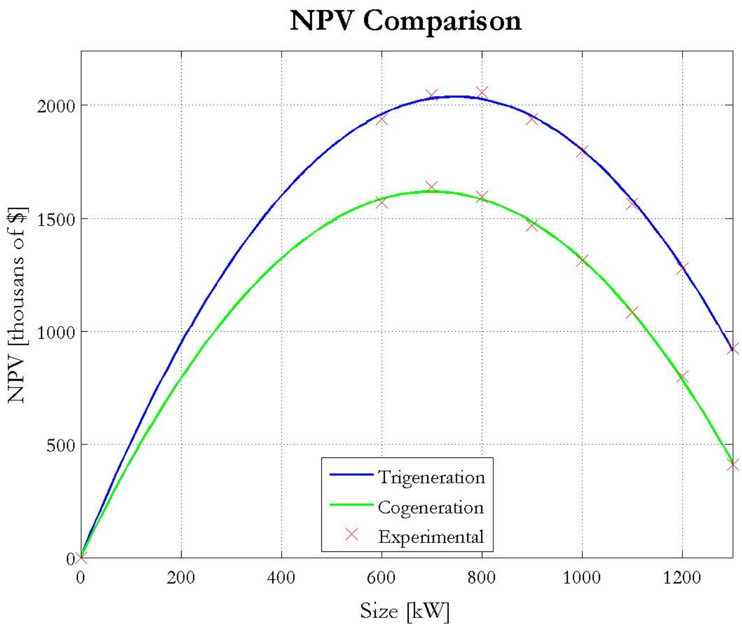

Figure 80: NPV comparison for cogeneration and trigeneration plants.

The economic analysis carried out for the trigeneration plant shows how the maximum NPV for the investment is obtained installing a trigeneration plant with a gas turbine of 800 [kW]. The value of NPV in this case is 2,057,036 USD. In figure 80 it is possible to compare the trend of the NPV for both the cogeneration and the trigeneration plant.In both the cases, the data have been interpolated using a quadratic polynomial. The curve referring to trigeneration plant shows a higher maximum and it occurs for a larger gas turbine size. Comparing the best cogeneration layout with the best trigeneration layout, a percentage increase for the NPV of the investment is noticed; this increase is about 25.7%.

The performance of the plants have been analyzed not only on the point of view of the economic benefits produced by the investment; an analysis concerning the reduction in source energy consumption has been carried out through the employment of the PRSEC and $PRSEC_{OS}$ indexes. This analysis is not influenced by the temporary economic framework, e.g., utilities price, investment cost or availability of financing for the investment. Conversely, it provides a measure of the environmental benefits achieved. However, because of the strong connection existing between source energy savings and economic savings, in both the cases the best results for the facility are achieved for the same sizes producing the highest economic savings: 700 [kW] for the cogeneration layout, 800 [kW] for the trigeneration layout. In both the cases, focusing only on the performance of the CHP plant ($PRSEC_{OS}$), the best performances are achieved for the smallest installed size (600 [kW]), resulting in a layout working in full load steady state conditions for the whole year. The obtained results are collected in Table XXIII. In this table it is possible to compare the different performance of both the layout analyzed. The common trend is represented by the reduction of performance of the CHP system ($PRSEC_{OS}$ index). Similarly the efficiency of the whole plant ($PRSEC$ index) reaches a maximum. Although a maximum exists in both the cases, it occurs for different sizes depending on the adopted layout.

From the comparison of these results with the one obtained by the analysis of a cogeneration plant, an important conclusion is obtained. The upgrade of a cogeneration plant into a trigeneration plant always provides the possibility to better exploits the wasted heat produced by the prime mover. This entails an increase of the optimal size of gas turbine. Changing

TABLE XXIII: FUEL CONSUMPTION FOR THE ANALYZED LAYOUTS - [MBTU].

	Cogeneration		**Trigeneration**	
Size [kW]	$PRSEC$	$PRSEC_{OS}$	$PRSEC$	$PRSEC_{OS}$
600	18.4%	29.1%	21.7%	33.8%
700	19.0%	27.0%	22.6%	31.5%
800	18.2%	24.7%	22.7%	29.4%
900	16.3%	21.2%	21.0%	26.2%
1000	14.3%	17.5%	19.3%	22.7%
1100	11.5%	13.2%	16.4%	18.6%
1200	8.1%	8.8%	12.9%	14.4%
1300	3.5%	3.5%	8.8%	9.4%

layout, the $PRSEC$ index increases by 3.7%. In this case, the overall percentage reduction in source energy consumption is of 22.7%.

These results confirm the feasibility and profitability of on-site power generation and underline the big improvements produced for the health care facility by the realization of a trigeneration system rather than a cogeneration system.

APPENDICES

Appendix A

HOSPITAL

A.1 FIRST FLOOR HOSPITAL MAP

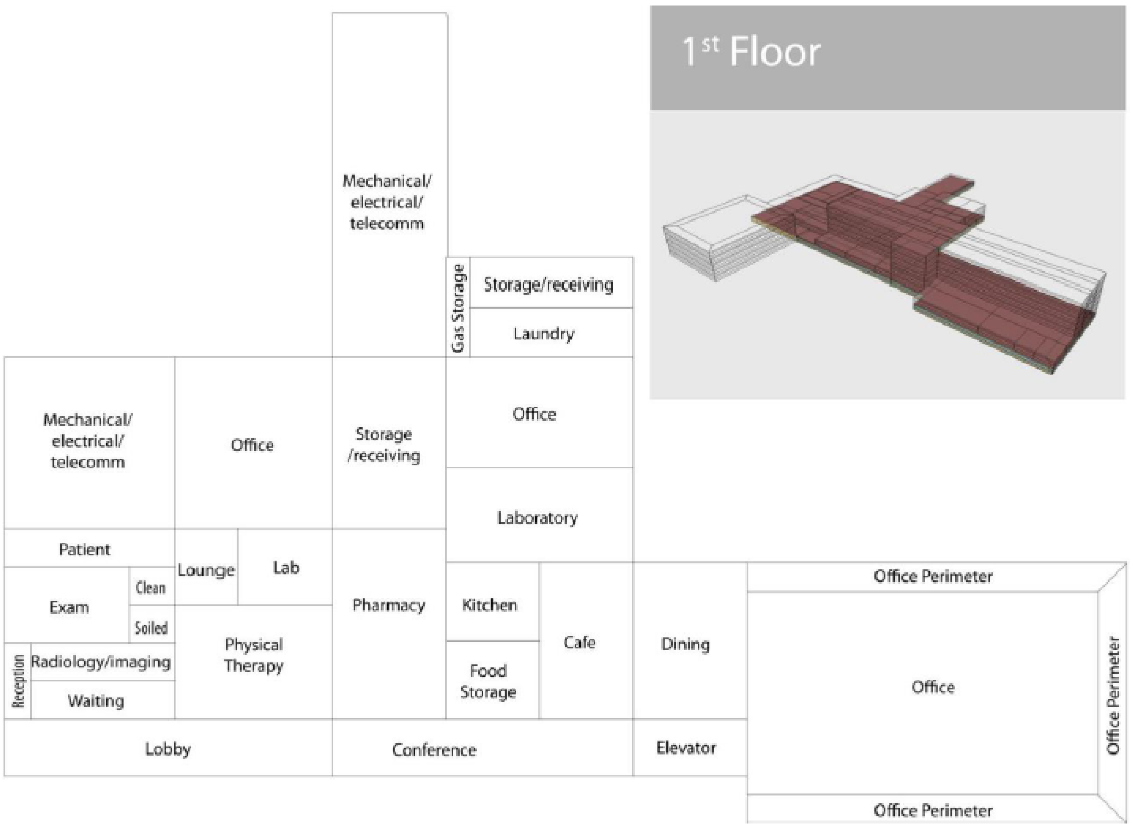

Figure 81: Map of the first floor of the prototype hospital.

APPENDIX A (Continued)

A.2 SECOND FLOOR HOSPITAL

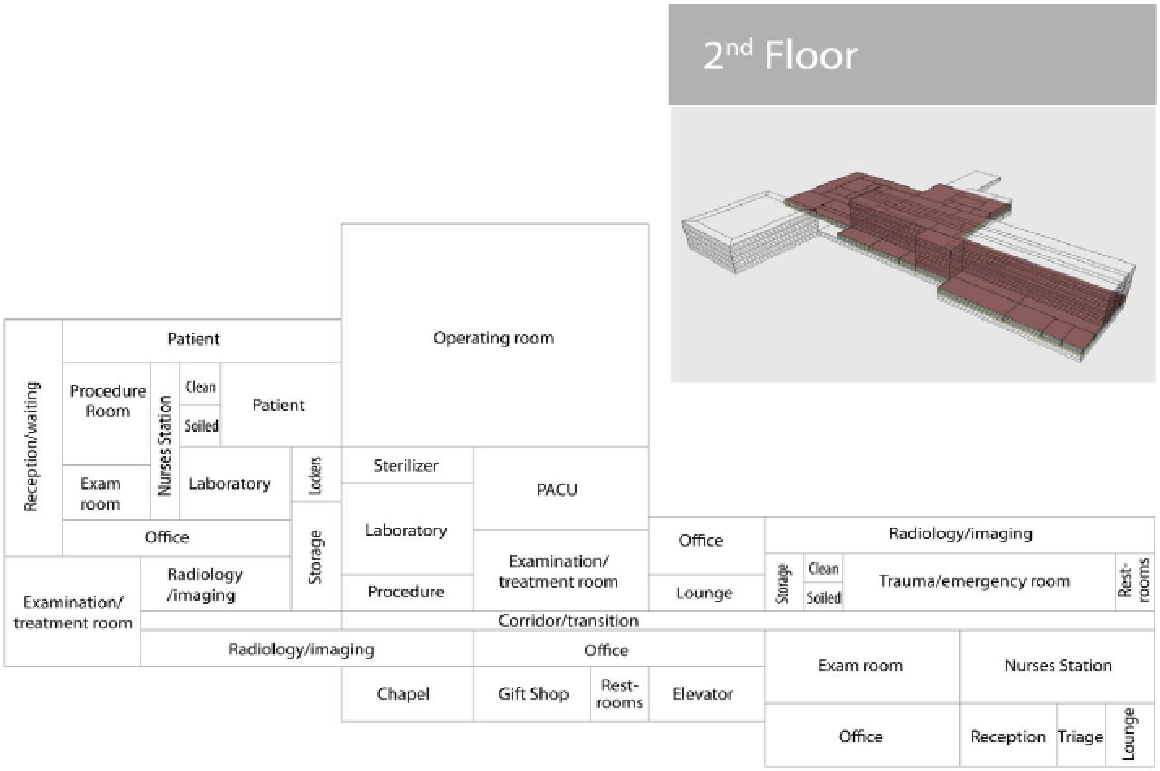

Figure 82: Map of the second floor of the prototype hospital.

APPENDIX A (Continued)

A.3 THIRD FLOOR HOSPITAL

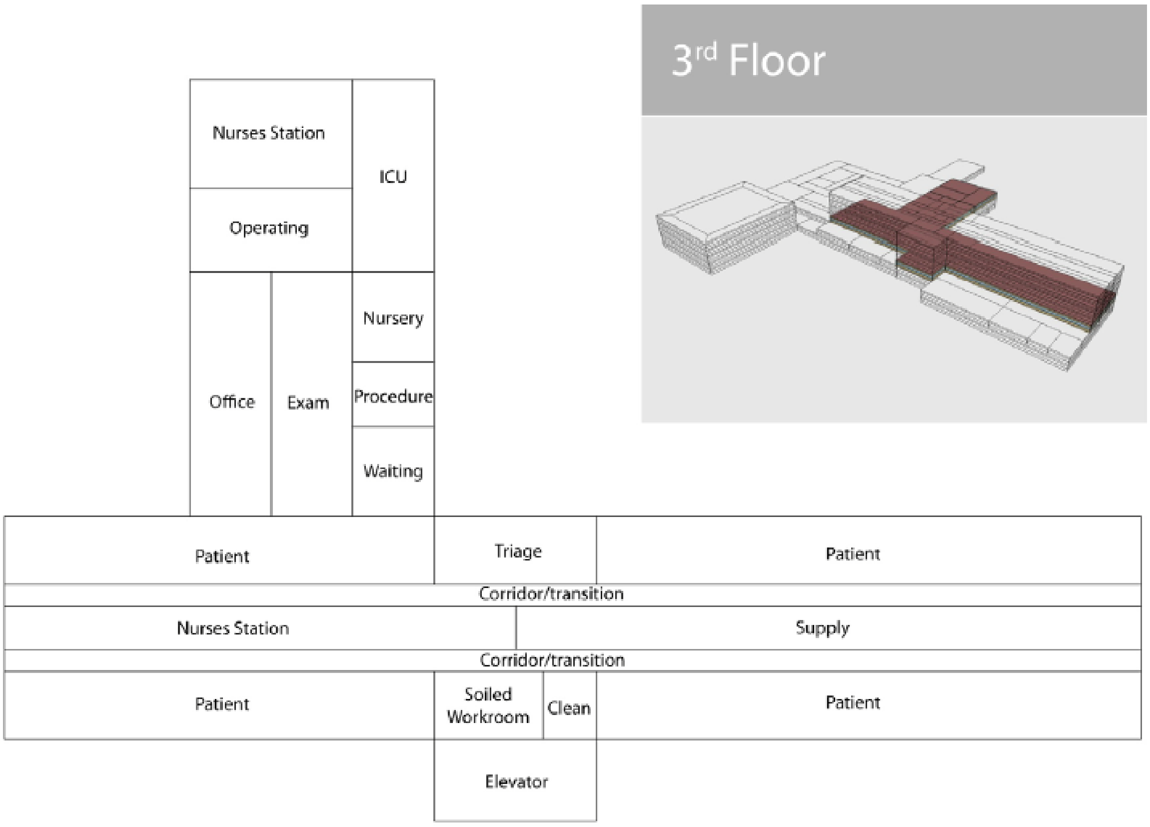

Figure 83: Map of the third floor of the prototype hospital.

APPENDIX A (Continued)

A.4 FORTH TO SEVENTH FLOORS HOSPITAL

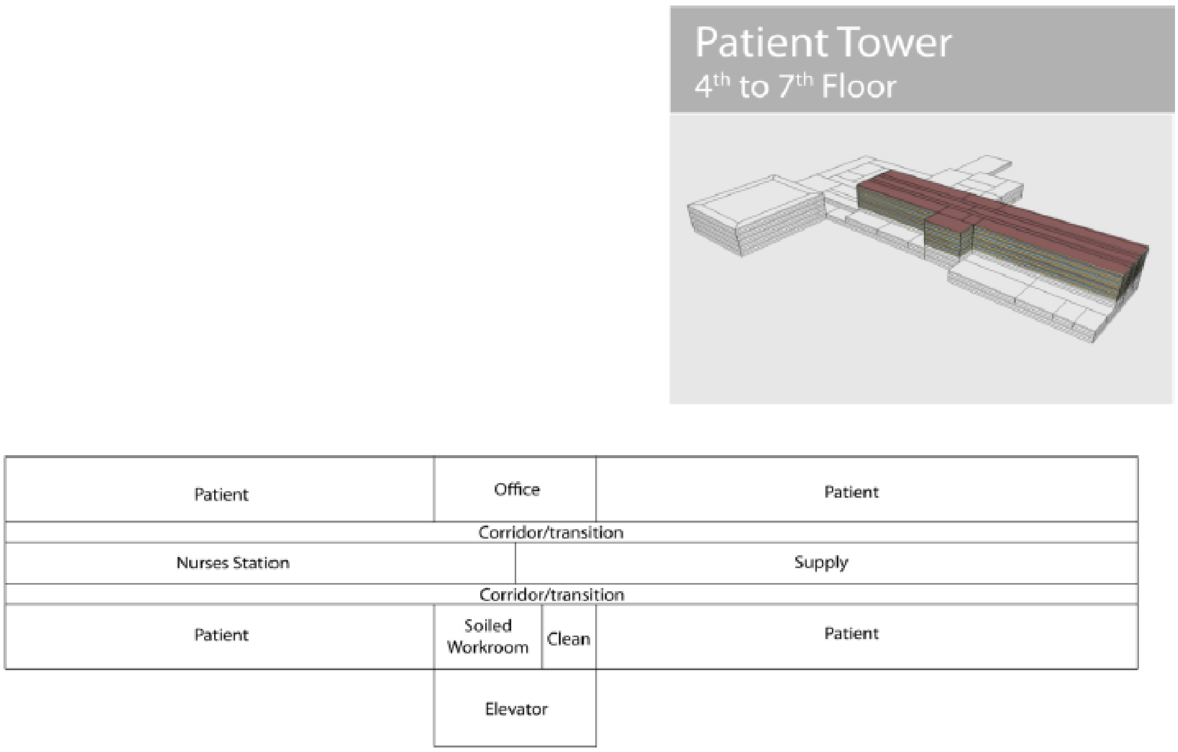

Figure 84: Map of the last three floors of the prototype hospital.

A.5 MEDICAL OFFICE BUILDING

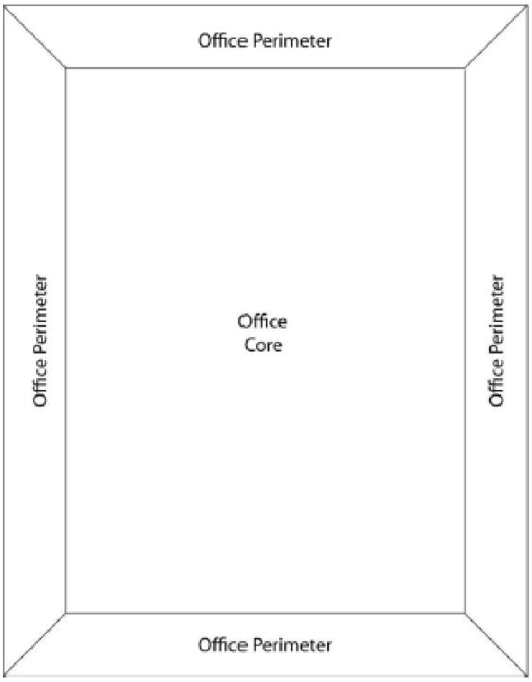

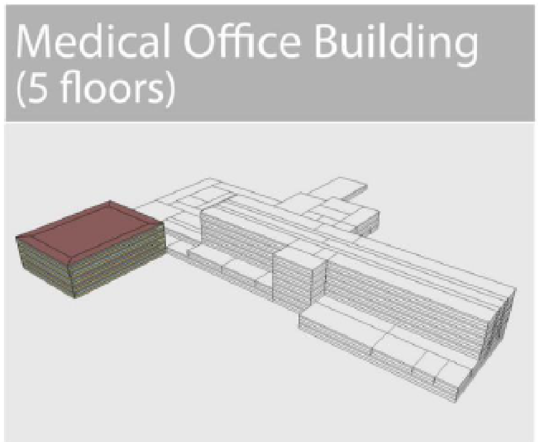

Figure 85: Map of the five floors of the MOB.

Appendix B

EQUATIONS

In this appendix the equations and the models derived in this thesis are reported in the same form required by eQuest®.

B.1 Gas Turbine Model

General parameters:

- Heat to input ratio=3.39;
- Min ratio=0.1;
- Max ratio=1.0;
- Start up time=0.17;

Performance curve coefficients for Gas Turbine heat to input ratio vs. partial load ratio:

- a=0.2006;
- b=1.9881;
- c=-1.2400;

Performance curve coefficients for Gas Turbine capacity vs. ambient temperature:

- a=1.1460;

- b=-0.0024;

Performance curve coefficients for Gas Turbine exhaust heat recovery vs. partial load ratio:

- a=0.2956;
- b=0.4930;
- c=0.2113;

B.2 Absorption Chiller Model

General parameters:

- electricity to input ratio=0.007
- heat to input ratio=1.2500
- chilled water temperature=44
- condenser temperature=85
- condenser flow=3.6
- max heat recovery condenser=0.0

Performance curve coefficients for ABS CHiller heat to input ratio vs. partial load ratio:

- a=1.2703
- b=-0.0079

APPENDIX B (Continued)

- c=0.000054

Performance curve coefficients for ABS CHiller heat to input ratio vs. chilled water temperature:

- a=0.3012

Performance curve coefficients for ABS CHiller capacity vs. chilled water temperature:

- a=1.9327
- b=0.0
- c=0.0
- d=-0.0152
- e=0.00005
- f=0.0

Appendix C

COGENERATION

C.1 Electric Demand Hourly Profile

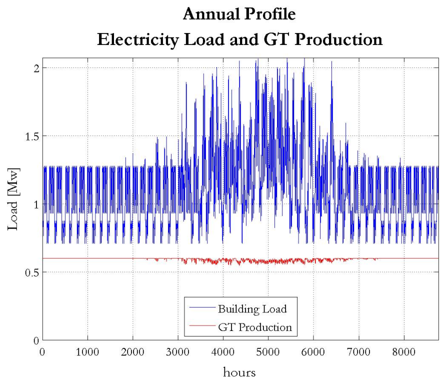

(a) Cogeneration 600 kw

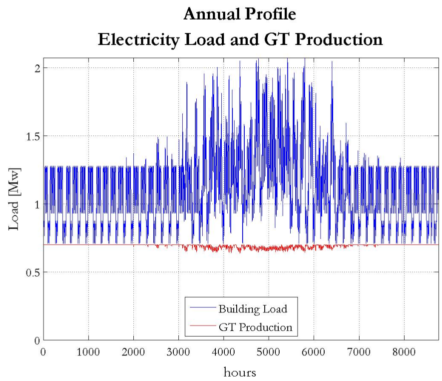

(b) Cogeneration 700 kw

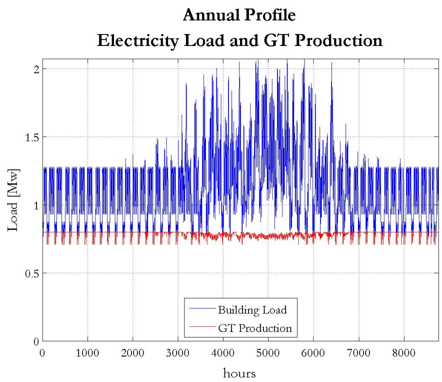

(c) Cogeneration 800 kw

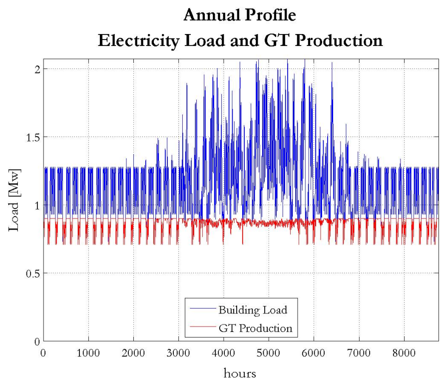

(d) Cogeneration 900 kw

Figure 86: Electrical duration curves for several proposed cogeneration layouts [1/2].

APPENDIX C (Continued)

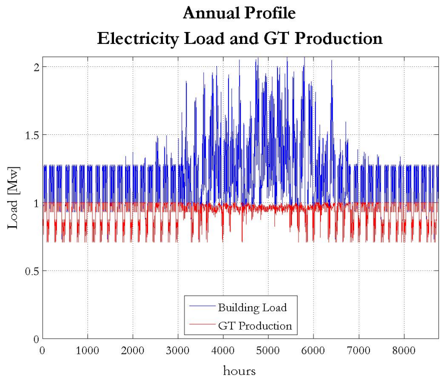

(a) Cogeneration 1000 kw

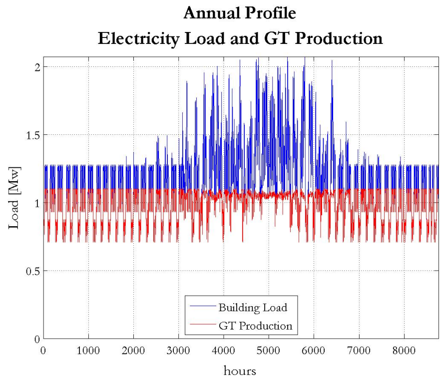

(b) Cogeneration 1100 kw

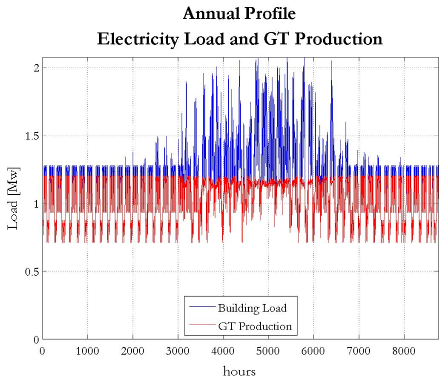

(c) Cogeneration 1200 kw

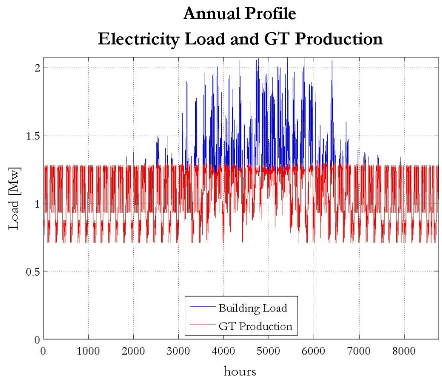

(d) Cogeneration 1300 kw

Figure 87: Changes in electrical duration curves for several proposed cogeneration layouts [2/2].

APPENDIX C (Continued)

C.2 Electric Demand Duration Curves

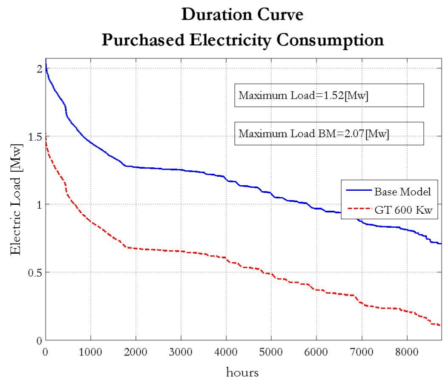

(a) Cogeneration 600 kw

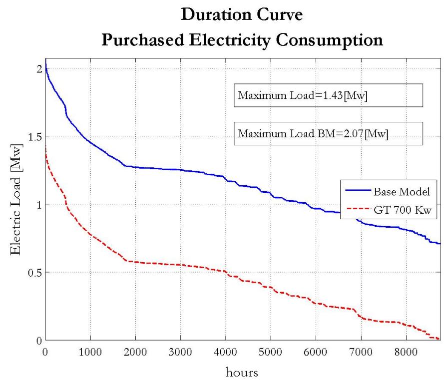

(b) Cogeneration 700 kw

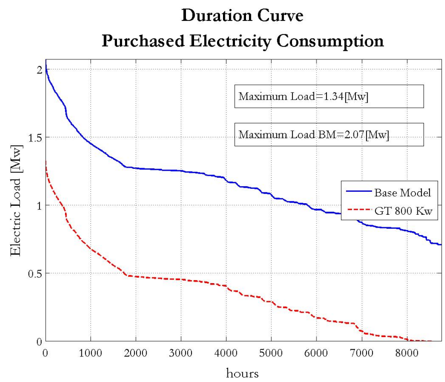

(c) Cogeneration 800 kw

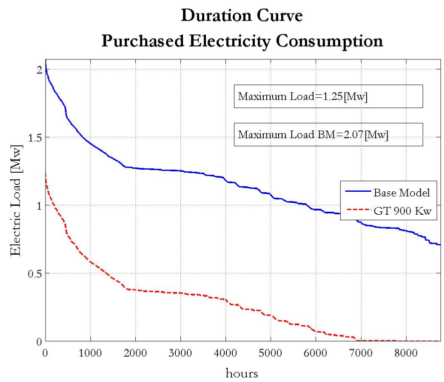

(d) Cogeneration 900 kw

Figure 88: Electrical duration curves for several proposed cogeneration layouts [1/2].

APPENDIX C (Continued)

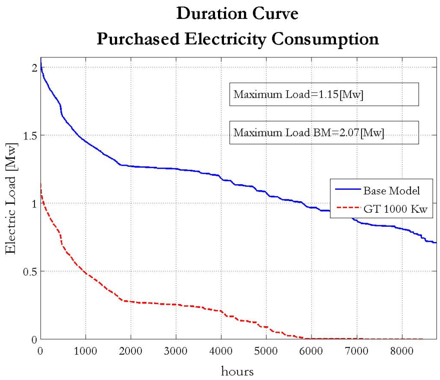

(a) Cogeneration 1000 kw

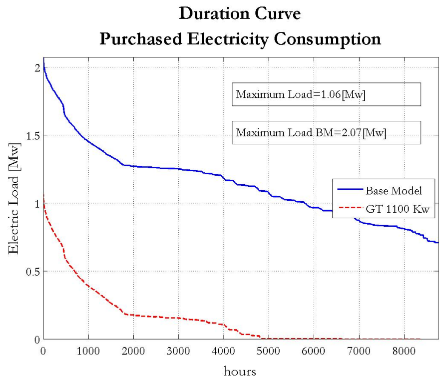

(b) Cogeneration 1100 kw

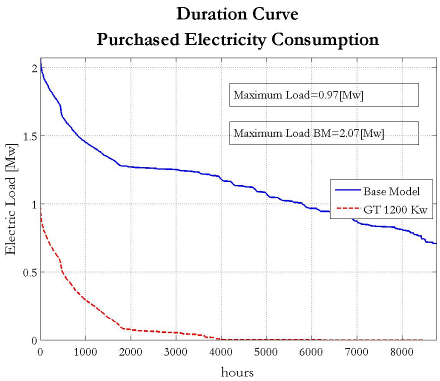

(c) Cogeneration 1200 kw

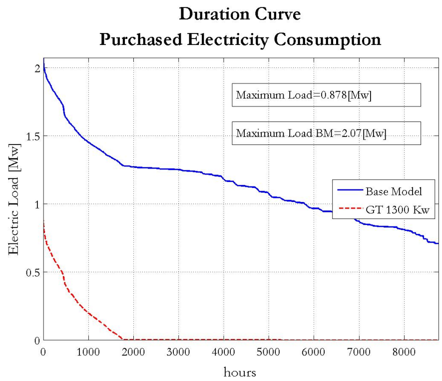

(d) Cogeneration 1300 kw

Figure 89: Electrical duration curves for several proposed cogeneration layouts [2/2].

APPENDIX C (Continued)

C.3 Monthly Electricity Production

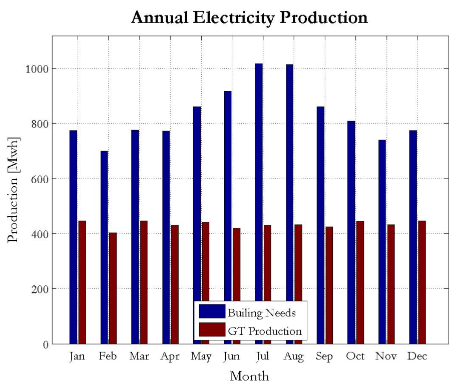

(a) Cogeneration 600 kw

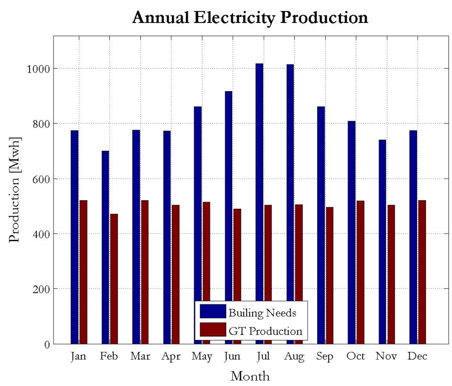

(b) Cogeneration 700 kw

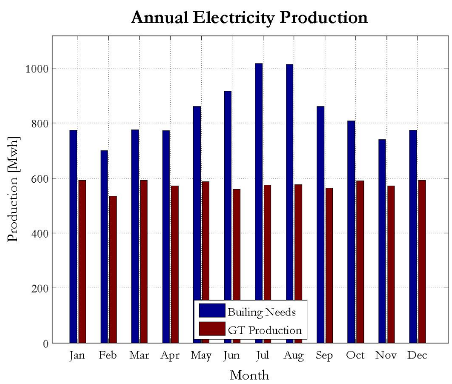

(c) Cogeneration 800 kw

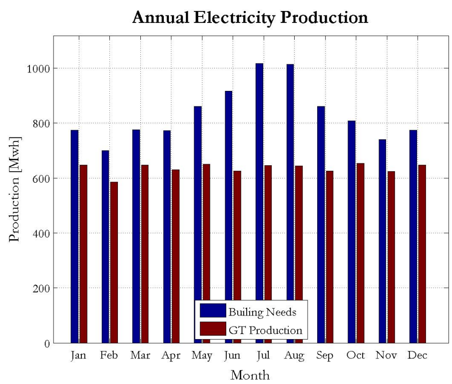

(d) Cogeneration 900 kw

Figure 90: Monthly electricity production for several proposed cogeneration layouts [1/2].

APPENDIX C (Continued)

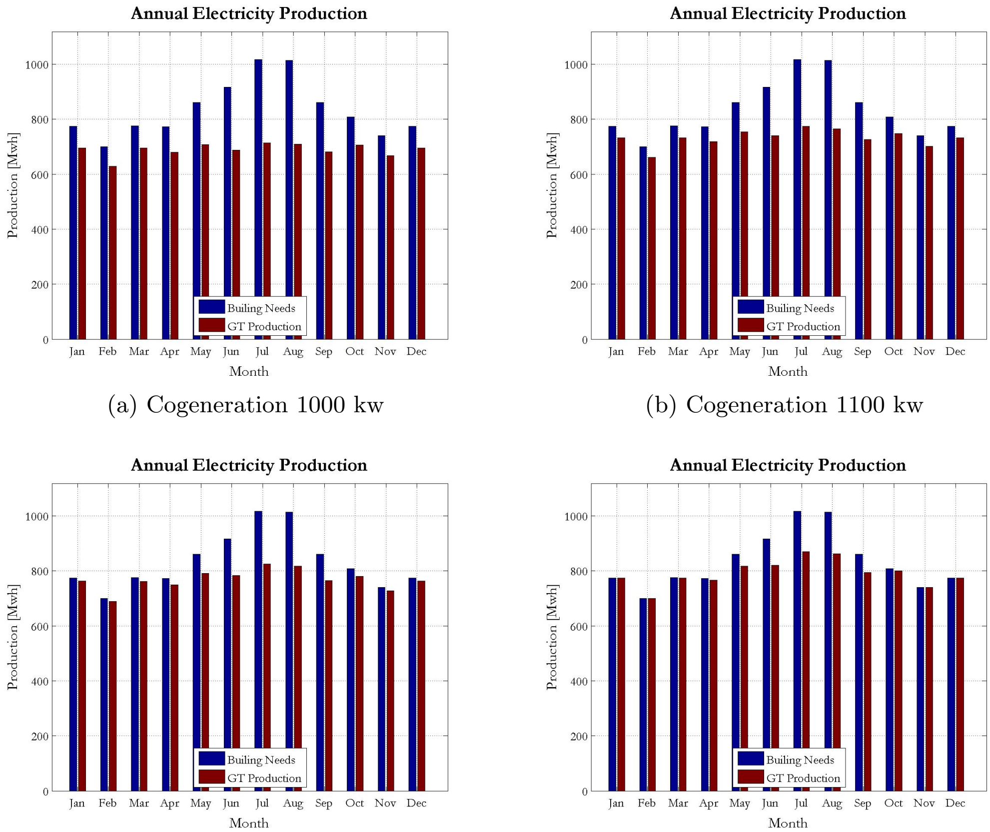

(a) Cogeneration 1000 kw

(b) Cogeneration 1100 kw

(c) Cogeneration 1200 kw

(d) Cogeneration 1300 kw

Figure 91: Monthly electricity production for several proposed cogeneration layouts [2/2].

APPENDIX C (Continued)

C.4 Duration Curves of Fuel Demand for Heating Purposes

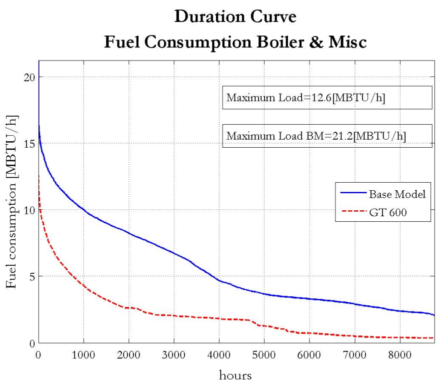

(a) Cogeneration 600 kw

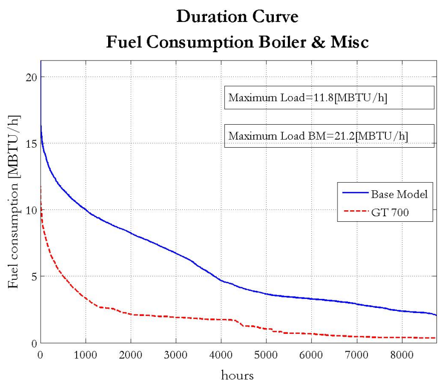

(b) Cogeneration 700 kw

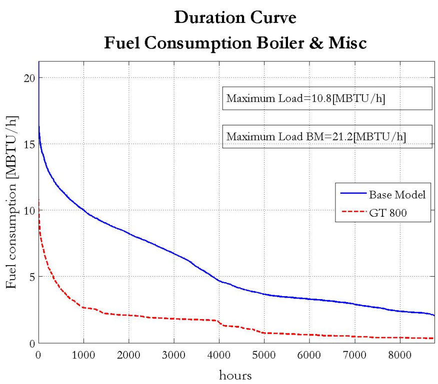

(c) Cogeneration 800 kw

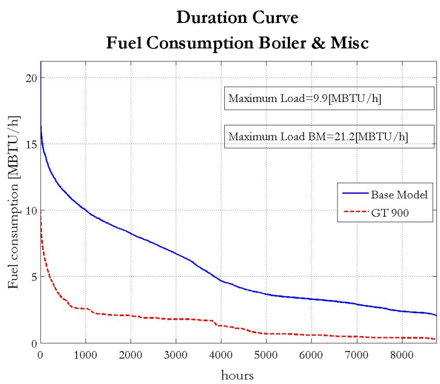

(d) Cogeneration 900 kw

Figure 92: Fuel for purposes other than gas turbine feeding. Duration curves. [1/2].

APPENDIX C (Continued)

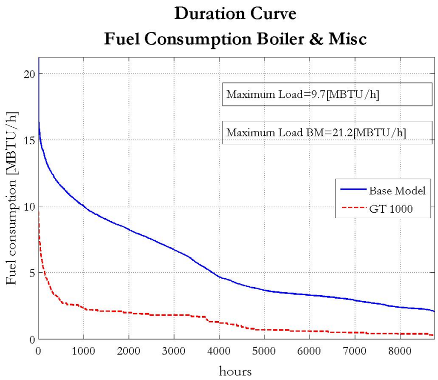

(a) Cogeneration 1000 kw

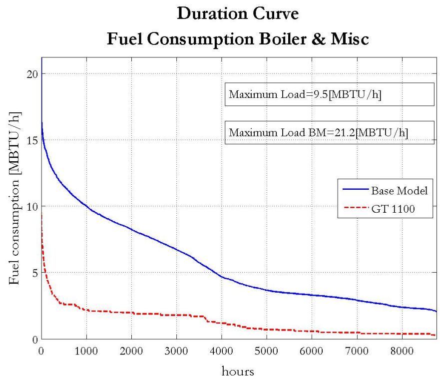

(b) Cogeneration 1100 kw

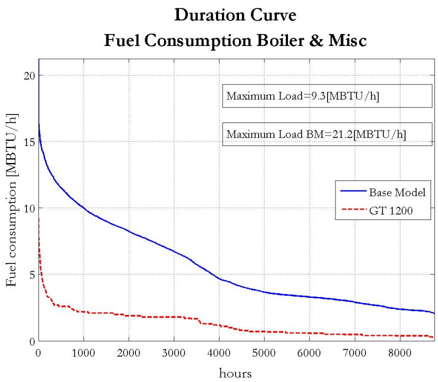

(c) Cogeneration 1200 kw

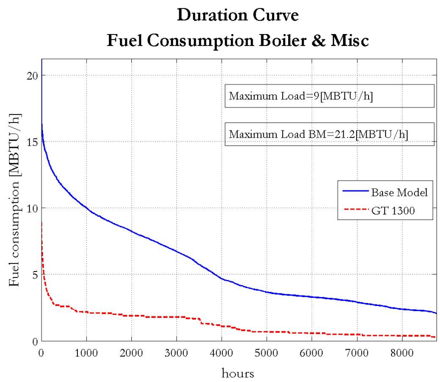

(d) Cogeneration 1300 kw

Figure 93: Fuel for purposes other than gas turbine feeding. Duration curves. [2/2].

APPENDIX C (Continued)

C.5 Monthly Fuel Consumption for Heating Purposes

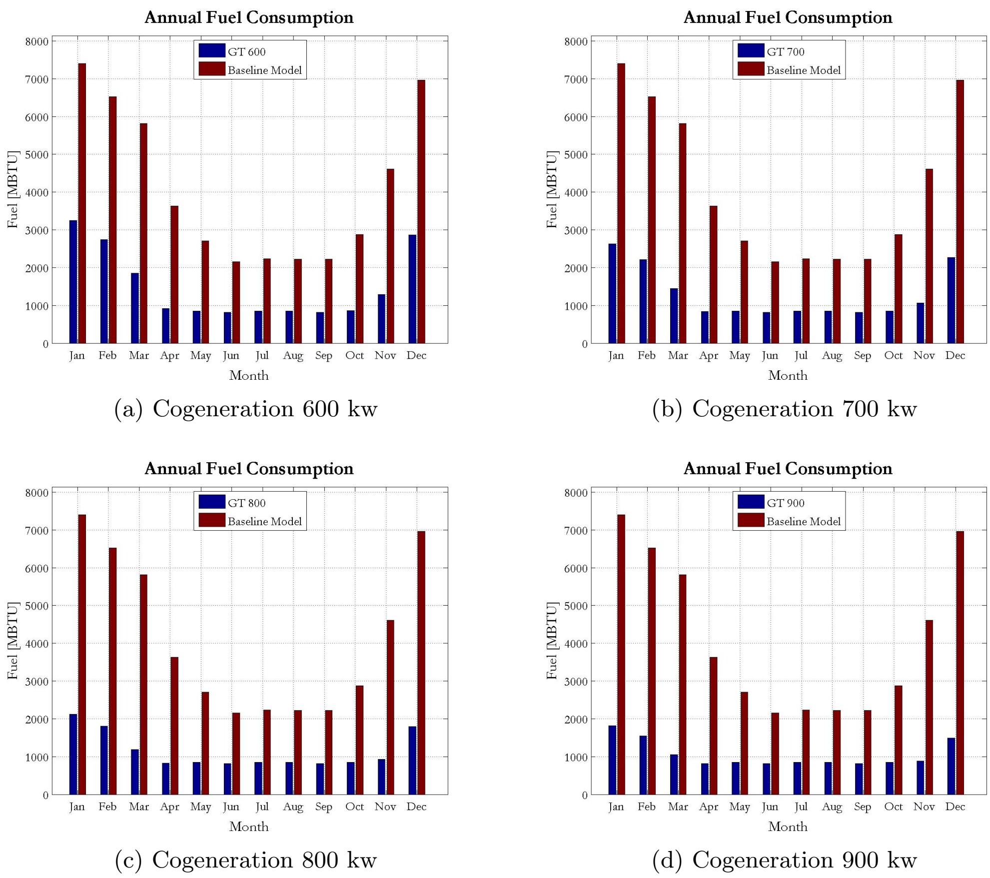

(a) Cogeneration 600 kw

(b) Cogeneration 700 kw

(c) Cogeneration 800 kw

(d) Cogeneration 900 kw

Figure 94: Monthly fuel consumption for heating and other purposes [1/2].

APPENDIX C (Continued)

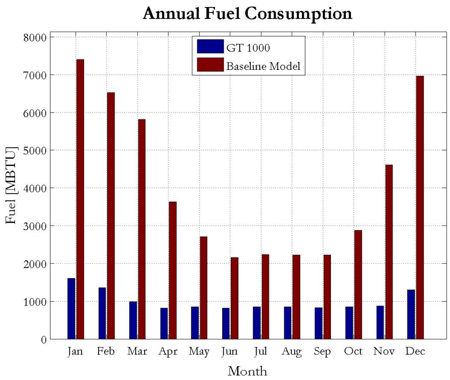

(a) Cogeneration 1000 kw

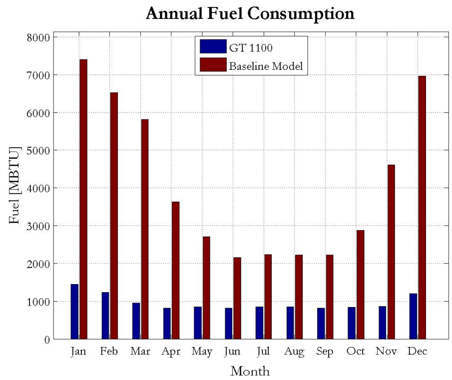

(b) Cogeneration 1100 kw

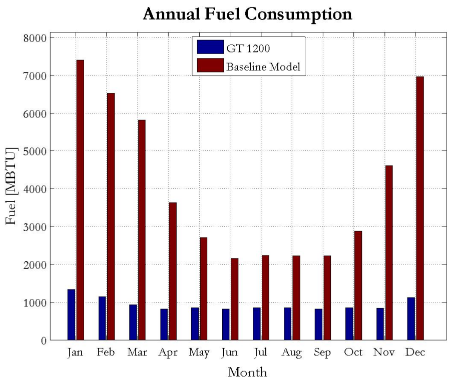

(c) Cogeneration 1200 kw

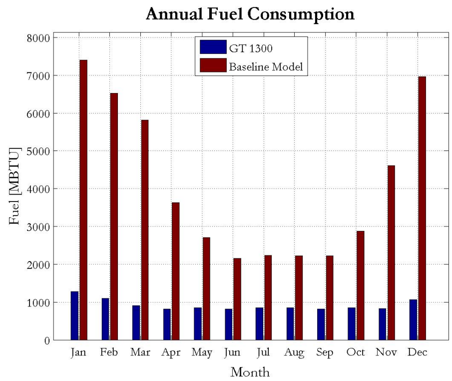

(d) Cogeneration 1300 kw

Figure 95: Monthly fuel consumption for heating and other purposes [2/2].

APPENDIX C (Continued)

C.6 Duration Curves of Overall Fuel Demand

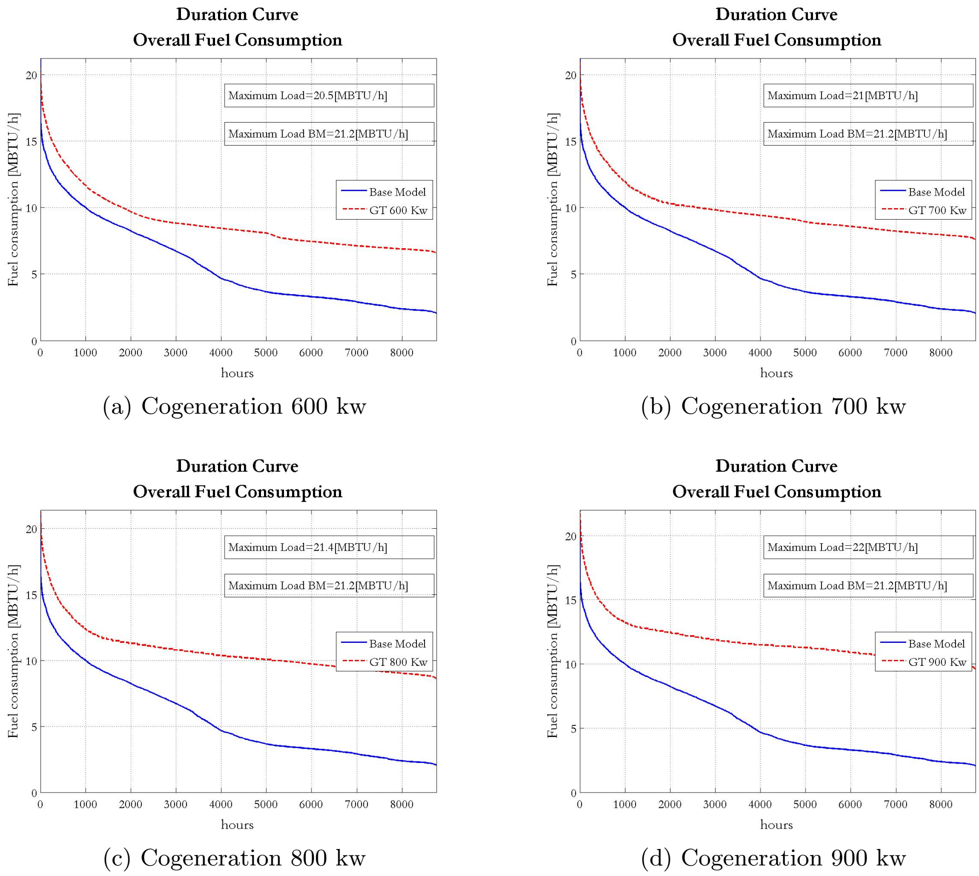

Figure 96: Overall fuel consumption. Duration curves. [1/2].

APPENDIX C (Continued)

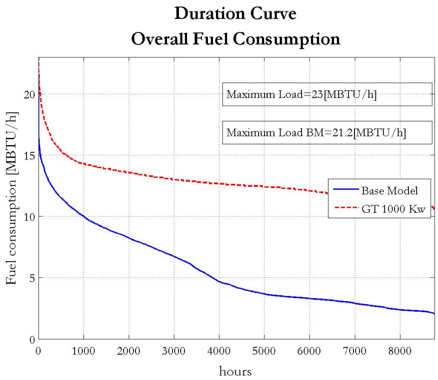

(a) Cogeneration 1000 kw

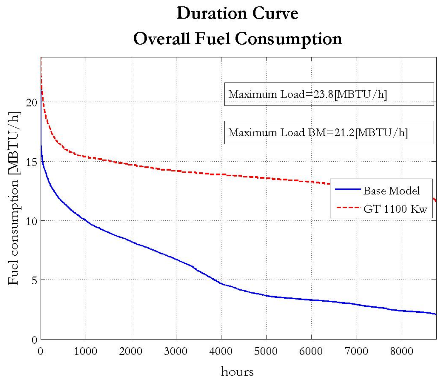

(b) Cogeneration 1100 kw

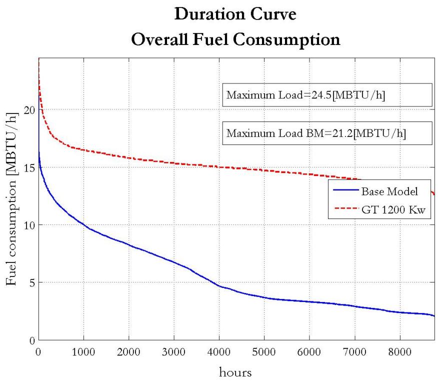

(c) Cogeneration 1200 kw

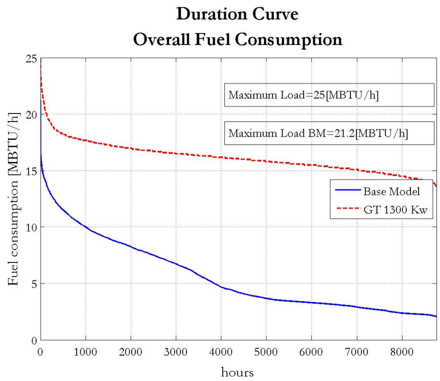

(d) Cogeneration 1300 kw

Figure 97: Overall fuel consumption. Duration curves. [2/2].

APPENDIX C (Continued)

C.7 Thermal Needs, Recovered Heat and WRH

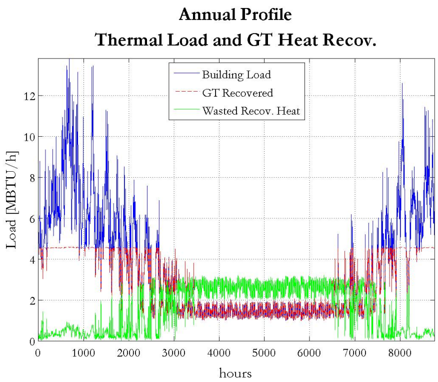

(a) Cogeneration 600 kw

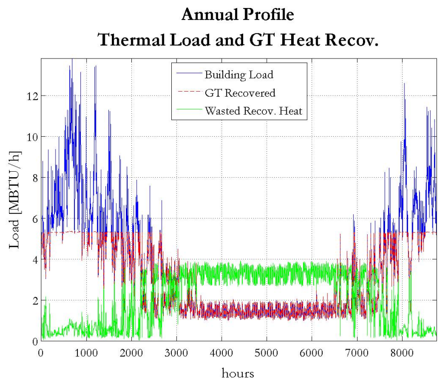

(b) Cogeneration 700 kw

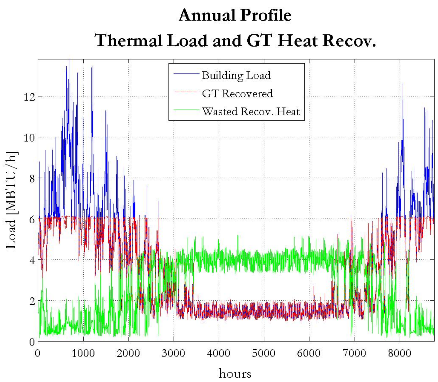

(c) Cogeneration 800 kw

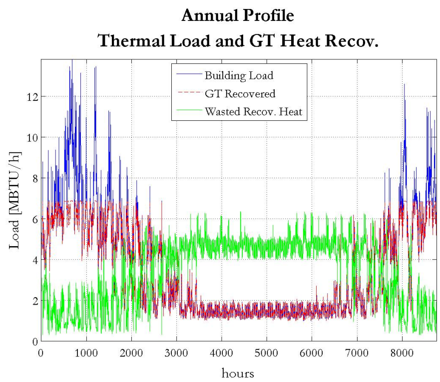

(d) Cogeneration 900 kw

Figure 98: Hourly profile of building thermal needs, recovered heat and WRH. [1/2].

APPENDIX C (Continued)

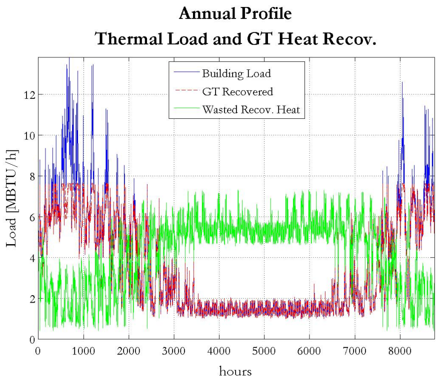

(a) Cogeneration 1000 kw

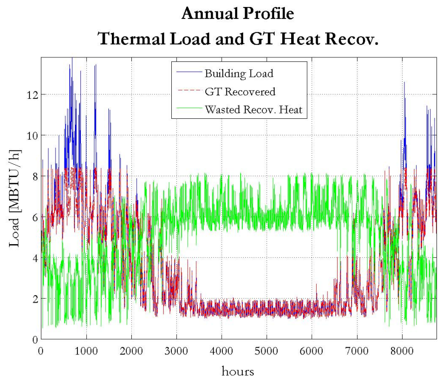

(b) Cogeneration 1100 kw

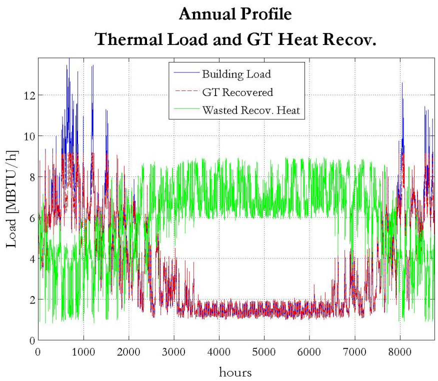

(c) Cogeneration 1200 kw

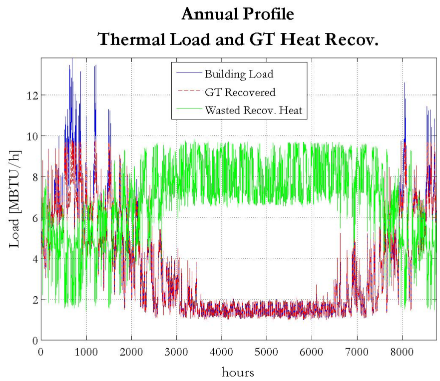

(d) Cogeneration 1300 kw

Figure 99: Hourly profile of building thermal needs, recovered heat and WRH. [2/2].

Appendix D

TRIGENERATION

D.1 Electric duration curves

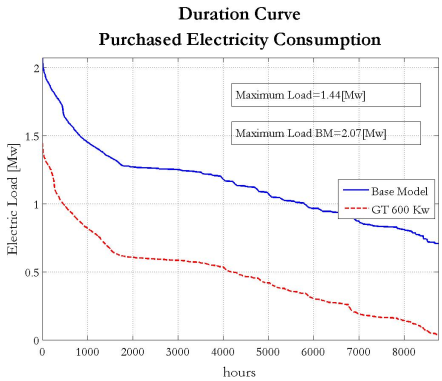

(a) Trigeneration 600 kw

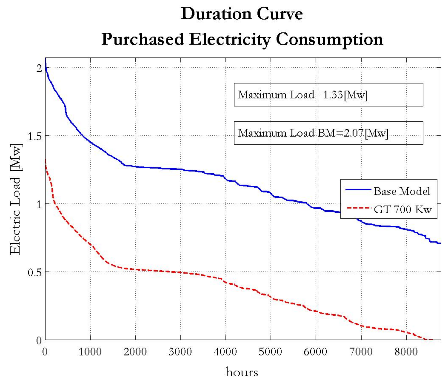

(b) Trigeneration 700 kw

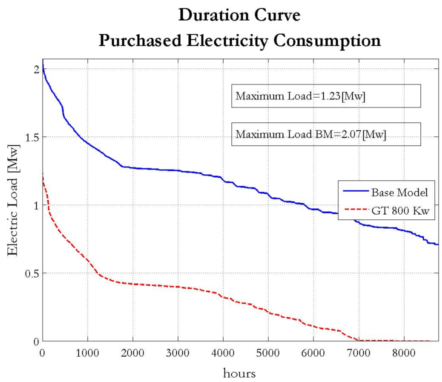

(c) Trigeneration 800 kw

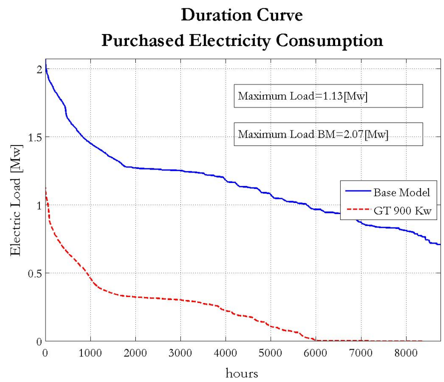

(d) Trigeneration 900 kw

Figure 100: Changes in electrical duration curves for several proposed trigeneration layouts [1/2].

APPENDIX D (Continued)

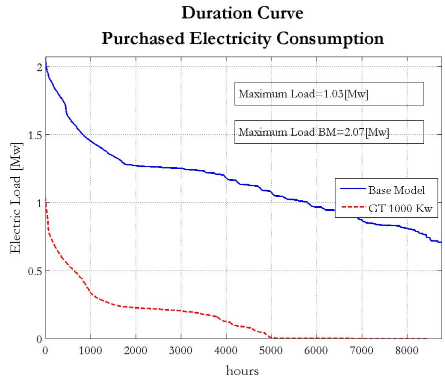

(a) Trigeneration 1000 kw

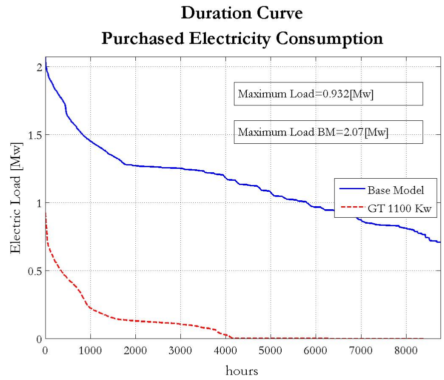

(b) Trigeneration 1100 kw

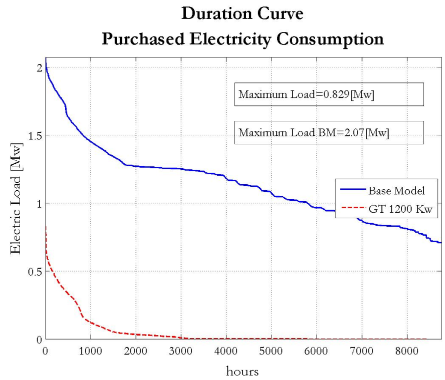

(c) Trigeneration 1200 kw

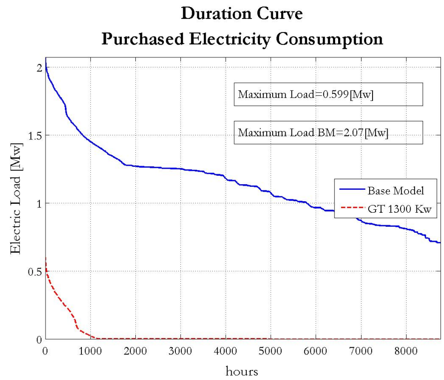

(d) Trigeneration 1300 kw

Figure 101: Changes in electrical duration curves for several proposed trigeneration layouts [2/2].

APPENDIX D (Continued)

D.2 Electric hourly profile

Hourly profile comparison for all the studied cases.

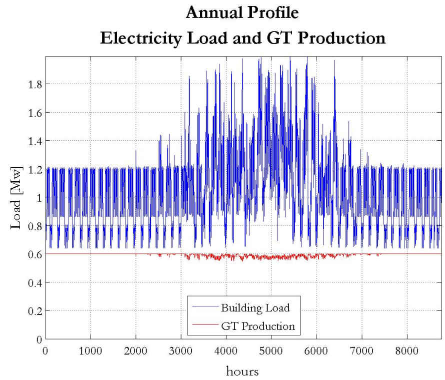

(a) Trigeneration 600 kw

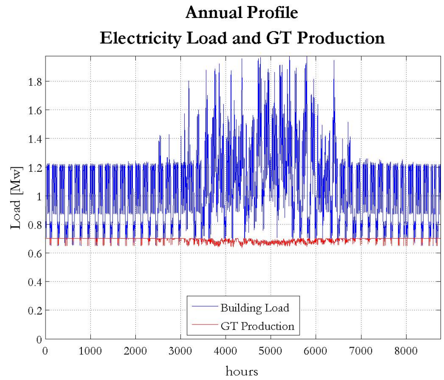

(b) Trigeneration 700 kw

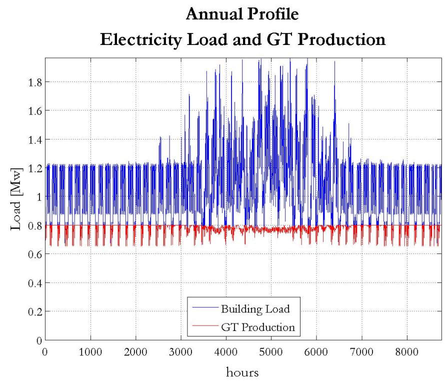

(c) Trigeneration 800 kw

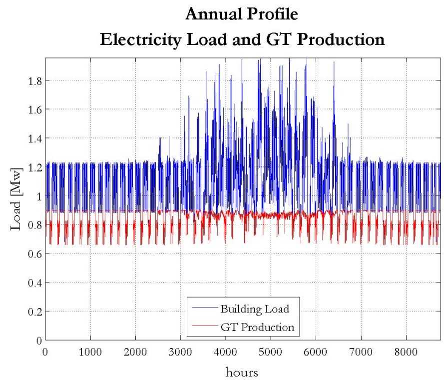

(d) Trigeneration 900 kw

Figure 102: Electrical duration curves for several proposed trigeneration layouts [1/2].

APPENDIX D (Continued)

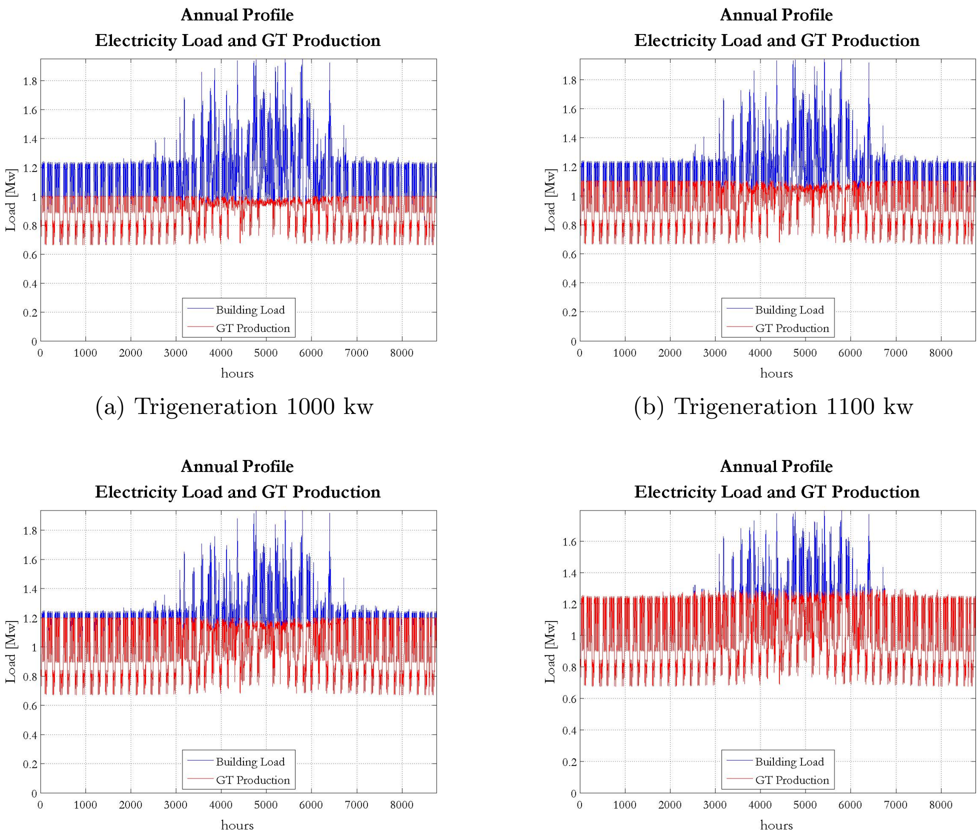

(a) Trigeneration 1000 kw

(b) Trigeneration 1100 kw

(c) Trigeneration 1200 kw

(d) Trigeneration 1300 kw

Figure 103: Changes in electrical duration curves for several proposed trigeneration layouts [2/2].

CITED LITERATURE

1. Haefke, C. and Cuttica, J.: Market sector fact sheet: Combined heat and power in hospitals. US DOE CHP Technical Assistance Partnership, 2013.

2. GE Jenbacher GmbH & Co OG: Studio di caso di motori a gas: Sistemi di cogenerazione negli ospedali. GE feasibility study - Retrived from https://www.ge-distributedpower.com/ on 01/28/2015, 2014.

3. Haefke, C. and Cuttica, J.: Market hospital potential business plan. US DOE Technical Assistance Partnerships, 2013.

4. Crino', A.: CHP Technologies in the Midwest of USA: Energy and Economic Evaluation of a CHP System. Master's thesis, Politecnico di Torino, 2014.

5. ASUE: Arbeitsgemeinschaft für Sparsamen und Umweltfreundlichen: Blockheizkraftwerke in Krankenhäusern. 2010.

6. Babus' Haq, R., Probert, S., and O'Callaghan, P.: Assessing the prospects and commercial viabilities of small-scale chp schemes. Applied energy, 31(1):19–30, 1988.

7. Bonnema, E., Studer, D., Parker, A., Pless, S., and Torcellini, P.: Large hospital 50% energy savings: Technical support document. National Renewable Energy Laboratory, 2010.

8. ANSI/ASHRAE: Standard 90.1-2004, standard methods of determining, expressing and comparing building energy performance and greenhouse gas emissions. American Society of Heating, Refrigerating and Air-Conditioning Engineers, Inc, 2010.

9. Hirsch, J. and et al.: equest user manual: topics. Building Energy Use and Analysis Program, 3, 2006.

10. Darrow, K., Tidball, R., Wang, J., and Hampson, A.: Catalogue of chp technologies. U.S. Environmental Protection Agency and U.S. Department of energy, Combined Heat And Power Partnership Report, 2014.

CITED LITERATURE (Continued)

11. Solar turbines: Turbomachinery systems for oil and gas application. 2011 Solar Turbine Catalog - Retrived from https://mysolar.cat.com on 02/27/2015, 2011.

12. Solar turbines: Solar turbine - product support. 2011 Solar Turbine Catalog - Retrived from https://mysolar.cat.com on 02/27/2015, 2011.

13. ISO International Organization for Standardization: Iso 3977-2: Gas turbines-part 2: Standard reference conditions and ratings. 1997.

14. Carapellucci, R. and Giordano, L.: The recovery of exhaust heat from gas turbines. 2012.

15. Kerr, T.: Combined heat and power: Evaluating the benefits of greater global investment. IEA, International Energy Agency website - Retrived from http://www.eia.gov/ on 01/22/2015, 2008.

16. Bourgeois, T., Dillingham, G., Panzarella, I., and Hampson, A.: Combined heat and power: Enabling resilient energy infrastructure for critical facilities. ICF International Paper, 2013.

17. ASHRAE: Standard 105-2004, energy standard for buildings except low rise residential buildings. American Society of Heating, Refrigerating and Air-Conditioning Engineers, Inc, 2010.

18. Sheikhi, A., Ranjbar, A., and Oraee, H.: Financial analysis and optimal size and operation for a multicarrier energy system. Energy and Buildings, 48:71–78, 2012.

19. Commonwealth Edison Company: Schedule of rates for electric service. Retrived from www.comed.com on 03/28/2015, 2014.

20. US Energy Information Administration: Average retail price of electricity to ultimate customers by end-use sector. (EIA) Report - Retrived from http://www.eia.gov/ on 04/01/2015, 2015.

21. US Energy Information Administration: Illinois natural gas industrial price. US Energy Information Administration (EIA) Report - Retrived from http://www.eia.gov/ on 04/01/2015, 2015.

22. De Vega, M., Almendros-Ibáñez, J. A., and Ruiz, G.: Performance of a libr-water absorption chiller operating with plate heat exchangers. Energy conversion and management, 47(18):3393–3407, 2006.

CITED LITERATURE (Continued)

23. YORK: Millennium yia single-effect absorption chillers. YORK Catalog - Retrived from http://www.johnsoncontrols.com/ on 02/05/2015, 2012.

24. YORK: Isoflow single-effect absorption chillers - catalog. YORK Catalog - Retrived from http://www.johnsoncontrols.com/ on 02/05/2015, 2012.

25. Standard, A.: 550/590-2003. Performance rating of water-chilling packages using the vapor compression cycle, Air-conditioning & Refrigeration Institute, 2003.

26. Al-Sulaiman, F. A., Hamdullahpur, F., and Dincer, I.: Trigeneration: a comprehensive review based on prime movers. International journal of energy research, 35(3):233–258, 2011.

27. Sieminski, A.: International energy outlook 2013. US Energy Information Administration (EIA) Report Number: DOE/EIA-0484, 2013.

28. Ng, K. C.: Thermodynamic tools for chiller diagnostics and optimization. Heat Transfer Engineering, 25(8):1–4, 2004.

29. TRANE: Quick reference for efficient chiller system design. 2011 TRANE Catalog - Retrived from https://www.trane.com on 02/15/2015, 2000.

VITA

Name:	Francesco Cicciarella
Education:	Master of Science in Mechanical Engineering
	University of Illinois at Chicago, USA, August 2015
	Master of Science in Energy and Nuclear Engineering
	Politecnico di Torino, Italy, July 2015
	Bachelor of Science in Energy Engineering
	Politecnico di Torino, Italy, March 2013
Honors:	TOP-UIC mobility scholarship for Double Degree program, 2014-2015
	Thesis under request scholarship, 2014-2015